The role of dentate granule cell age and morphology in seizure-induced plasticity.

by

Alison Leigh Althaus

A dissertation submitted in partial fulfillment
of the requirements for the degree of
Doctor of Philosophy
(Neuroscience)
in The University of Michigan
2015

Doctoral Committee:

Professor Jack M Parent, Chair
Professor Roman J Giger
Professor Richard I Hume
Associate Professor Geoffrey G Murphy
Professor Michal R Zochowski

For Mom and Dad

Acknowledgements

The work presented in this dissertation represents a collaborative effort by many talented individuals. First and foremost is my advisor, Jack Parent. Without his mentorship and support none of this work could have been accomplished. In addition, I am fortunate to have had many excellent mentors and role models throughout my graduate career, and of principle importance has been the mentorship of Geoff Murphy. I wish also to acknowledge the continued support of those whose encouragement initially prompted me to seek a career in science; including my high school biology teacher Dee Blatchford and my first research mentor David Wagner.

My colleagues in the Parent and Murphy laboratories have given so much of their time and energy to the betterment of this work. Chief among them is Helen Zhang, who is not only a talented scientist, but also a paragon of collegiality. Though all members of both laboratories have provided scientific assistance or moral support, I want to especially thank Dr. Shannon Moore, Dr. Michelle Kron, Xixi Du, Stephanie Temme, Liz Messenger, Duriel Hardy, Nick Kransz, J.P. Purtell, and Elena Gueorguiev.

Finally, I could not have persevered without love and support of my friends and family. To Nate, you keep me afloat. To Aaron and Adam, your

accomplishments keep me humble. To Mom and Dad, I owe everything to you. To my cohort, thank you, I'm an anteater.

Table of Contents

List of Figures

Chapter 1

Chapter 2

Chapter 3

Chapter 4

List of Tables

Chapter 2

List of Abbreviations

DGC = Dentate Granule Cell

TLE = Temporal Lobe Epilepsy

SE = Status Epilepticus

NSC = Neural Stem Cell

DCX = Doublecortin

BDNF = Brain Derived Neurotrophic Factor

FGF-2 = Fibroblast Growth Factor 2

VEGF = Vascular Endothelial Growth Factor

SGZ = Subgranular Zone

GCL = Granule Cell Layer

KA = Kainic Acid

HBD = Hilar Basal Dendrite

MFS = Mossy Fiber Sprouting

OML = Outer Molecular Layer

MML = Middle Molecular Layer

IML = Inner Molecular Layer

aCSF = artificial Cerebral Spinal Fluid

SFA = Spike Frequency Accommodation

AP = Action Potential

sAHP = slow Afterhyperpolarization

ADP = Afterdepolarization

RMP = Resting Membrane Potential

RV = retrovirus

GFP = Green Fluorescent Protein

YFP = Yellow Fluorescent Protein

syp = synaptophysin

PTX = picrotoxin

TTX = tetrodotoxin

IEI = Interevent Interval

Abstract

Epilepsy is a debilitating disease that often has a profoundly negative impact on quality of life for patients. Temporal lobe epilepsy (TLE) is a common type of medically intractable epilepsy among adults. In TLE, spontaneous seizures begin in temporal lobe structures, including the hippocampus, before progressing to cortical structures. As a result, pathological changes within the hippocampus are hypothesized to play a critical role in epileptogenesis. However, the relationship between observed neuropathology and the development of seizure activity is not well understood, and some aberrant neuronal features that appear to be pathological may actually participate in reparative plasticity. The dentate gyrus is a region of particular interest for epilepsy-related plasticity because of its position as a gate for much of the incoming excitatory input to the hippocampus. In addition, it is capable of a unique type of neuronal plasticity, due to ongoing adult neurogenesis in this region. Indeed, DGCs born after an epileptogenic insult in rodent models are much more likely to display aberrant, pro-excitatory morphology than those that were mature at the time of insult.

We hypothesized that these adult-born DGCs with aberrant morphology are also the most likely to display pro-excitatory physiological features. Hilar ectopic DGCs are common in tissue from TLE patients and animal models, but

rare in healthy controls. We recorded from hilar ectopic and normotopic (located in the granule cell layer) DGCs from both rat and human TLE tissue and found increased excitability in rat DGCs, but decreased excitability in human DGCs. These data present a conflicting view of the role of ectopic DGCs in hyperexcitability, but they also highlight important discrepancies between the human disease and the rodent disease model, which are explored in chapter 2.

We also hypothesized that adult-born DGCs would contribute more than neonatal-born DGCs (which would be mature at the time of epileptogenesis), to aberrant inter-connectivity of DGCs. We labeled neonatal- and adult-born populations of DGCs using retrovirus carrying a fluorescent-tagged synaptophysin to study mossy fiber axonal reorganization in the rat pilocarpine TLE model. Interestingly, we found no major differences, either qualitative or quantitative, in axonal plasticity between the two birthdated populations. Thus, axonal reorganization is independent of adult-neurogenesis in the rat TLE model. Subsets of neonatal and adult-born DGCs are capable of remarkable plasticity in response to epileptogenesis, and the implications of this are discussed in chapter 3.

The work presented in this dissertation provides new insight into the role of DGC birthdate and morphology for excitability in epilepsy. It is more complex than was previously suggested. We have shown that both neonatal- and adult-born, can exhibit features consistent with increased excitability in TLE, but not all adult-born DGCs appear to promote excitability. To gain more comprehensive insight into the implications of these various seizure-related changes, these data

should be integrated into computational models in future studies.

Chapter 1

Introduction

Epilepsy is a complex and diverse neurological disorder characterized by spontaneous, recurrent seizures. Despite being a recognized neurological illness for millennia, underlying mechanisms of epilepsy are not well understood. Of the large variety of epilepsy syndromes, temporal lobe epilepsy (TLE) is the most common in adults. It is also one of the most intractable: in more than 30% of persons with TLE, seizure activity is not controlled by pharmacotherapy (Engel & Pedley 1998).

The causes of TLE are largely unknown and probably vary across patients. In many cases, the onset of spontaneous seizures is preceded by an initial precipitating injury, which is believed to play a causal role in the development of epilepsy. Precipitating injuries are different from patient to patient, ranging from prolonged febrile seizures, to nervous system infections like bacterial meningitis, to traumatic brain injury and others. However, most people who experience these insults will not go on to develop epilepsy (Harvey et al 1997). For those that do, the latent period (time between the injury and onset of seizures) is highly variable. All of these factors contribute to the difficulty

of understanding the process of epileptogenesis, which involves cellular and molecular changes leading to the generation of spontaneous recurrent seizures.

In many TLE patients, removal of the seizure focus, which includes the hippocampus and other antero-medial temporal lobe structures, alleviates seizures. These resected tissues, along with post-mortem tissues, often display hippocampal sclerosis, which includes pyramidal cell death, astrogliosis, and structural reorganization within the dentate gyrus (Engel & Pedley 1998). Pathology in the dentate gyrus is of particular relevance to those interested in adult neurogenesis, because the dentate is a well-established region of ongoing neurogenesis in the adult human brain (Eriksson et al 1998).

Modeling TLE in laboratory animals

TLE is a heterogeneous disease: patients present at all ages, have had a variety of precipitating injuries (or, in many cases, no injury), experience a wide range of seizure numbers and severity, and tissues exhibit varying degrees of histopathology (Engel 1996). Fortunately, many animal models have been developed and validated that recapitulate many different aspects of the disease. These models most commonly involve rodents, but other species have been utilized as well, yielding important contributions to the understanding of human disease.

TLE is often acquired after a precipitating insult such as a prolonged febrile seizure, although there are some inherited forms of TLE associated with

focal brain malformations (Berkovic et al 1996, Engel 1996). Laboratory models therefore typically rely on an induced brain insult to elicit seizure activity. These insults range from relatively minor, such as low doses of chemoconvulsants that induce acute, self-limited seizures, to moderate, such as electrical kindling, which chronically alters network excitability, to severe, such as induced status epilepticus (SE), which causes spontaneous recurrent seizures for the duration of the animal's life. While this means that tools to study important and diverse questions in the field are readily available, it also presents a challenge when considering discrepant data. When results cannot be replicated across models, it is difficult to determine whether different findings are equally valid because models recapitulate different manifestations of the disease, or because the model(s) in question fails to properly model the relevant aspect of the disease. For this reason, it is necessary to select an appropriate model to address a specific question relevant to the human disease.

The most common models use SE, a prolonged period of continuous seizures, as the initial precipitating injury (analogous to a prolonged febrile seizure) to subsequently produce spontaneous seizures in rodents. In these models, SE is induced by chemoconvulsants (usually pilocarpine or kainic acid) or electrical stimulation, and then spontaneous seizures develop after a latent period lasting days to weeks. Structural changes in the hippocampi of these animals arise within hours to days of SE, and after weeks to months much of the hippocampal histopathology resembles that seen in hippocampal tissue from human TLE patients (Buckmaster 2004). Within the dentate gyrus, this

histopathology includes hilar and pyramidal cell death, dentate granule cell (DGC) layer dispersion, sprouting of mossy fibers, and ectopic locations of DGC bodies (Dudek & Sutula 2007, Houser 1992) (Figure 1.1). The severity of this pathology can vary across individual animals, and by induction method, but is generally greater the longer SE is allowed to proceed uninterrupted (Buckmaster 2004).

The rodent data presented in this dissertation was collected using adult male, Sprague Dawley rats that were treated with a high dose of pilocarpine-hydrochloride to induce SE, which was terminated with diazepam after 90 minutes. This model was chosen because animals rapidly and reliably undergo epileptogenesis, and consistently develop spontaneous recurrent seizures and DGC histopathology. Therefore, this model is a good tool for examining the conditions that create DGC histopathology and how aberrant plasticity impacts the function of networks. However, because of the severity of injury in these animals, it is difficult to use this model to determine which aspects of the seizure-related plasticity are necessary or sufficient for epileptogenesis.

The impact of seizures on adult neural stem cell NSC proliferation

Under basal laboratory conditions, about 9,000 new DGCs are generated daily in the young adult rat (Cameron & McKay 2001). Typically, 25-40% of newly generated DGCs survive and functionally integrate into the dentate gyrus network (Kempermann et al 2003, Tashiro et al 2007). However, the number of

cells generated and the proportion that survive into maturity are dynamically regulated and can be influenced by both physiological and pathological stimuli at many different stages.

For example, exercise, and traumatic brain injury stimulate the division of specific subsets of dentate NSCs, while stress and learning depress NSC division (Brown et al 2003, Dobrossy et al 2003, Pham et al 2003, Yu et al 2008). Interestingly, learning has the opposite effect on the survival of newly generated DGCs; along with environmental enrichment, it enhances the number of immature DGCs that survive into maturity (Dobrossy et al 2003, Kempermann et al 1997, van Praag et al 1999). Prolonged seizures influence adult dentate gyrus neurogenesis to a greater extent and at all stages in the neurogenic process. They modulate the proliferation of multiple NSC types, as well as the survival, maturation, and integration of adult-generated DGCs.

Effects on different populations of NSCs

The population of NSCs in the adult dentate gyrus is complex and heterogeneous, and the heterogeneity is not well understood. For a comprehensive review, see (Duan et al 2008, Faigle & Song 2013). Determining the responses of the different subsets of NSC to seizure activity requires a nuanced approach to identifying NSC subpopulations that has not yet been undertaken in TLE models. However, many studies have distinguished the responses of at least two different progenitor populations to seizure activity. Radial glia-like stem cells are multipotent stem cells which are typically

quiescent but participate in the early proliferative response to SE in the rodent dentate gyrus (**Figure 1.2**) (Huttmann et al 2003, Kronenberg et al 2003, Lugert et al 2010, Seri et al 2004, Suh et al 2007). Doublecortin (DCX)-expressing neural progenitors substantially increase in number several days after the initial SE episode and, depending on the severity and duration of SE, continue to accumulate for up to four weeks afterward (Jessberger et al 2005, Jessberger et al 2007b, Parent et al 1999, Parent et al 1997). DCX-expressing cells are committed to a neuronal fate (Francis et al 1999); thus, most of the proliferating progenitor cells generate new neurons after SE. The survival of these post-SE-generated cells, however, is closely tied to seizure severity and duration (Mohapel et al 2004). Interestingly, proliferation can be dramatically increased even with a mild seizure stimulus. In fact a single, discrete electrical stimulation-induced discharge is sufficient to increase neurogenesis several weeks later (Bengzon et al 1997).

Effects of chronic seizures and aging

Fewer studies have focused on neurogenesis in the chronic phase of epilepsy. Although it is well known that basal levels of neurogenesis decline with age in the rodent dentate gyrus (Kuhn et al 1996), it is unclear how chronic epilepsy influences this age-related decline. Recent work suggests that five months after chemoconvulsant-induced SE, rats have dramatically reduced basal neurogenesis compared to same-aged controls (Hattiangady et al 2004). Although the mechanism for this reduction is unknown, it may result from

impaired NSC function in the epileptic brain, or perhaps from a reduction in the available “NSC pool.” However, others have found that six months after electrically-induced SE, epileptic animals do not show a decrease in basal neurogenesis compared to age-matched controls (Bonde et al 2006), highlighting the variability between models and the importance of understanding how different models relate to human disease.

The age of an animal at the onset of SE is also an important factor in the NSC response. Typically, epilepsy is induced in juvenile/young adult rodents (one to four months of age). Animals within this age range have equivalent levels of post-SE neurogenesis, despite slight decreases in basal neurogenesis (Gray et al 2002). However, 24-month-old animals, and in some experiments even those as young as 12 months, do not show increased neurogenesis in response to an epileptogenic insult (Hattiangady & Shetty 2008, Rao et al 2008). Importantly, this finding is not the result of a general unresponsiveness of NSCs in aged animals, since increased neurogenesis in response to voluntary exercise is maintained in senescent animals (van Praag et al 2005). Instead, the differential response suggests a specific reduction in NSC activation by seizures in the aged brain, either directly or indirectly through reduced effects of seizures on other cells in the neurogenic niche.

Possible mechanisms of proliferative response to seizures

Clues as to why the NSC response differs between experimental models or with age requires a better understanding of the molecular mechanisms that

lead to enhanced proliferation after an epileptogenic insult. Part of the difficulty in studying this phenomenon is the fact that molecular mechanisms mediating adult neurogenesis in the intact dentate gyrus are not completely understood. Recent evidence suggests that many of the same processes involved in neurogenesis during brain development also regulate adult neurogenesis (Faigle & Song 2013). Some of these molecular processes are also stimulated by SE (Elliott & Lowenstein 2004). For example, data indicate that SE alters Notch1 and Sonic hedgehog signaling in a manner that would promote cell proliferation (Banerjee et al 2005, Sibbe et al 2012). Trophic factors such as brain derived neurotrophic factor (BDNF), fibroblast growth factor-2 (FGF-2) and vascular endothelial growth factor (VEGF) are increased in hippocampal tissue after SE (Gall 1993, Isackson et al 1991, Newton et al 2003, Warner-Schmidt & Duman 2007), and are also known regulators of adult neurogenesis (Faigle & Song 2013). An important consideration, however, is that changes observed in these signaling cascades after epileptic insults may be incidental to the fact that proliferation has been stimulated, rather than the direct mechanism of stimulation.

Importantly, neuronal activity itself can modulate NSC proliferation (Deisseroth et al 2004). This effect is mediated through calcium channels, NMDA receptors, and possibly GABA-A receptors expressed by NSCs (Deisseroth et al 2004, Tozuka et al 2005). In the dentate gyrus, zinc is an additional potential link between neural activity and NSC proliferation. Zinc is normally released from DGC axon terminals, and zinc chelation after SE

reduces NSC proliferation (Kim et al 2012). Activity dependent epigenetic modifications are also associated with altered NSC proliferation after single electroconvulsive seizures or chemoconvulsant-induced SE (Jessberger et al 2007a, Ma et al 2009), although in one of these settings neurogenesis is modulated indirectly through epigenetic changes in mature DGCs (Ma et al 2009). The myriad of diverse signals that have been reported to mediate NSC proliferation after discrete seizures or SE cannot be explained by differences in epilepsy models because the same models are often used in a number of different studies. Rather, because seizures elicit many changes in neural tissue, it is likely that within any given model different signals converge to produce a robust seizure-induced neurogenic response.

Seizure impact on DGC maturation and integration

The percentage of adult-generated DGCs that survive the initial activity dependent selection process is highly variable, even under baseline conditions. Some studies have reported as much as 75% survival, others as little as 30%, likely reflective of species and strain differences (Dayer et al 2003, Kempermann et al 2003, Snyder et al 2009, Tashiro et al 2007). In SE models, the percentage of post-SE generated cells that survive and mature seems to be, in part, a function of the severity of SE (Mohapel et al 2004) and a consequence of inflammation in the epileptic hippocampus (Ekdahl et al 2003). The environmental changes that take place during epileptogenesis, as well as in the

setting of chronic epilepsy, affect the maturation and integration of the surviving, seizure-generated DGCs. Moreover, whether these changes influence DGC progenitors to develop in a pro- or anti-epileptic fashion may itself be a function of model severity.

Seizures affect the rate of DGC maturation

In intact animals, adult-born DGCs progress through distinct maturation stages over a period of 3-4 months, after which they are fully integrated into the pre-existing network and are indistinguishable from peri-natally generated DGCs, (Esposito et al 2005, Laplagne et al 2006, Piatti et al 2006, Toni et al 2008, van Praag et al 2002, Zhao et al 2006). Each stage of maturation is regulated by both intrinsic and extrinsic mechanisms. GABA plays an important role at many stages (Ge et al 2007). Because of the high internal chloride concentration of adult neural progenitors and immature neurons, GABA depolarizes the membrane and elicits an excitatory response that is necessary for proper development (Ge et al 2006, Overstreet Wadiche et al 2005, Tozuka et al 2005). Since the developing cells do not respond to glutamatergic inputs until they are about two weeks post-mitotic (Piatti et al 2006), tonic and synaptic GABA inputs drive much of the early activity-related development. This effect is, in part, mediated by the basic helix-loop-helix transcription factor NeuroD1, which is activated by GABA-driven activity and is required for survival and maturation of DGCs (Gao et al 2009, Tozuka et al 2005). Many SE models show profound changes to GABAergic activity in the dentate gyrus, due to the death of

inhibitory interneurons and changes in the structure and function of the remaining interneurons (Dudek & Sutula 2007, Thind et al 2010, Zhang et al 2009). A direct relationship between altered GABA signaling and altered neurogenesis has not been explored in the context of TLE models, but this is a promising area for future research. Changes in network activity and in levels of growth factor expression also affect the rate of maturation and integration of adult-born DGCs (Piatti et al 2011, Waterhouse et al 2012). Not surprisingly, seizures also strongly affect the rate of DGC development. Under baseline conditions, DGC dendrites do not reach the outer molecular layer until around 21 days after birth (Toni et al 2007). However, some DGCs born after or near the time of SE develop extensive dendritic arbors almost a week sooner and receive excitatory inputs well before their counterparts in control brains (Overstreet-Wadiche et al 2006).

Aberrant DGC migration in epilepsy

In addition to speeding up maturation and integration, alterations in the local environment of the dentate gyrus after SE lead to abnormal DGC morphological features and physiology. Adult-born DGCs are generated in the subgranular zone (SGZ), between the granule cell layer (GCL) and the hilus. Normally, as they mature, they migrate into the GCL where their dendrites receive excitatory inputs from perforant path fibers. After SE, a subset of the newly generated DGCs migrates aberrantly into the hilus where they are innervated by mossy fiber axons (Jessberger et al 2007b, Kron et al 2010,

Parent et al 2006, Pierce et al 2005). Newborn DGCs continue to migrate ectopically even in chronic epilepsy after the level of neurogenesis has returned to baseline (Bonde et al 2006), suggesting that permanent changes to the epileptic network underlie the aberrant migration. Although the causes of aberrant migration are not well understood, reelin, a migratory signal that is involved in embryonic development, is one interesting candidate. Reelin signaling is important for proper migration of adult born neurons in the dentate gyrus (Gong et al 2007, Teixeira et al 2012), and is potently disrupted by SE (Gong et al 2007). Importantly, the loss of reelin signaling within individual DGC progenitors in an otherwise normal animal is sufficient to induce ectopic migration of the affected cells (Teixeira et al 2012).

Loss of reelin signaling has also been linked to aberrant locations of mature DGCs in the intra-hippocampal kainate model of SE (Heinrich et al 2006). In this model, the chemoconvulsant kainic acid (KA) is delivered directly into the hippocampus of one hemisphere. This induces SE and robust cellular pathology, including dispersion of the granule cell body layer, in the ipsilateral (injected) hippocampus. This dispersion, which can be observed rapidly following the KA injection, is not associated with an increase in neurogenesis (Fahrner et al 2007), likely due to disruption of the dentate NSC niche from severe injury. Thus, work from different animal models indicates that dispersion of the normally compact granule cell body layer may result from both acute changes to the structure of mature DGCs and from chronic changes that impair migration of developing DGCs.

Due to their aberrant location and inputs, hilar ectopic DGCs are thought to play an important role in the formation of a recurrent excitatory network after SE (Parent & Lowenstein 2002, Scharfman & Gray 2007). In addition to being innervated by mossy fiber axons, hilar ectopic DGCs send their axon collaterals to the molecular layer to form aberrant synapses onto DGC apical dendrites (Scharfman et al 2000). Functionally, they receive more excitatory inputs than DGCs located in the GCL (Zhan et al 2010, Zhang et al 2012), and they become partially synchronized with pyramidal cells in area CA3 (Scharfman et al 2000). However, hilar ectopic DGCs are probably not the only drivers of aberrant excitatory activity in the epileptic dentate gyrus. Many, perhaps most, other DGCs participate to some extent in the formation of the abnormal epileptic network. A major difficulty in defining the net effects of altered DGC neurogenesis on epileptogenesis, however, is that the DGCs in the granule cell layer, even those only generated after SE, are likely to be a heterogeneous population, with some contributing to excess excitability, others having a more neutral response, and still others perhaps playing a compensatory role by developing reduced excitability.

Aberrant dendritic morphology in epilepsy

One sub-population that is believed to contribute to abnormal recurrent excitation is DGCs with hilar basal dendrites (HBDs) (Dashtipour et al 2003, Ribak et al 2000, Shapiro et al 2005, Shapiro & Ribak 2006, Thind et al 2008). Normally, basal dendrites are transient structures on immature DGCs of

rodents that do not become synaptically integrated (Seress & Pokorny 1981). After SE, however, synapses rapidly develop onto HBDs (Shapiro et al 2007), leading to spine formation (Jessberger et al 2007b, Walter et al 2007) and an overall increase in primarily excitatory inputs onto the cell (Thind et al 2008). These HBDs persist once the cell has reached maturity (Ribak et al 2000, Walter et al 2007). Recent work also indicates that DGCs with a prominent HBD are more likely to have a very high spine density on their apical dendrites when compared with other DGCs born at the same time (Murphy et al 2011), The mechanism for the increased presence of DGCs with HBDs after SE is not entirely understood, although the fact that HBDs are part of a normal developmental stage for DGCs may be a clue. Only DGCs that are in the process of developing at the onset of SE, or those born afterward, show increased rates of HBD persistence (Jessberger et al 2007b, Kron et al 2010, Walter et al 2007). Thus, DGCs developing in this abnormal environment may be unable to retract their HBDs, or alternatively, they may regrow previously retracted HBDs, though this is less likely. Importantly, HBDs have been linked not only to anatomical measures of excitability, but also to increased physiological excitation (Austin & Buckmaster 2004).

Despite the fact that hilar ectopic DGCs and those with HBDs comprise a minority of the total population, the degree to which they are hyper-innervated suggests that they may have a powerful influence on overall network excitability. Two recent studies suggest that pro-excitatory changes in a relatively small subset of DGCs are sufficient to induce epileptic activity. In one, computational

modeling of an epileptic dentate gyrus showed that the configuration of synaptic connectivity that most reliably produced seizure-like activity was one in which a small subset of DGCs (5%) were highly interconnected (Morgan & Soltesz 2008). By keeping constant the total number of synapses in the network, and changing only the distribution of the recurrent DGC inputs, Morgan and Soltesz found that a network containing the highly interconnected DGC “hubs” was strongly activated by a relatively mild input. In a separate study, Pun and colleagues used a conditional transgenic mouse to delete phosphatase and tensin homolog (PTEN) in dentate gyrus progenitors and thereby alter the development of a subset of adult-born DGCs in the context of an otherwise normal brain. The genetically altered DGCs displayed HBDs, increased spine density, and ectopic migration into the hilus, similar to DGCs present in models of epilepsy. Remarkably, although only 9-24% of DGCs developed these abnormal features, animals subsequently developed spontaneous recurrent seizures (Pun et al 2012). Together, these studies indicate that small populations of DGCs can play a pivotal role in the development of seizure activity, and they highlight the need for a better understanding of individual DGC abnormalities in the context of TLE.

Axonal reorganization in epilepsy

Mossy fiber sprouting (MFS) is another important feature of TLE. Under normal conditions, DGC axons, which are also called mossy fibers, project throughout the hilus and to CA3 (Blaabjerg & Zimmer 2007). In TLE and animal

models, mossy fiber axons also extend through the GCL and into the supragranular inner molecular layer, where they innervate the apical dendrites of other DGCs (Buckmaster et al 2002). This results in an excitatory feedback loop that is proposed to underlie recurrent activation of DGCs and therefore the development or spread of spontaneous seizure activity (Sutula & Dudek 2007). It has been difficult to determine whether specific subpopulations of DGCs selectively participate in MFS. Initially, the hypothesis was put forward that adult-generated-DGCs developing after an epileptogenic insult are responsible for MFS (Parent & Lowenstein 1997); however, a study using irradiation to suppress neurogenesis provided evidence that ablating DGCs born after SE failed to prevent MFS within 4 weeks after SE (Parent et al 1999). With the use of the more precise retrovirus birthdating methods, subsequent work suggested that only cells that were developing during SE or born afterward contributed to MFS (Kron et al 2010). Using superior labeling technology, more recent data, which is discussed in Chapter 3 of this dissertation, now show that cells that were mature at SE do indeed contribute to MFS. Nevertheless, the role of MFS, at least in the supragranular inner molecular layer, in epileptogenesis remains controversial.

Functional significance of adult neurogenesis in TLE

As stated above, some DGCs generated after SE appear to show decreased excitability, perhaps as a means of compensating for the overall hyper-excitability within the network. Several recent studies have used

fluorescent reporter labeling using retroviruses or transgenic mice to identify DGCs born after SE in order to characterize the morphological and physiological characteristics of this population. On one extreme, nearly all of the adult-born DGCs examined in an adult rat electrical stimulation-induced SE model displayed strongly reduced excitation and increased inhibition (Jakubs et al 2006), suggesting an anti-epileptogenic role for this population as a whole. In other studies of rodent chemoconvulsant TLE models, many of the adult-born DGCs display pro-excitatory features and receive increased excitatory inputs (Kron et al 2010, Walter et al 2007, Wood et al 2011). Still others report a more mixed population, in which some cells clearly display anatomical evidence of pro-excitatory features (Jessberger et al 2007b), while others have features that are consistent with reduced excitation (Murphy et al 2011). The variability in the proportion of cells that might be “pro-excitatory” as opposed to “pro-inhibitory” in these models may reflect the use of different SE induction protocols. The type of induction protocol can have a dramatic affect on the development of chronic epilepsy, affecting number and severity of spontaneous seizures. Moreover, post-SE generated DGCs that are continuously exposed to seizures during their development show increased excitatory activity, even without a dramatic increase in aberrant morphology (Wood et al 2011).

Therapeutic potential of targeting endogenous NSCs

The structural and functional heterogeneity of DGCs born after SE is one major challenge when considering the best way to target these cells for

therapeutic intervention. Certainly aberrant integration of and increased excitatory inputs onto some of these cells seems to indicate that they have a pathological role in the development of spontaneous seizures. Supporting this idea is the fact that as little as 9% of aberrantly connected DGCs in an otherwise normal animal is sufficient to induce spontaneous seizures (Pun et al 2012). However, the subset of cells in this same population that display pro-inhibitory features in some epilepsy models may be an important part of the brain's attempt to balance excess network excitability. Experimental efforts to eliminate the entire population of DGCs that are born in response to SE as a means of understanding the overall impact of this population on seizure development yield mixed results. Treatment with anti-mitotic agents after chemoconvulsant-induced SE resulted in reduced seizure frequency (Jung et al 2004, Jung et al 2006), suggesting a net excitatory effect of this population on the network. However, focal brain irradiation to suppress neurogenesis in a kindling model increased seizure activity (Raedt et al 2007), a finding that may indicate a net inhibitory effect of post-SE neurogenesis. Despite the differences in SE models and means of reducing neurogenesis in these experiments, taken together the results suggest that a targeted approach that can address aberrant integration of this cell population without interfering with the development of compensatory mechanisms may be the most effective strategy.

Another, perhaps larger, challenge is to understand how the findings in rodent models relate to the human disease. When considering this question, it is important to note that TLE manifestations in patients are even more diverse than

in animal models. Thus, it is perhaps incorrect to try to identify a model that "most closely" resembles the human disease. Instead, it seems most relevant to focus on the salient features in the different models.

Increased neurogenesis, per se, has not been convincingly demonstrated in human tissue from adult TLE patients (Fahrner et al 2007), but there is evidence for increased numbers of neural progenitors in the dentate gyrus of some patients (Crespel et al 2005). However, one must be cautious when drawing conclusions from post-mortem human tissue or specimens obtained from epilepsy surgery to treat drug-resistant seizures. Often, this tissue comes from patients who have had seizures for many years and therefore may not reflect the same structural changes that initially led to epilepsy development. Because experimental tissue from patients in early stages of TLE is largely unavailable, it has been difficult to determine whether hippocampal neurogenesis is affected early in the disease. Interestingly, there is some evidence of increased neurogenesis in very young children after an epileptogenic insult (Blumcke et al 2001).

The presence of hilar ectopic DGCs in human TLE tissue is described, but is not found in every patient (Parent et al 2006, Parent & Murphy 2008, Scharfman & Gray 2007). Although lack of hilar ectopic DGCs in some tissues could be due to a number of factors, the same issues related to early versus late stage disease course apply when comparing findings in human tissue to experimental models. In addition to this caveat, another potential issue is the fact that the method for identifying cell types based on expression of

endogenous markers identified in rodent cells may not be completely effective in human tissue. Thus, the presence of hilar ectopic DGCs could be missed if investigators only use one method for detection (Scharfman & Gray 2007). Nonetheless, hilar ectopic DGCs are present and functionally integrated in tissue from at least some patients with TLE (Parent et al 2006, Parent & Murphy 2008). Chapter 2 of this dissertation discusses the first investigation of the physiology of this aberrant population of DGCs in human tissue.

Although the increased presence of HBDs on developing and newborn DGCs after SE is a feature of many different models and represents an important opportunity for increased recurrent excitatory input between DGCs, the relevance of this finding to human TLE is also unclear. While mature DGCs in rodent tissue rarely (<6%) have HBDs (Kron et al 2010, Walter et al 2007), they are more common on DGCs in non-epileptic humans (10%) and non-human primates (25%) (Seress 1992). However, several studies suggest that the number of cells with HBDs is increased in human TLE (Franck et al 1995, von Campe et al 1997), raising the possibility that HBDs contribute to increased recurrent innervation. It is unknown whether inputs to these structures are altered in TLE patients and more work is needed to understand the potential importance of HBDs in human TLE.

In addition to contributing to seizure generation or spread, the aberrant integration of post-SE born DGCs may have other adverse effects on the epileptic brain. Great interest exists in understanding the normal function of adult neurogenesis, and though there are no definitive answers yet, a number of

studies have found links between disrupted neurogenesis and altered learning and memory (Deng et al 2010). Although seizures in human TLE and in animal models affect many other structures besides the dentate gyrus, the potential relationship between aberrant neurogenesis and cognitive impairments in epileptic animals and human patients is intriguing. Also of interest is the reduction of neurogenesis that occurs in some animals in later stages of chronic TLE (Hattiangady et al 2004), and the increased incidence of major depression in patients with TLE (Hermann et al 2000). Because the presence of DGC neurogenesis appears to be a critical aspect of the effect of anti-depressants, at least in some mouse strains (Santarelli et al 2003), patients with TLE and comorbid major depression may benefit doubly from a therapy that corrects aberrant neurogenesis or stimulates normal neurogenesis.

Dissertation Aims

This thesis describes an investigation into the impact of DGC birthdate and morphology on DGC contribution to the development of TLE. DGCs born after SE are more likely to exhibit aberrant, seizure-related features, but the physiological implications of these changes are not fully understood. In chapter 2, the question of whether hilar ectopic DGCs have greater intrinsic excitability than normotopic DGCs was addressed in both rat and human TLE tissue. The results indicate that ectopic DGCs have altered excitability compared to normotopic, but they also highlight potential discrepancies between the disease and the disease

model. Chapter 3 describes an investigation into the relationship between DGC birthdate and mossy fiber reorganization after SE. The data indicate that axonal plasticity is robust in both cells that were mature at SE as well as those born afterward. Finally, Chapter 4 provides preliminary insight into the relationship between aberrant morphology and synaptic input.

References

Austin JE, Buckmaster PS. 2004. Recurrent excitation of granule cells with basal dendrites and low interneuron density and inhibitory postsynaptic current frequency in the dentate gyrus of macaque monkeys. *The Journal of comparative neurology* 476: 205-18

Banerjee SB, Rajendran R, Dias BG, Ladiwala U, Tole S, Vaidya VA. 2005. Recruitment of the Sonic hedgehog signalling cascade in electroconvulsive seizure-mediated regulation of adult rat hippocampal neurogenesis. *The European journal of neuroscience* 22: 1570-80

Bengzon J, Kokaia Z, Elmer E, Nanobashvili A, Kokaia M, Lindvall O. 1997. Apoptosis and proliferation of dentate gyrus neurons after single and intermittent limbic seizures. *Proceedings of the National Academy of Sciences of the United States of America* 94: 10432-7

Berkovic SF, McIntosh A, Howell RA, Mitchell A, Sheffield LJ, Hopper JL. 1996. Familial temporal lobe epilepsy: a common disorder identified in twins. *Annals of neurology* 40: 227-35

Blaabjerg M, Zimmer J. 2007. The dentate mossy fibers: structural organization, development and plasticity. *Progress in brain research* 163: 85-107

Blumcke I, Schewe JC, Normann S, Brustle O, Schramm J, et al. 2001. Increase of nestin-immunoreactive neural precursor cells in the dentate gyrus of pediatric patients with early-onset temporal lobe epilepsy. *Hippocampus* 11: 311-21

Bonde S, Ekdahl CT, Lindvall O. 2006. Long-term neuronal replacement in adult rat hippocampus after status epilepticus despite chronic inflammation. *The European journal of neuroscience* 23: 965-74

Brown J, Cooper-Kuhn CM, Kempermann G, Van Praag H, Winkler J, et al. 2003. Enriched environment and physical activity stimulate hippocampal but not olfactory bulb neurogenesis. *The European journal of neuroscience* 17: 2042-6

Buckmaster PS. 2004. Laboratory animal models of temporal lobe epilepsy. *Comparative medicine* 54: 473-85

Buckmaster PS, Zhang GF, Yamawaki R. 2002. Axon sprouting in a model of temporal lobe epilepsy creates a predominantly excitatory feedback circuit. *The Journal of neuroscience : the official journal of the Society for Neuroscience* 22: 6650-8

Cameron HA, McKay RD. 2001. Adult neurogenesis produces a large pool of new granule cells in the dentate gyrus. *The Journal of comparative neurology* 435: 406-17

Crespel A, Rigau V, Coubes P, Rousset MC, de Bock F, et al. 2005. Increased number of neural progenitors in human temporal lobe epilepsy. *Neurobiology of disease* 19: 436-50

Dashtipour K, Wong AM, Obenaus A, Spigelman I, Ribak CE. 2003. Temporal profile of hilar basal dendrite formation on dentate granule cells after status epilepticus. *Epilepsy research* 54: 141-51

Dayer AG, Ford AA, Cleaver KM, Yassaee M, Cameron HA. 2003. Short-term and long-term survival of new neurons in the rat dentate gyrus. *The Journal of comparative neurology* 460: 563-72

Deisseroth K, Singla S, Toda H, Monje M, Palmer TD, Malenka RC. 2004. Excitation-neurogenesis coupling in adult neural stem/progenitor cells. *Neuron* 42: 535-52

Deng W, Aimone JB, Gage FH. 2010. New neurons and new memories: how does adult hippocampal neurogenesis affect learning and memory? *Nature reviews. Neuroscience* 11: 339-50

Dobrossy MD, Drapeau E, Aurousseau C, Le Moal M, Piazza PV, Abrous DN. 2003. Differential effects of learning on neurogenesis: learning increases or decreases the number of newly born cells depending on their birth date. *Molecular psychiatry* 8: 974-82

Duan X, Kang E, Liu CY, Ming GL, Song H. 2008. Development of neural stem cell in the adult brain. *Current opinion in neurobiology* 18: 108-15

Dudek FE, Sutula TP. 2007. Epileptogenesis in the dentate gyrus: a critical perspective. *Progress in brain research* 163: 755-73

Ekdahl CT, Claasen JH, Bonde S, Kokaia Z, Lindvall O. 2003. Inflammation is detrimental for neurogenesis in adult brain. *Proceedings of the National Academy of Sciences of the United States of America* 100: 13632-7

Elliott RC, Lowenstein DH. 2004. Gene expression profiling of seizure disorders. *Neurochemical research* 29: 1083-92

Engel J, Jr. 1996. Introduction to temporal lobe epilepsy. *Epilepsy research* 26: 141-50

Engel J, Pedley TA. 1998. *Epilepsy : a comprehensive textbook*. Philadelphia: Lippincott-Raven.

Eriksson PS, Perfilieva E, Bjork-Eriksson T, Alborn AM, Nordborg C, et al. 1998. Neurogenesis in the adult human hippocampus. *Nature medicine* 4: 1313-7

Esposito MS, Piatti VC, Laplagne DA, Morgenstern NA, Ferrari CC, et al. 2005. Neuronal differentiation in the adult hippocampus recapitulates embryonic development. *J Neurosci* 25: 10074-86

Fahrner A, Kann G, Flubacher A, Heinrich C, Freiman TM, et al. 2007. Granule cell dispersion is not accompanied by enhanced neurogenesis in temporal lobe epilepsy patients. *Experimental neurology* 203: 320-32

Faigle R, Song H. 2013. Signaling mechanisms regulating adult neural stem cells and neurogenesis. *Biochimica et biophysica acta* 1830: 2435-48

Francis F, Koulakoff A, Boucher D, Chafey P, Schaar B, et al. 1999. Doublecortin is a developmentally regulated, microtubule-associated protein expressed in migrating and differentiating neurons. *Neuron* 23: 247-56

Franck JE, Pokorny J, Kunkel DD, Schwartzkroin PA. 1995. Physiologic and morphologic characteristics of granule cell circuitry in human epileptic hippocampus. *Epilepsia* 36: 543-58

Gall CM. 1993. Seizure-induced changes in neurotrophin expression: implications for epilepsy. *Experimental neurology* 124: 150-66

Gao Z, Ure K, Ables JL, Lagace DC, Nave KA, et al. 2009. Neurod1 is essential for the survival and maturation of adult-born neurons. *Nature neuroscience* 12: 1090-2

Ge S, Goh EL, Sailor KA, Kitabatake Y, Ming GL, Song H. 2006. GABA regulates synaptic integration of newly generated neurons in the adult brain. *Nature* 439: 589-93

Ge S, Pradhan DA, Ming GL, Song H. 2007. GABA sets the tempo for activity-dependent adult neurogenesis. *Trends in neurosciences* 30: 1-8

Gong C, Wang TW, Huang HS, Parent JM. 2007. Reelin regulates neuronal progenitor migration in intact and epileptic hippocampus. *J Neurosci* 27: 1803-11

Gray WP, May K, Sundstrom LE. 2002. Seizure induced dentate neurogenesis does not diminish with age in rats. *Neuroscience letters* 330: 235-8

Harvey AS, Berkovic SF, Wrennall JA, Hopkins IJ. 1997. Temporal lobe epilepsy in childhood: clinical, EEG, and neuroimaging findings and syndrome classification in a cohort with new-onset seizures. *Neurology* 49: 960-8

Hattiangady B, Rao MS, Shetty AK. 2004. Chronic temporal lobe epilepsy is associated with severely declined dentate neurogenesis in the adult hippocampus. *Neurobiology of disease* 17: 473-90

Hattiangady B, Shetty AK. 2008. Implications of decreased hippocampal neurogenesis in chronic temporal lobe epilepsy. *Epilepsia* 49 Suppl 5: 26-41

Heinrich C, Nitta N, Flubacher A, Muller M, Fahrner A, et al. 2006. Reelin deficiency and displacement of mature neurons, but not neurogenesis, underlie the formation of granule cell dispersion in the epileptic hippocampus. *J Neurosci* 26: 4701-13

Hermann BP, Seidenberg M, Bell B. 2000. Psychiatric comorbidity in chronic epilepsy: identification, consequences, and treatment of major depression. *Epilepsia* 41 Suppl 2: S31-41

Houser CR. 1992. Morphological changes in the dentate gyrus in human temporal lobe epilepsy. *Epilepsy research. Supplement* 7: 223-34

Houser CR, Miyashiro JE, Swartz BE, Walsh GO, Rich JR, Delgado-Escueta AV. 1990. Altered patterns of dynorphin immunoreactivity suggest mossy fiber reorganization in human hippocampal epilepsy. *The Journal of neuroscience : the official journal of the Society for Neuroscience* 10: 267-82

Huttmann K, Sadgrove M, Wallraff A, Hinterkeuser S, Kirchhoff F, et al. 2003. Seizures preferentially stimulate proliferation of radial glia-like astrocytes in the adult dentate gyrus: functional and immunocytochemical analysis. *The European journal of neuroscience* 18: 2769-78

Isackson PJ, Huntsman MM, Murray KD, Gall CM. 1991. BDNF mRNA expression is increased in adult rat forebrain after limbic seizures: temporal patterns of induction distinct from NGF. *Neuron* 6: 937-48

Jakubs K, Nanobashvili A, Bonde S, Ekdahl CT, Kokaia Z, et al. 2006. Environment matters: synaptic properties of neurons born in the epileptic adult brain develop to reduce excitability. *Neuron* 52: 1047-59

Jessberger S, Nakashima K, Clemenson GD, Jr., Mejia E, Mathews E, et al. 2007a. Epigenetic modulation of seizure-induced neurogenesis and cognitive decline. *The Journal of neuroscience : the official journal of the Society for Neuroscience* 27: 5967-75

Jessberger S, Romer B, Babu H, Kempermann G. 2005. Seizures induce proliferation and dispersion of doublecortin-positive hippocampal progenitor cells. *Experimental neurology* 196: 342-51

Jessberger S, Zhao C, Toni N, Clemenson GD, Jr., Li Y, Gage FH. 2007b. Seizure-associated, aberrant neurogenesis in adult rats characterized with retrovirus-mediated cell labeling. *The Journal of neuroscience : the official journal of the Society for Neuroscience* 27: 9400-7

Jung KH, Chu K, Kim M, Jeong SW, Song YM, et al. 2004. Continuous cytosine-b-D-arabinofuranoside infusion reduces ectopic granule cells in adult rat hippocampus with attenuation of spontaneous recurrent seizures following pilocarpine-induced status epilepticus. *The European journal of neuroscience* 19: 3219-26

Jung KH, Chu K, Lee ST, Kim J, Sinn DI, et al. 2006. Cyclooxygenase-2 inhibitor, celecoxib, inhibits the altered hippocampal neurogenesis with attenuation of spontaneous recurrent seizures following pilocarpine-induced status epilepticus. *Neurobiology of disease* 23: 237-46

Kempermann G, Gast D, Kronenberg G, Yamaguchi M, Gage FH. 2003. Early determination and long-term persistence of adult-generated new neurons in the hippocampus of mice. *Development* 130: 391-9

Kempermann G, Kuhn HG, Gage FH. 1997. More hippocampal neurons in adult mice living in an enriched environment. *Nature* 386: 493-5

Kim JH, Jang BG, Choi BY, Kwon LM, Sohn M, et al. 2012. Zinc chelation reduces hippocampal neurogenesis after pilocarpine-induced seizure. *PloS one* 7: e48543

Kron MM, Zhang H, Parent JM. 2010. The developmental stage of dentate granule cells dictates their contribution to seizure-induced plasticity. *The Journal of neuroscience : the official journal of the Society for Neuroscience* 30: 2051-9

Kronenberg G, Reuter K, Steiner B, Brandt MD, Jessberger S, et al. 2003. Subpopulations of proliferating cells of the adult hippocampus respond differently to physiologic neurogenic stimuli. *The Journal of comparative neurology* 467: 455-63

Kuhn HG, Dickinson-Anson H, Gage FH. 1996. Neurogenesis in the dentate gyrus of the adult rat: age-related decrease of neuronal progenitor proliferation. *The Journal of neuroscience : the official journal of the Society for Neuroscience* 16: 2027-33

Laplagne DA, Esposito MS, Piatti VC, Morgenstern NA, Zhao C, et al. 2006. Functional convergence of neurons generated in the developing and adult hippocampus. *PLoS biology* 4: e409

Lugert S, Basak O, Knuckles P, Haussler U, Fabel K, et al. 2010. Quiescent and active hippocampal neural stem cells with distinct morphologies respond

selectively to physiological and pathological stimuli and aging. *Cell stem cell* 6: 445-56

Ma DK, Jang MH, Guo JU, Kitabatake Y, Chang ML, et al. 2009. Neuronal activity-induced Gadd45b promotes epigenetic DNA demethylation and adult neurogenesis. *Science (New York, N.Y* 323: 1074-7

Mohapel P, Ekdahl CT, Lindvall O. 2004. Status epilepticus severity influences the long-term outcome of neurogenesis in the adult dentate gyrus. *Neurobiology of disease* 15: 196-205

Morgan RJ, Soltesz I. 2008. Nonrandom connectivity of the epileptic dentate gyrus predicts a major role for neuronal hubs in seizures. *Proceedings of the National Academy of Sciences of the United States of America* 105: 6179-84

Murphy BL, Pun RY, Yin H, Faulkner CR, Loepke AW, Danzer SC. 2011. Heterogeneous integration of adult-generated granule cells into the epileptic brain. *The Journal of neuroscience : the official journal of the Society for Neuroscience* 31: 105-17

Newton SS, Collier EF, Hunsberger J, Adams D, Terwilliger R, et al. 2003. Gene profile of electroconvulsive seizures: induction of neurotrophic and angiogenic factors. *J Neurosci* 23: 10841-51

Overstreet Wadiche L, Bromberg DA, Bensen AL, Westbrook GL. 2005. GABAergic signaling to newborn neurons in dentate gyrus. *Journal of neurophysiology* 94: 4528-32

Overstreet-Wadiche LS, Bromberg DA, Bensen AL, Westbrook GL. 2006. Seizures accelerate functional integration of adult-generated granule cells. *The Journal of neuroscience : the official journal of the Society for Neuroscience* 26: 4095-103

Parent JM, Elliott RC, Pleasure SJ, Barbaro NM, Lowenstein DH. 2006. Aberrant seizure-induced neurogenesis in experimental temporal lobe epilepsy. *Annals of neurology* 59: 81-91

Parent JM, Lowenstein DH. 1997. Mossy fiber reorganization in the epileptic hippocampus. *Current opinion in neurology* 10: 103-9

Parent JM, Lowenstein DH. 2002. Seizure-induced neurogenesis: are more new neurons good for an adult brain? *Progress in brain research* 135: 121-31

Parent JM, Murphy GG. 2008. Mechanisms and functional significance of aberrant seizure-induced hippocampal neurogenesis. *Epilepsia* 49 Suppl 5: 19-25

Parent JM, Tada E, Fike JR, Lowenstein DH. 1999. Inhibition of dentate granule cell neurogenesis with brain irradiation does not prevent seizure-induced mossy fiber synaptic reorganization in the rat. *J Neurosci* 19: 4508-19

Parent JM, Yu TW, Leibowitz RT, Geschwind DH, Sloviter RS, Lowenstein DH. 1997. Dentate granule cell neurogenesis is increased by seizures and contributes to aberrant network reorganization in the adult rat hippocampus. *J Neurosci* 17: 3727-38

Pham K, Nacher J, Hof PR, McEwen BS. 2003. Repeated restraint stress suppresses neurogenesis and induces biphasic PSA-NCAM expression in the adult rat dentate gyrus. *The European journal of neuroscience* 17: 879-86

Piatti VC, Davies-Sala MG, Esposito MS, Mongiat LA, Trinchero MF, Schinder AF. 2011. The timing for neuronal maturation in the adult hippocampus is modulated by local network activity. *J Neurosci* 31: 7715-28

Piatti VC, Esposito MS, Schinder AF. 2006. The timing of neuronal development in adult hippocampal neurogenesis. *The Neuroscientist : a review journal bringing neurobiology, neurology and psychiatry* 12: 463-8

Pierce JP, Melton J, Punsoni M, McCloskey DP, Scharfman HE. 2005. Mossy fibers are the primary source of afferent input to ectopic granule cells that are born after pilocarpine-induced seizures. *Experimental neurology* 196: 316-31

Pun RY, Rolle IJ, Lasarge CL, Hosford BE, Rosen JM, et al. 2012. Excessive activation of mTOR in postnatally generated granule cells is sufficient to cause epilepsy. *Neuron* 75: 1022-34

Raedt R, Boon P, Persson A, Alborn AM, Boterberg T, et al. 2007. Radiation of the rat brain suppresses seizure-induced neurogenesis and transiently enhances excitability during kindling acquisition. *Epilepsia* 48: 1952-63

Rao MS, Hattiangady B, Shetty AK. 2008. Status epilepticus during old age is not associated with enhanced hippocampal neurogenesis. *Hippocampus* 18: 931-44

Ribak CE, Tran PH, Spigelman I, Okazaki MM, Nadler JV. 2000. Status epilepticus-induced hilar basal dendrites on rodent granule cells contribute to recurrent excitatory circuitry. *The Journal of comparative neurology* 428: 240-53

Santarelli L, Saxe M, Gross C, Surget A, Battaglia F, et al. 2003. Requirement of hippocampal neurogenesis for the behavioral effects of antidepressants. *Science (New York, N.Y* 301: 805-9

Scharfman HE, Goodman JH, Sollas AL. 2000. Granule-like neurons at the hilar/CA3 border after status epilepticus and their synchrony with area CA3 pyramidal

cells: functional implications of seizure-induced neurogenesis. *J Neurosci* 20: 6144-58

Scharfman HE, Gray WP. 2007. Relevance of seizure-induced neurogenesis in animal models of epilepsy to the etiology of temporal lobe epilepsy. *Epilepsia* 48 Suppl 2: 33-41

Seress L. 1992. Morphological variability and developmental aspects of monkey and human granule cells: differences between the rodent and primate dentate gyrus. *Epilepsy research. Supplement* 7: 3-28

Seress L, Pokorny J. 1981. Structure of the granular layer of the rat dentate gyrus. A light microscopic and Golgi study. *Journal of anatomy* 133: 181-95

Seri B, Garcia-Verdugo JM, Collado-Morente L, McEwen BS, Alvarez-Buylla A. 2004. Cell types, lineage, and architecture of the germinal zone in the adult dentate gyrus. *The Journal of comparative neurology* 478: 359-78

Shapiro LA, Figueroa-Aragon S, Ribak CE. 2007. Newly generated granule cells show rapid neuroplastic changes in the adult rat dentate gyrus during the first five days following pilocarpine-induced seizures. *The European journal of neuroscience* 26: 583-92

Shapiro LA, Korn MJ, Ribak CE. 2005. Newly generated dentate granule cells from epileptic rats exhibit elongated hilar basal dendrites that align along GFAP-immunolabeled processes. *Neuroscience* 136: 823-31

Shapiro LA, Ribak CE. 2006. Newly born dentate granule neurons after pilocarpine-induced epilepsy have hilar basal dendrites with immature synapses. *Epilepsy research* 69: 53-66

Sibbe M, Haussler U, Dieni S, Althof D, Haas CA, Frotscher M. 2012. Experimental epilepsy affects Notch1 signalling and the stem cell pool in the dentate gyrus. *The European journal of neuroscience* 36: 3643-52

Snyder JS, Choe JS, Clifford MA, Jeurling SI, Hurley P, et al. 2009. Adult-born hippocampal neurons are more numerous, faster maturing, and more involved in behavior in rats than in mice. *J Neurosci* 29: 14484-95

Suh H, Consiglio A, Ray J, Sawai T, D'Amour KA, Gage FH. 2007. In vivo fate analysis reveals the multipotent and self-renewal capacities of Sox2+ neural stem cells in the adult hippocampus. *Cell stem cell* 1: 515-28

Sutula T, Cascino G, Cavazos J, Parada I, Ramirez L. 1989. Mossy fiber synaptic reorganization in the epileptic human temporal lobe. *Annals of neurology* 26: 321-30

Sutula TP, Dudek FE. 2007. Unmasking recurrent excitation generated by mossy fiber sprouting in the epileptic dentate gyrus: an emergent property of a complex system. *Progress in brain research* 163: 541-63

Tashiro A, Makino H, Gage FH. 2007. Experience-specific functional modification of the dentate gyrus through adult neurogenesis: a critical period during an immature stage. *J Neurosci* 27: 3252-9

Teixeira CM, Kron MM, Masachs N, Zhang H, Lagace DC, et al. 2012. Cell-autonomous inactivation of the reelin pathway impairs adult neurogenesis in the hippocampus. *The Journal of neuroscience : the official journal of the Society for Neuroscience* 32: 12051-65

Thind KK, Ribak CE, Buckmaster PS. 2008. Synaptic input to dentate granule cell basal dendrites in a rat model of temporal lobe epilepsy. *The Journal of comparative neurology* 509: 190-202

Thind KK, Yamawaki R, Phanwar I, Zhang G, Wen X, Buckmaster PS. 2010. Initial loss but later excess of GABAergic synapses with dentate granule cells in a rat model of temporal lobe epilepsy. *The Journal of comparative neurology* 518: 647-67

Toni N, Laplagne DA, Zhao C, Lombardi G, Ribak CE, et al. 2008. Neurons born in the adult dentate gyrus form functional synapses with target cells. *Nature neuroscience* 11: 901-7

Toni N, Teng EM, Bushong EA, Aimone JB, Zhao C, et al. 2007. Synapse formation on neurons born in the adult hippocampus. *Nature neuroscience* 10: 727-34

Tozuka Y, Fukuda S, Namba T, Seki T, Hisatsune T. 2005. GABAergic excitation promotes neuronal differentiation in adult hippocampal progenitor cells. *Neuron* 47: 803-15

van Praag H, Christie BR, Sejnowski TJ, Gage FH. 1999. Running enhances neurogenesis, learning, and long-term potentiation in mice. *Proceedings of the National Academy of Sciences of the United States of America* 96: 13427-31

van Praag H, Schinder AF, Christie BR, Toni N, Palmer TD, Gage FH. 2002. Functional neurogenesis in the adult hippocampus. *Nature* 415: 1030-4

van Praag H, Shubert T, Zhao C, Gage FH. 2005. Exercise enhances learning and hippocampal neurogenesis in aged mice. *J Neurosci* 25: 8680-5

von Campe G, Spencer DD, de Lanerolle NC. 1997. Morphology of dentate granule cells in the human epileptogenic hippocampus. *Hippocampus* 7: 472-88

Walter C, Murphy BL, Pun RY, Spieles-Engemann AL, Danzer SC. 2007. Pilocarpine-induced seizures cause selective time-dependent changes to adult-generated hippocampal dentate granule cells. *The Journal of neuroscience : the official journal of the Society for Neuroscience* 27: 7541-52

Warner-Schmidt JL, Duman RS. 2007. VEGF is an essential mediator of the neurogenic and behavioral actions of antidepressants. *Proceedings of the National Academy of Sciences of the United States of America* 104: 4647-52

Waterhouse EG, An JJ, Orefice LL, Baydyuk M, Liao GY, et al. 2012. BDNF promotes differentiation and maturation of adult-born neurons through GABAergic transmission. *J Neurosci* 32: 14318-30

Wood JC, Jackson JS, Jakubs K, Chapman KZ, Ekdahl CT, et al. 2011. Functional integration of new hippocampal neurons following insults to the adult brain is determined by characteristics of pathological environment. *Experimental neurology* 229: 484-93

Yu TS, Zhang G, Liebl DJ, Kernie SG. 2008. Traumatic brain injury-induced hippocampal neurogenesis requires activation of early nestin-expressing progenitors. *J Neurosci* 28: 12901-12

Zhan RZ, Timofeeva O, Nadler JV. 2010. High ratio of synaptic excitation to synaptic inhibition in hilar ectopic granule cells of pilocarpine-treated rats. *Journal of neurophysiology* 104: 3293-304

Zhang W, Huguenard JR, Buckmaster PS. 2012. Increased excitatory synaptic input to granule cells from hilar and CA3 regions in a rat model of temporal lobe epilepsy. *The Journal of neuroscience : the official journal of the Society for Neuroscience* 32: 1183-96

Zhang W, Yamawaki R, Wen X, Uhl J, Diaz J, et al. 2009. Surviving hilar somatostatin interneurons enlarge, sprout axons, and form new synapses with granule cells in a mouse model of temporal lobe epilepsy. *The Journal of neuroscience : the official journal of the Society for Neuroscience* 29: 14247-56

Zhao C, Teng EM, Summers RG, Jr., Ming GL, Gage FH. 2006. Distinct morphological stages of dentate granule neuron maturation in the adult mouse hippocampus. *The Journal of neuroscience : the official journal of the Society for Neuroscience* 26: 3-11

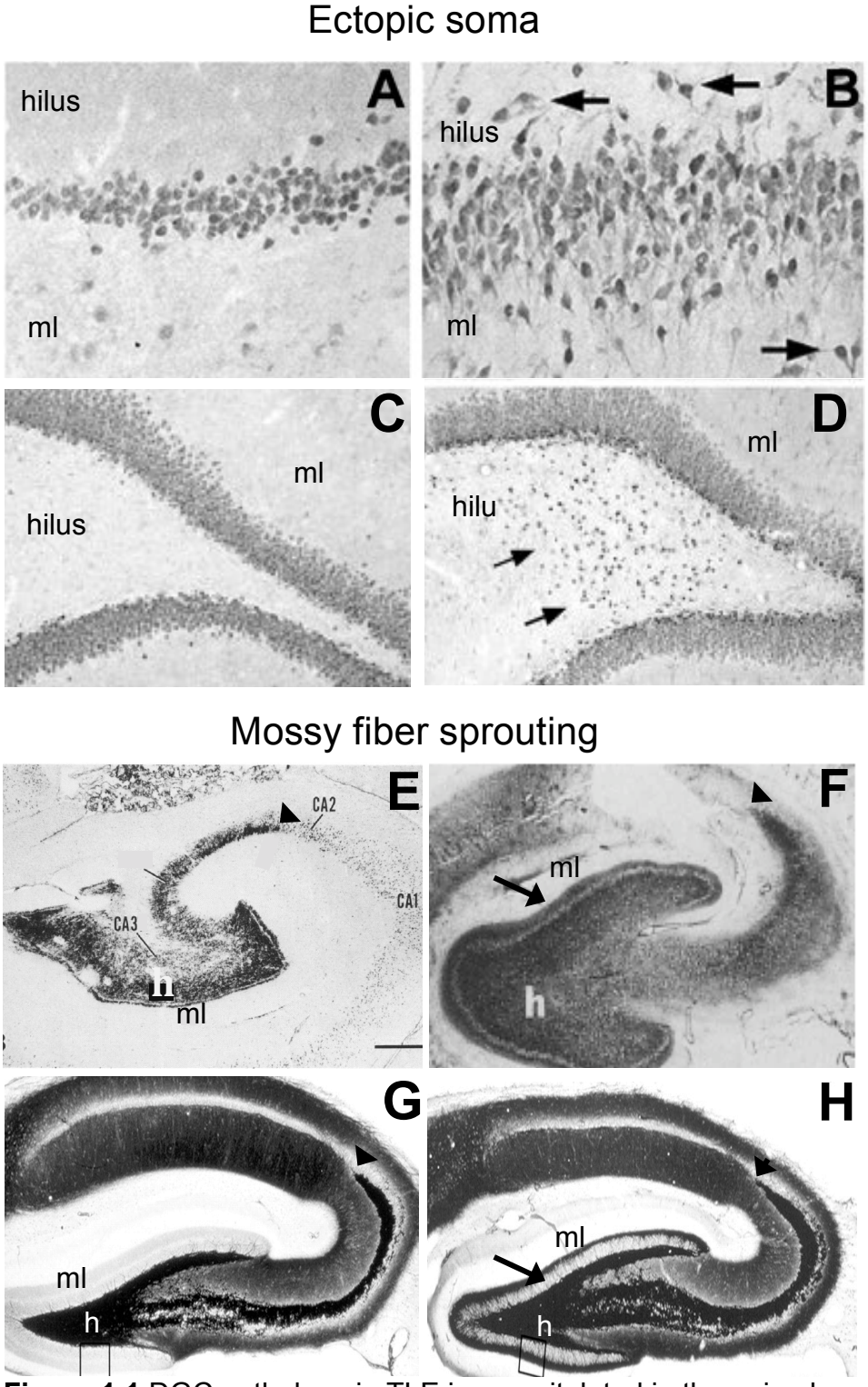

Figure 1.1 DGC pathology in TLE is recapitulated in the animal model. **A-D.** Images showing ectopic location of DGC cell bodies in the dentate gyrus of human TLE and rat model tissue compared with control. Arrows indicate ectopic DGCs. **A.** DGCs labeled for neuronal nuclear protein (NeuN) in the GCL of a control human tissue section. **B.** DGCs labeled for NeuN in the GCL and hilus

and molecular layer (ml) of TLE patient tissue section. Arrows show hilar and molecular layer DGCs. **C.** DGCs labeled for DGC specific marker prospero homeobox-1 (prox-1) in the GCL of a sham-treated rat tissue section. **D.** DGCs labeled for prox-1 in the GCL and hilus of an epileptic rat tissue section. Arrows indicate hilar ectopic DGCs. Images from A-D were reproduced from (Parent et al 2006).
E-F. Images showing MFS in the inner molecular layer of tissue from human TLE and rat model tissue compared with control. Mossy fibers were labeled with Timm's stain. Arrows indicate MFS in the IML, arrowheads indicate termination of mossy fiber axons in CA2. **E.** Sample image of a region of dentate gyrus from healthy human tissue that lacks MFS in the IML. **F.** Section of human hippocampus showing MFS in the IML. **G.** Tissue section from a sham-treated rat which lacks MFS in the IML. **F.** Tissue section from an epileptic rat with MFS in the IML. Image from E was reproduced from (Houser et al 1990) Image from F was reproduced from (Sutula et al 1989). Images from G and H were reproduced from (Buckmaster et al 2002).

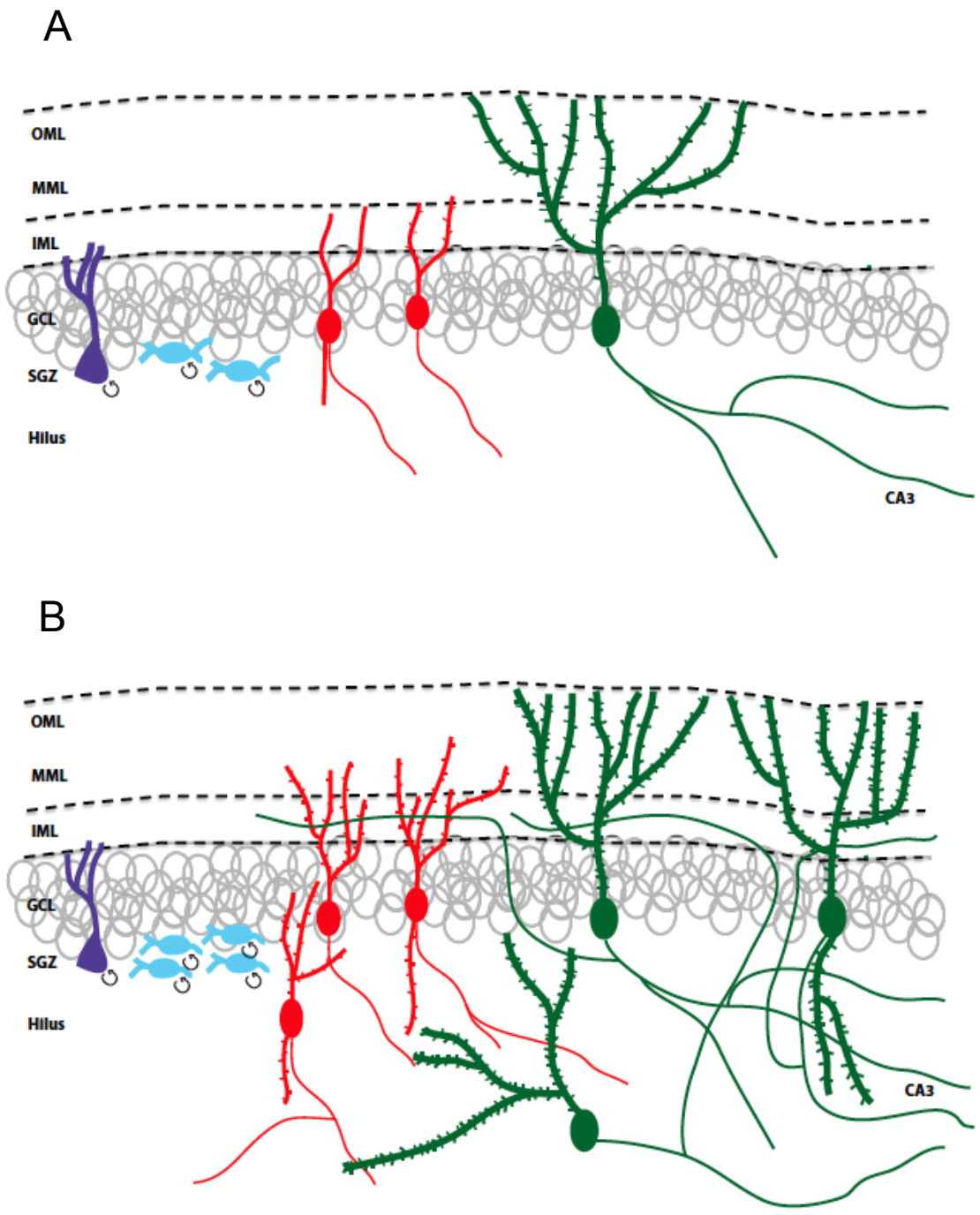

Figure 1.2 Schematic images of NSC and DGC organization within the intact (**A**) or epileptic (**B**) adult dentate gyrus. Purple structure represents a radial glia-like stem cell, blue represents amplifying neural progenitors, red represents immature DGCs, and green represents mature DGCs. OML = outer molecular layer, MML = middle molecular layer, IML = inner molecular layer, GCL = granule cell layer,

SGZ = subgranular zone. **A.** In an intact animal, the radial glia-like stem cell and amplifying progenitors are present in the SGZ. Radial glia-like cells are relatively quiescent and unlikely to be dividing at any given time. Amplifying progenitors are a relatively proliferative population and more likely to be dividing. Immature neurons are beginning to develop processes and may have a transient hilar basal dendrite, but it does not receive synaptic input. Mature DGCs, including those born in adulthood, have fully arborized dendritic trees that extend to the outer molecular layer and mossy fiber axons that branch in the hilus and extend out to area CA3. **B**. In an animal with epilepsy, radial glia-like stem cells may be activated early after SE in some models, but still generally remain quiescent. Amplifying progenitors, however, are commonly upregulated by seizure activity in many models. Immature neurons develop more rapidly, showing longer processes and more dendritic spines. Some immature neurons migrate ectopically into the hilus, where they remain throughout maturity. Once the cells mature, they may retain hilar basal dendrites, persist ectopically in the hilus, or sprout mossy fiber axons into the inner molecular layer.

Chapter 2

Intrinsic neurophysiological properties of hilar ectopic and normotopic dentate granule cells in human temporal lobe epilepsy and a rat model

Summary

Hilar ectopic dentate granule cells (DGCs) are a salient feature of aberrant plasticity in human temporal lobe epilepsy (TLE) and most rodent models of the disease. Recent evidence from rodent TLE models suggests that hilar ectopic DGCs contribute to hyperexcitability within the epileptic hippocampal network. Here we investigate the intrinsic excitability of DGCs from humans with TLE and the rat pilocarpine TLE model with the objective of comparing the neurophysiology of hilar ectopic DGCs to their normotopic counterparts in the granule cell layer (GCL). We recorded from 36 GCL and 7 hilar DGCs from human TLE tissue. Compared to GCL DGCs, hilar DGCs in patient tissue exhibited lower action potential (AP) firing rates, more depolarized AP threshold, and differed in single AP waveform, consistent with an overall decrease in excitability. To evaluate the intrinsic neurophysiology of rat hilar ectopic DGCs, we made recordings from retrovirus-birthdated, adult-born DGCs 2-4 months after pilocarpine-induced status epilepticus (SE) or sham treatment. Hilar DGCs from epileptic rats exhibited higher AP firing rates than normotopic DGCs from epileptic or control animals. They also displayed more depolarized resting

membrane potential and wider AP waveforms, indicating an overall increase in excitability. The contrasting findings between disease and disease model may reflect differences between the late stage disease tissue available from human surgical specimens and the earlier disease stage examined in the rat TLE model. These data represent the first neurophysiological characterization of ectopic DGCs from human hippocampus and prospectively birthdated ectopic DGCs in a rodent TLE model. They provide novel evidence for alterations in intrinsic excitability of aberrantly integrated DGCs in TLE, and highlight potentially important differences between the human disease and a commonly used disease model.

Introduction

Temporal lobe epilepsy (TLE) is the most common type of medically intractable epilepsy (Ramey et al 2013). The mechanisms of TLE pathogenesis are not well understood, but the hippocampus is widely believed to be a critical structure for seizure development and progression. In some cases, patients with refractory TLE undergo surgical resection of the affected tissue, including the hippocampus, as a means of seizure suppression. This procedure provides the unique opportunity to study the neurophysiology of living human brain tissue. Previous work has demonstrated that resected hippocampal tissue from TLE patients displays physiological features consistent with hyperexcitability (Dietrich et al 1999, Franck et al 1995, Selke et al 2006, Surges et al 2012).

The hippocampal dentate gyrus is strongly implicated in epileptogenesis, largely because of its well-documented plasticity in TLE. Aberrant plasticity such as mossy fiber sprouting, persistent hilar basal dendrites, and ectopic location of adult-born dentate granule cells (DGCs) have all been implicated in hyperexcitability and have been described in both human and experimental TLE (de Lanerolle et al 1989, Houser et al 1990, Parent et al 2006, Scharfman & Gray 2007, Sutula et al 1989, von Campe et al 1997). Recent work suggests that, in rodent TLE models, hilar ectopic DGCs represent the subset of DGCs most predisposed to hyperexcitability in the epileptic network (Scharfman et al 2000, Scharfman & Pierce 2012, Zhan et al 2010). However, the intrinsic neurophysiology of hilar ectopic DGCs has not been studied in human tissue, nor has it been thoroughly characterized in rodent models. In this study, we compare intrinsic excitability of hilar ectopic DGCs to normotopic DGCs (those in the granule cell layer; GCL) from human TLE tissue. We also compare birthdated hilar ectopic and normotopic DGCs in the rat pilocarpine status epilepticus (SE) model to assess alterations in intrinsic excitability in a more controlled experimental paradigm.

Methods

Human tissues acquisition

Surgical specimens were obtained from 24 patients (9 male, 15 female) ages 19-57 years at surgery (mean 37.7 ± 11.4), with mean epilepsy duration of 18.1 ±

12.1 years. All patients had a history of failed antiepileptic drug (AED) treatment, and 22 of the 24 were being treated by one or more of the following drugs at the time of surgery: lamotrigine, valproic acid, phenytoin, levetiracetam, zonisamide, carbamazepine, oxcarbazepine, phenobarbital, clonazepam, lorazepam, gabatril, felbamate, topiramate, lacosamide, and gabapentin. Only two subjects had their AEDs tapered at the time of surgery. All patients participated after informed consent, in accordance with the University of Michigan Institutional Review Board.

Animals

Animal procedures were performed using protocols approved by the University Committee on Use and Care of Animals of the University of Michigan. Animals were purchased from Charles River and kept under a constant 12 hour light/dark cycle with access to food and water *ad libitum.* Epileptic animals and sham controls were generated as described previously (Kron et al 2010). Briefly, eight week-old male Sprague Dawley rats were pretreated with atropine methylbromide (5 mg/kg i.p.; Sigma-Aldrich, St. Louis, MO) 20 minutes prior to pilocarpine hydrochloride (340 mg/kg i.p.; Sigma-Aldrich, St. Louis, MO) for epileptic animals, or an equivalent volume of 0.9% saline for sham animals. After 90 minutes of SE, seizures were terminated with diazepam (10 mg/kg i.p.; Hospira Inc, Lake Forest, IL). In our hands, 90% (by observation) to 100% (by video/EEG recording) of animals treated according to this protocol exhibit spontaneous behavioral seizures after at least 1 week of recovery. Sham

controls were treated with diazepam two hours after the saline injection. Four days after SE/sham treatment, animals were injected with green fluorescent protein (GFP)-expressing retrovirus (RV) bilaterally into the dentate gyrus as described previously (Kron et al 2010). Acute slice recordings were made 2-4 months after SE/sham treatment.

Slice preparation (Human)

Tissue was acquired in the operating room from subjects undergoing anterior temporal lobectomy with amygdalo-hippocampectomy or selective amygdalo-hippocampectomy for medically refractory epilepsy. Clinical evaluation to localize the region of seizure onsets included neuroimaging and video-electroencephalographic ictal recordings with scalp and, in some cases, intracranial electrodes. During surgery, care was taken to maintain hippocampal perfusion until it was resected en bloc and immediately placed in ice cold Hibernate A (Brain Bits, LLC, Springfield IL). All reagents for the following solutions were obtained from Fisher Scientific, Fair Lawn, NJ unless otherwise specified. The tissue was transferred on ice as quickly as possible (5-7 minutes) back to the laboratory where it was transferred to ice cold, oxygenated, cutting solution containing (in mM): 206 sucrose, 2.8 KCl, 1 $MgCl_2 \bullet 6H_2O$, 1.25 NaH_2PO_4, 1 $CaCl_2$, 10 D-Glucose, 26 $NaHCO_3$, 0.4 Ascorbic Acid (pH 7.4). Slices (400 μm thickness) were cut perpendicular to the anterior-posterior axis with a vibrating blade microtome (VT1000S, Leica Microsystems Inc, Buffalo Grove, IL), allowed to recover for 15 minutes in 34^0C, oxygenated N-methyl D-

glutamine (NMDG) based solution containing (in mM): 92 NMDG (Sigma Aldrich St. Louis, MO), 2.5 KCl, 1.2 NaH_2PO_4, 30 $NaHCO_3$, 20 HEPES, 25 Glucose, 5 sodium ascorbate (Sigma Aldrich St. Louis, MO), 2 thiourea (Sigma, Aldrich St. Louis, MO), 3 sodium pyruvate (Gibco Life Technologies, Grand Island, NY), 10 $MgSO_4 \bullet 7H_2O$ (Sigma Aldrich, St. Louis, MO), 0.5 $CaCl_2 \bullet 2H_2O$. (pH adjusted to 7.35 with 10N HCl). We find that recovery in this solution provides a significant improvement in the health of slices made from both rat and human tissue (Zhao et al 2011). Slices were then rested for at least 1 hour at RT in aCSF containing (in mM): 124 NaCl, 2.8 KCl, 2 $MgSO_4$, 1.25 NaH_2PO_4, 2 $CaCl_2$, 10 D-Glucose, 26 $NaHCO_3$, 0.4 Ascorbic acid (pH 7.4) before being transferred individually to the recording chamber and continuously perfused (~1.5mL/min) with oxygenated aCSF heated to 32^0C.

Slice preparation (Rodent)

Animals were anesthetized with isoflourane (Vet One, Boise, ID) and transcardially perfused with ice-cold cutting solution (as above) for 60 seconds. After decapitation, brains were rapidly removed and rested for 2 minutes in ice cold, oxygenated cutting solution. Brains were then blocked to isolate the hippocampus and 400 μm-thick sections were cut in the coronal plane with a vibrating blade microtome (VT1000S, Leica Microsystems Inc, Buffalo Grove, IL) in ice cold, oxygenated cutting solution, and from that point on were treated identically to human tissue slices.

Electrophysiological recordings and analysis

Cells were visualized using epifluorescence and infrared differential interference contrast (IR-DIC) optics. For human neurons, only IR-DIC was used to visualize and patch. Rodent GFP+ DGCs were first identified under epifluorescence (525 nm emission filter), then visualized and patched using IR-DIC. Whole cell current clamp recordings were obtained using borosilicate glass electrodes (Sutter Instruments, Novato, CA) with a 4-7 MΩ open tip resistance. Pipettes contained 0.3% biocytin (Sigma Aldrich, St. Louis, MO) in internal solution made with either (in mM): 120 potassium methyl sulfate (Sigma Aldrich, St. Louis, MO) or 120 potassium gluconate (Sigma Aldrich, St. Louis, MO), and 20 KCl, 10 HEPES, 0.2 EGTA, 2 $MgCl•6H_2O$, 4 Na_2 ATP, 0.3 Tris-GTP, 7 phosphocreatine, pH adjusted to 7.25 with KOH. Recordings were obtained using a Dagan Cornerstone amplifier (Minneapolis, MN) in bridge mode, filtered at 2 kHz and digitized at 10 kHz. Data were acquired using pClamp 10.0. Synaptic stimuli were delivered via a glass theta electrode filled with aCSF and positioned in the molecular layer.

Seal resistances of >1 GΩ were achieved before breaking into whole cell mode. Resting membrane potential (RMP) was determined in each cell immediately after break in. Each neuron was sequenced through a series of current clamp protocols to determine input resistance, sag ratio, spike frequency accommodation (SFA), action potential (AP) properties, and post-burst slow afterhyperpolarization (sAHP). Sag was determined by injecting hyperpolarizing steps to -0.1 pA and calculated as the ratio of the steady state response over the

peak negative potential. To measure AP threshold and spike properties, short (10 ms) current steps were delivered at increasing amplitudes of 15 pA until a single AP was elicited. Threshold was defined as the membrane potential measured just before the spike upstroke. Spike height was measured from threshold to peak, and half-width was defined as the width (in ms) of the spike at half maximal height. Input resistance and spike train firing properties were assessed by longer intracellularly injected current steps (-150 pA to 500 pA, 500 or 1000 ms). Input resistance was determined by the slope of the linear portion of the V/I plot generated by all traces that did not contain AP firing. SFA index was determined in traces that contained 4 or more APs by dividing the interspike intervals by the interspike interval of the first two spikes in a given train. Cells were not all driven by the same levels of injected current. As a result, firing frequency of each group was determined by generating scatter plots of the data for every cell and fitting each data set with a Poisson regression line through the origin.

In a subset of cells, sAHP was measured by eliciting 5 or 6 APs in a 100 ms time period, with cells either at their resting potential or held at 5 mV below AP threshold. The magnitude of the sAHP was then determined by comparing the membrane potential immediately prior to the 100 ms current injection with the membrane potential 1 second after the end of the current step. Synaptic input was also assessed in a subset of cells by placing a stimulating electrode in the molecular layer and delivering stimulations of increasing magnitude, to elicit maximum EPSP response or AP firing in the post-synaptic cell.

Immunohistochemistry

Following recording, slices were immediately placed in 4% paraformaldehyde (Sigma Aldrich, St. Louis, MO) in phosphate buffered saline (PBS) (pH 7.4), and refrigerated for up to 1 week. For biocytin visualization, slices were rinsed with PBS and endogenous peroxidase activity was quenched with 0.1% hydrogen peroxide in 10% methanol and PBS. After a second wash in PBS, slices were permeabilized with 2% Triton X-100 (Sigma Aldrich, St. Louis, MO) in PBS and then incubated at room temperature in avidin/biotinylated enzyme complex (Vector Labs, Burlingame, CA). After 1-2 days, slices were rinsed with PBS and then reacted with 3,3'-Diaminobenzidine (Invitrogen, Grand Island, NY) until the cells could be visualized. Slices were slide-mounted before cresyl violet counterstaining and coverslipping. Images were acquired on a Leica DSM-IRB inverted microscope (Leica Microsystems Inc, Buffalo Grove, IL) connected to a SPOT Flex digital camera (SPOT Imaging Solutions, Sterling Heights, MI).

Statistics

Off-line analysis was completed in Clampfit and statistical comparisons were made using GraphPad Prism 6 software. RMP, input resistance, sag ratio, AP threshold, AP spike height, and AP half-width were compared between groups using one way ANOVA with Tukey's post-hoc test for multiple comparisons. Data are presented as mean +/- SEM with the significance level set at $p < 0.05$. SFA distribution and single AP type distribution were compared

between groups using Fisher's Exact test with the significance level set at $p < 0.05$. Data are presented as contingency histograms. The slopes of the lines describing AP firing rate were generated using the nonlinear regression, line through the origin function in Prism. The best-fit values for slope were compared using the extra sum of squares F test with the significance level set at $p < 0.05$. Mean amplitudes of sAHP were compared using unpaired student's t-test (human) or one way ANOVA (rodent), with data presented as mean +/- SEM and the significance level set at $p < 0.05$.

Results

In the present study we investigated intrinsic neurophysiological properties of DGCs in tissue resected from subjects with intractable TLE, as well as from pilocarpine or sham treated rats. Results from cells in human tissue are discussed first, followed by results from rodent cells.

Differentiating DGCs from interneurons.

We used a set of neurophysiological criteria to distinguish DGCs from dentate interneurons, and DGC morphology and cell location were confirmed with biocytin staining in a subset of cases (**Figure 2.1**). Intrinsic membrane properties are reported in **Table 2.1**. Neurophysiological characteristics that identify DGCs include SFA, a hyperpolarized RMP (more negative than -60mV), and lack of sag current (Fournier & Crepel 1984, Fricke & Prince 1984, Staley et

al 1992). A SFA index value was calculated for each cell that fired at least four APs in response to depolarizing current steps (**Figure 2.2**). This value is approximately 1 for cells that do not accommodate and becomes larger as the degree of accommodation increases. In our data set, 6 cells showed no accommodation (SFA index 0.9-1.2), and were therefore classified as interneurons (**Figure 2.2A$_3$**). An additional 5 cells exhibited weak accommodation (SFA index 2.0-3.0), but had other features that did not fit the electrophysiological profile of a DGC, such as obvious sag current and depolarized RMP (less negative than -60mV). These cells were also classified as interneurons; all 11 cells were excluded from further analysis. The remaining 43 cells in this data set fit the neurophysiological criteria for DGCs.

Spike frequency accommodation

Pro-excitatory changes in SFA have been reported in DGCs from human TLE tissue (Dietrich et al 1999). In fact, it has been suggested that DGCs with a reduced SFA are an aberrant subpopulation of DGCs in TLE (Selke et al 2006). Since ectopic location also defines an aberrant subpopulation of DGCs that is thought to be pro-excitatory (Hester & Danzer 2013, Scharfman et al 2000, Zhan et al 2010), we asked whether ectopic DGCs show reduced SFA compared to normotopic DGCs in the GCL. We calculated SFA index values for all cells that fired 4 or more APs within a single current step; 17 GCL and 4 hilar neurons displayed strong accommodation (index value ≥ 3.0: **Figure 2.2 A$_1$**, **B**), 9 GCL and 2 hilar neurons displayed weak accommodation (index value 2.0-3.0: **Figure**

2.2 A_2, **B**). However, SFA index could not be calculated for 10 GCL and 1 hilar cells, which are called “low-firing” neurons because they could not be induced to fire more than 3 APs in response to prolonged injected current (**Figure 2.2 A_4**). We observed no significant difference ($p = 0.75$, Fisher’s Exact test) in the distribution of firing patterns between DGCs in the hilus or the GCL (**Figure 2.2 C**).

Firing frequency

A common method of assessing intrinsic excitability is to measure the number of APs fired by a cell in response to somatic current injection. We delivered current steps of increasing magnitude to DGCs in the hilus and GCL and compared their responses. There was considerable variation in the AP firing response and amount of injected current required to drive AP firing in individual DGCs, regardless of cell location. Poisson regression lines through the data from each group revealed that DGCs in the hilus exhibited a modest but statistically significant reduction in firing rates when compare to DGCs in the GCL (slope of 0.01 ± 0.0014 vs. 0.023 ± 0.0012 respectively; $p < 0.0001$, extra sum of squares F test; **Figure 2.3**).

Post-burst afterhyperpolarization

Dentate granule neurons exhibit a post-burst AHP (Podlogar & Dietrich 2006, Tanner et al 2011), and the slow component (sAHP) is thought to regulate firing rate and SFA in neurons (Faber & Sah 2003). Therefore, we hypothesized

that the sAHP would be larger in ectopic relative to normotopic DGCs, and that this might account for the decreased firing frequency observed in ectopic DGCs. Subsets of cells (6 in the hilus and 30 in the GCL) were driven to fire at 50 Hz for 100 ms. The sAHP was measured at 1000 ms after the offset of the current step. Notably, it has been suggested that DGCs in human tissue from TLE patients do not exhibit a sAHP (Dietrich et al 1999). While we did not observe sAHP in 30% of cells tested, we did record a sAHP of at least -0.27 mV amplitude in the majority of cells. However, there was no difference in the mean sAHP amplitude between the two groups ($p = 0.76$, unpaired t-test) (**Figure 2.4**). We observed some heterogeneity in the post-burst AHP waveform among DGCs, but there was also no difference in the amplitude of the medium AHP (measured at 250 ms after the current offset) between the two groups ($p = 0.83$, unpaired t-test) (**Figure 2.4**).

Individual action potential waveform

Although several reports have described the repetitive firing properties of human DGCs, there is relatively little data carefully evaluating single AP waveforms. Therefore, we investigated the properties of individual APs by eliciting a single spike with a 10 ms current injection at the AP threshold (**Figure 2.5**). We observed two distinct shapes of AP traces: APs with (**Figure 2.5 A_1**) or without (**Figure 2.5 A_2**, **A_3**) an afterdepolarization (ADP). Both AP waveforms were observed in cells in the GCL, with a majority of GCL cells exhibiting an ADP. However, AP traces from cells recorded in the hilus (**Figure 2.5 B**) all

lacked ADP. In a subset of cells in both the hilus and GCL, molecular layer stimulation could drive a cell to fire a single AP. Interestingly, we observed distinct AP shapes with this type of stimulation as well (**Figure 2.5 C_1**, **C_2**).

sAHP amplitude and disease duration

Hilar ectopic DGCs have been shown in multiple animal models of TLE to exhibit anatomical and physiological features of disease-related plasticity (Althaus & Parent 2014, Parent & Murphy 2008). By comparing recordings from ectopic DGCs to normotopic DGCs, we identified neurophysiological features that we believe are likely to represent disease-related plasticity in human TLE. These features include reduced firing frequency in response to injected current, a higher AP threshold, and an AP waveform without an ADP. Since the tissue included in this study came from patients with a wide range of disease duration (time from clinical diagnosis of TLE to surgical resection of 18.78 ± 12.10 years), we examined whether disease duration correlated with differences in these neurophysiological features. Using Pearson correlation analysis, we found no correlation between the patients' disease duration and sAHP amplitude (R^2 = 0.033, p = 0.29), firing rate (R^2 = 0.039, p = 0.40), SFA index (R^2 = 0.00057, p = 0.91) or ADP amplitude (R^2 = 0.040, p = 0.24). However, in the absence of control tissue (e.g. from patients with extrahippocampal, nonepileptic lesions) we have limited ability to determine whether the observed differences are caused by disease-related plasticity in a subpopulation of DGCs, normal biological variability, or uncontrolled variables in our sample population.

Neurophysiology of ectopic DGCs in a rodent TLE model

To study mechanistic questions of DGC abnormalities in TLE under more controlled conditions, we turned to the pilocarpine-induced status epilepticus (SE) model in adult male rats. This model allows comparison to non-seizure controls and avoids confounds present for human tissue. These confounds include variability in age of seizure onset and severity, medication history, gender, and birthdates of individual DGCs. DGCs are generated in the human and rodent brain throughout adulthood and into senescence (Eriksson et al 1998, Kuhn et al 1996). In rodent models of TLE, DGC age at the onset of epileptogenesis is a critical factor in determining the cell's response to the insult. Cells that are born after the epileptogenic insult show the greatest degree of morphological disease-related plasticity, and are the only DGCs that migrate ectopically (Jessberger et al 2007, Kron et al 2010, Walter et al 2007). Using the rodent model and retroviral reporter labeling to birthdate and prospectively identify specific DGC cohorts, we directly compared hilar ectopic DGCs with normotopic DGCs that were the same age with respect to SE, as well as to similar aged, birthdated cells in intact tissue.

Confirming DGC identity

In animals that underwent SE, GFP labeled cells (Kron et al 2010) were patched from throughout the GCL and the hilus. In sham treated animals, fluorescent cells were only present in the GCL. In a subset of experiments, DGC

morphology and location was confirmed with biocytin staining (**Figure 2.6 A**, **B**). All cells that were patched in rodent tissue exhibited neurophysiological features characteristic of DGCs including SFA, hyperpolarized RMP, and lack of sag current (**Table 2**). In a subset of sham treated animals, GFP-negative cells were patched from the GCL to determine whether the RV labeling affected the cells' intrinsic properties. We found that GFP-negative cells (n = 13) exhibited RMP of -75.79 ± 1.340, IR of 302.57 ± 33.30, were mostly low firing (10 out of 13), and had a prominent ADP. The values for GFP-negative cells were not significantly different from those of GFP-positive cells from sham animals ($p > 0.05$ for RMP and $p > 0.05$ for R_{in}, student's t-test). These data suggest that the RV-GFP does not alter the intrinsic neurophysiological properties of DGCs that were measured in this study.

Firing behavior in response to injected current steps

In total, we made successful recordings from 45 RV-GFP-labeled DGCs in SE rats and 6 labeled cells from sham treated rats. Most DGCs (n=30) from all groups were low firing (i.e. fired 3 AP or less even at the maximal amplitude of injected current). All adult-born DGCs from control tissue fired less than 3 AP in response to this stimulation intensity (**Figure 2.7 A**, **D**). The DGCs from SE tissue that fired 4 or more APs in response to prolonged somatic current injection (n=15) all exhibited strong accommodation, with a SFA index of at least 3.0 (**Figure 2.7 B**). Interestingly, a subset of both normotopic and ectopic cells from pilocarpine-treated animals fired unique AP doublets (**Figure 2.7 C**). These cells

were classified as burst firing because the two APs were within 10 ms of one another and on the same depolarizing envelope (Metz et al 2005). There was no significant difference in the distribution of low firing, strongly accommodating, or burst firing cells between normotopic and ectopic DGCs in pilocarpine-treated animals (**Figure 2.7 D**, p = 0.73 Fisher's Exact test).

Firing frequency in response to somatic current injection

We were surprised to find that ectopic DGCs in human tissue tended to fire fewer APs in response to injected current than normotopic DGCs, although there has been some recent evidence in rats that some cells born after an epileptogenic insult, albeit in the GCL, show an overall reduction in excitability (Jakubs et al 2006). To determine whether hilar DGCs have lower firing rates than their age-matched normotopic counterparts, we compared the firing frequency of hilar ectopic and normotopic DGCs in tissue from rats that experienced SE (**Figure 2.8**). DGCs from sham treated animals were excluded from this analysis because none of these cells fired APs in response to current levels ≤ 130 pA. For each cell, we plotted the number of APs evoked by current injections of increasing amplitudes and fit the data from each group with Poisson regression lines through the origin. In contrast to the data from human TLE patients, ectopic DGCs from epileptic rats displayed modest but significant increased firing rates when compared to their normotopic counterparts (slope 0.032 ± 0.0038 vs 0.017 ± 0.0014 respectively; $p < 0.0001$, extra sum of squares F test).

Post-burst slow afterhyperpolarization

Although sAHP was not a primary determinant of cell firing frequency in human DGCs, we wanted to assess whether the more controlled environment of the rodent tissue might reveal a relationship between sAHP and firing frequency. Post-burst sAHP was recorded in a subset of cells from each group (3 sham, 27 normotopic, 6 ectopic; **Figure 2.9 A**). The waveform of the post-burst AHP in rodent DGCs differed somewhat from that recorded in most human cells, but DGCs in both sham and SE treated rats exhibited a prominent sAHP. In the rodent DGCs, as in human, the mean amplitudes of the sAHP were not significantly different between any of the groups (**Figure 2.9 B**; p = 0.31, one-way ANOVA).

Individual action potential waveform

When individual APs were evoked with brief current injections, we observed two distinct AP shapes in the recordings from rodent cells (**Figure 2.10 A_1**, **A_2**). However, in contrast to what was observed from human DGCs, cells without an ADP were much rarer in the rodent tissue. Only 1 in 6 sham cells, 4 in 38 normotopic, and 1 in 7 hilar cells lacked ADP. There was no difference between ectopic and normotopic DGCs, or between these groups and sham treated DGCs, in the distribution of cells where the AP lacked an ADP (**Figure 10 B**) (p = 0.91,Fisher's exact test). Because ADP size is correlated with burst firing in other cell types (Metz et al 2005), we measured the amplitude of the ADP

relative to RMP at 5 ms after the fast repolarization phase to determine if there was a relationship in our data set between ADP size and burst firing. Interestingly, the mean amplitude of ADP for burst firing cells (25.11 ± 0.84) was significantly larger than the mean ADP amplitude for non-burst firing cells (15.39 ± 1.1) from SE tissue ($p < 0.0001$, unpaired t-test).

Discussion

The goal of this study was to determine whether hilar ectopic DGCs in TLE display altered intrinsic neurophysiological features when compared to normotopic DGCs in the GCL. We examined ectopic DGCs from resected human TLE tissue and from pilocarpine rat TLE model tissue. The recordings from human neurons provided powerful data because they allowed us rare insight into living, diseased human brain function. However, the lack of human control tissue and uncontrolled variables somewhat limited the ability to draw definitive conclusions about the nature of neurophysiological differences observed among human DGCs. Combining human and rodent studies provided greater insight into the likely relationship between intrinsic neurophysiology in human DGCs and epileptogenesis.

The primary findings are that hilar DGCs in hippocampal tissue from epileptic patients tend to fire fewer APs in response to somatic current injection, have a more depolarized AP threshold, and lack an ADP after a single AP. These features all suggest decreased excitability. While this may seem counter-intuitive

because disease-related plasticity is often thought of as being pro-epileptogenic, and therefore pro-excitatory, there is evidence from multiple rodent models for the development of compensatory mechanisms that may reduce excitability after epileptogenesis (Jakubs et al 2006, Peng et al 2013, Zhan & Nadler 2009, Zhang et al 2009). One possible explanation for the lower firing frequency in the human tissue is that ectopic DGCs represent a subset of DGCs that develop compensatory mechanisms to reduce excitability. However, our recordings from rat tissue suggest that hilar DGCs are actually more excitable than their normotopic counterparts, and normotopic DGCs in an SE animal are more excitable than their sham control counterparts. These results are consistent with previous reports suggesting ectopic DGCs from rodent tissue are more active (Dashtipour et al 2001, Scharfman et al 2000, Zhan & Nadler 2009).

This discrepancy between results from human and rodent cells may be due to species related differences, but it could also stem from qualitative differences between the disease and the disease model. The pilocarpine SE model mimics severe epilepsy, but our recordings are made 2-4 months post SE, which is early in the chronic stage. Conversely, the patients who participated in this study had experienced seizures for 18.1 ± 12.3 years and were refractory to multiple anti-seizure medications. Their tissue is likely reflective of the late stage of the disease. Perhaps hilar DGCs exhibit increased excitability early in the course of epilepsy, but over time develop compensatory or homeostatic mechanisms to intrinsically reduce their activity levels. One such mechanism might be a shift toward more depolarized AP threshold, which we observed in

this population. Alternatively, hyperexcitable ectopic DGCs may initially be present during early epileptogenic stages, but might be selectively eliminated over the course of the disease, biasing the surviving population toward hypoexcitability. To our knowledge the intrinsic excitability of hilar ectopic DGCs in late stage rodent model tissue remains unknown, and we believe this is an important area for further research. However, it is important to acknowledge the variability in firing rate among individual cells. In this data set from human tissue, DGCs in the GCL have the capacity to be more excitable than DGCs in the hilus. However, this does not necessarily mean that GCL DGCs increase overall network excitability and hilar cells decrease network excitability. Likewise, it is not necessarily true that only ectopic DGCs from rodent tissue contribute to increased network excitability. Rather, there may be cell autonomous factors, in addition to location, that contribute to the overall role of individual cells in modulating network properties.

The size of the sAHP is thought to play a role in regulating firing frequency in some neurons (Faber & Sah 2003). However, we found no difference in the sAHP amplitude between hilar and GCL DGCs in human, suggesting that the lower firing frequency is not correlated with a larger sAHP. Similarly, we found no relationship between sAHP amplitude and firing frequency in rodent DGCs: there was no significant difference in sAHP amplitude among control, normotopic-SE or ectopic-SE groups, and the sAHP amplitude did not correlate with number of APs generated regardless of cell location.

We observed considerable qualitative variability in the shape of the AHP waveform among human DGCs, which was far less prevalent among rodent DGCs. The AHP of most human DGCs had a fast peak (as seen in Figure 2.4A_1 and A_2), some had a prominent medium peak (as seen in Figure 2.4A_1), and 70% had a slow component. In contrast, the AHP of nearly all rodent DGCs examined lacked discernible fast and middle peaks, but had a slow component (as seen in Figure 2.9A_1–A_3). Our data suggest the possibility of calcium dysregulation as an underlying factor in the observed physiological variability and uncoupling of AHP and firing frequency. Calcium and calcium-activated potassium conductances regulate numerous aspects of neuronal firing, including the post-burst AHP (Faber & Sah 2003). However, the relative heterogeneity among human DGCs – which is not present among rodent DGCs – suggests that these cells experience dysregulated calcium homeostasis in a variety of cell autonomous ways. For example, SK channels are important in some cell types for producing the post-burst mAHP (Faber & Sah 2003), which varies considerably among cells in our data set. BK channels, which also contribute to the AHP (Faber & Sah 2003), are altered in a rodent model of epilepsy (Pacheco Otalora et al 2008). Therefore, it is reasonable to hypothesize that SK and BK channels could both be differentially expressed among individual DGCs.

Previous reports using tissue from human TLE patients have implicated changes in SFA as a feature of disease-related plasticity (Dietrich et al 1999, Selke et al 2006). Non-epileptic rodent and human DGCs (DGCs from tissue that was resected due to tumors) typically exhibit strong accommodation (Selke et al

2006, Staley et al 1992). Dietrich et al. and Selke et al. found that, in human TLE tissue, some DGCs exhibited weak or no SFA, which they attributed to loss of interspike mAHP. We also found that some human DGCs were weakly accommodating; however, we rarely observed interspike mAHPs, even when cells exhibited strong accommodation. Interestingly, there was no difference in distribution of weakly and strongly accommodating cells between hilar and GCL DGCs, suggesting that a weak SFA may not be an identifying feature of the most aberrant subset of DGCs from human TLE tissue. We did, however, find a trend toward a positive correlation (R^2 = 0.115, p = 0.078 Pearson correlation analysis) when we examined the relationship between sAHP and SFA index for individual cells, irrespective of cell location. This suggests that the post-burst sAHP may contribute to regulating SFA in human DGCs in TLE. Interestingly, SFA of rodent DGCs was less heterogeneous; all exhibited strong accommodation or low firing activity. This suggests that a change in SFA is not a necessary feature of an epileptic network. However, it is also possible that altered SFA is an important feature of TLE in humans that the rat pilocarpine model fails to recapitulate.

Hilar DGCs from human TLE hippocampal specimens all exhibited a single AP waveform that lacked a prominent ADP, while the majority of GCL DGCs exhibited an AP waveform with an ADP. Previous work characterizing the AP of DGCs from other species suggested that, under normal conditions, AP waveforms from nearly all DGCs contain a prominent ADP (Aradi & Holmes 1999, Dudek et al 1976, Zhang et al 1993). As such, an AP waveform that lacks ADP may represent a shift from normal neurophysiology. In sham treated rats,

the majority of cells exhibited an AP waveform with a prominent ADP. Interestingly, a comparable percentage of both normotopic and ectopic DGCs from epileptic rodents also exhibited an ADP+ AP waveform. Therefore, the chronic epilepsy phase in rodents does not appear to be associated with an altered DGC ADP following a single AP.

It is important to note that ADP+ and ADP- denote only the most obvious differences in the AP waveforms that we observed. There was considerable qualitative variability in the shape of the AP waveforms within each ADP-defined group, which was most pronounced among DGCs from human tissue. Similar to the variability observed in the human AHP waveforms, we propose that dysregulation of calcium conductances underlies the heterogeneity in AP waveforms from human DGCs. In intact rodents, the ADP is primarily generated by T-type calcium channels (Zhang et al 1993). However, the shape of the ADP can be influenced by other calcium and calcium-activated channels. Using computational modeling to study the complement of calcium and calcium-activated currents that could produce DGC firing behavior, Aradi and Holmes (Aradi & Holmes 1999) confirmed that T-type channels are critical for generating an ADP+ AP waveform, but also found that other combinations of L-type, N-type, BK and SK channels regulated ADP waveforms in ways that closely mimic many of the shapes we observed in the human DGCs. Importantly, calcium is not alone in regulating the ADP. Persistent sodium current can influence the ADP in some cell types, and it is altered in both clinical and experimental TLE (Agrawal et al 2003, Azouz et al 1996, Chen et al 2011, Vreugdenhil et al 2004).

In DGCs from rodent tissue, epilepsy related changes in ADP could be driving the burst firing that we observed in a subset of neurons. About 15% of ectopic and normotopic cells from pilocarpine-treated rat tissue fired AP doublets (in some cases triplets). This type of burst firing has been described previously, but was only found in hilar ectopic DGCs and was thought to be related to dendritic morphology or the age of the individual cell (Zhan & Nadler 2009). Cells born after SE in the rodent model are the most likely to develop aberrant features, and are the only group susceptible to ectopic migration (Kron et al 2010). As a result, the ectopic cells from the prior study would all have been born after SE, while the normotopic cells could have been born well before SE. Our method of birthdating adult-born DGCs provides high confidence that they were all generated after the onset of epileptogenesis and were at least 8 weeks old and functionally mature at the time of recording. This suggests that the age of the cell with respect to SE, rather than the cell's location, may be the more important factor in its propensity for burst firing. This propensity for burst firing might be driven by an increase in T-type calcium channels, similar to what has been reported for CA1 pyramidal cells in a rat model of TLE (Su et al 2002).

Though some of the intrinsic properties of DGCs in the rodent epileptic tissue were less heterogeneous than DGCs from human tissue, important epilepsy-related changes were present among rodent DGCs. Recordings from the rodent hippocampus revealed that the birthdated DGCs all displayed strong SFA or low firing activity, similar size and shape of post-burst AHP, and most exhibited a single AP waveform that included a large ADP. However, notable

differences between DGCs of sham treated and SE animals were an increase in firing rate, the emergence of burst firing, and a more depolarized RMP. These differences all point to an increase in intrinsic excitability of DGCs born after SE as compared to adult-born DGCs in a sham treated animal.

In summary, we have found that hilar ectopic DGCs from human TLE tissue were less excitable than normotopic DGCs in the GCL. Interestingly, we found the opposite relationship in pilocarpine-treated rat tissue; hilar ectopic DGCs were more excitable than normotopic DGCs and, furthermore, normotopic DGCs were more excitable than DGCs from sham treated rats. We believe the discrepancies between results from the human disease and the disease model are related, at least in part, to the different stages of the disease. Human tissue was obtained from patients who had experienced epilepsy for many years, sometimes decades, and represents the late stage of disease. The rat model is designed to mimic severe epilepsy, but recordings were made early in the chronic stage of the disease. Unfortunately, due to the relatively small sample size, our human tissue data set was not amenable to a subgroup analysis of subjects with the shortest epilepsy durations. Furthermore, it is not clear how disease progression in rodent models compares to that in humans.

The discrepancies may also result from unresolved species-related differences or limitations of the animal model. Perhaps DGCs from healthy human tissue are naturally more heterogeneous than DGCs from rodent tissue. Alternatively, human DGCs may exhibit features of disease-related plasticity that rodent DGCs would not exhibit regardless of the stage of disease. Rodent

models are more homogenous by design, but there is still heterogeneity present among individual animals within any given model. More data from later stage epileptic rodents and from patients earlier in the disease course would help determine whether animal models can recapitulate the same level of heterogeneity seen in the human tissue.

References

Agrawal N, Alonso A, Ragsdale DS. 2003. Increased persistent sodium currents in rat entorhinal cortex layer V neurons in a post-status epilepticus model of temporal lobe epilepsy. *Epilepsia* 44: 1601-4

Althaus AL, Parent JM. 2014. Role of adult neurogenesis in seizure-induced hippocampal remodeling and epilepsy. In *Endogenous Stem Cell-Based Brain Remodeling in Mammals*, ed. J M.-P., KS G. Boston, MA: Springer US : Imprint: Springer

Aradi I, Holmes WR. 1999. Role of multiple calcium and calcium-dependent conductances in regulation of hippocampal dentate granule cell excitability. *Journal of computational neuroscience* 6: 215-35

Azouz R, Jensen MS, Yaari Y. 1996. Ionic basis of spike after-depolarization and burst generation in adult rat hippocampal CA1 pyramidal cells. *The Journal of physiology* 492 (Pt 1): 211-23

Chen S, Su H, Yue C, Remy S, Royeck M, et al. 2011. An increase in persistent sodium current contributes to intrinsic neuronal bursting after status epilepticus. *Journal of neurophysiology* 105: 117-29

Dashtipour K, Tran PH, Okazaki MM, Nadler JV, Ribak CE. 2001. Ultrastructural features and synaptic connections of hilar ectopic granule cells in the rat dentate gyrus are different from those of granule cells in the granule cell layer. *Brain research* 890: 261-71

de Lanerolle NC, Kim JH, Robbins RJ, Spencer DD. 1989. Hippocampal interneuron loss and plasticity in human temporal lobe epilepsy. *Brain research* 495: 387-95

Dietrich D, Clusmann H, Kral T, Steinhauser C, Blumcke I, et al. 1999. Two electrophysiologically distinct types of granule cells in epileptic human hippocampus. *Neuroscience* 90: 1197-206

Dudek FE, Deadwyler SA, Cotman CW, Lynch G. 1976. Intracellular responses from granule cell layer in slices of rat hippocampus: perforant path synapse. *Journal of neurophysiology* 39: 384-93

Eriksson PS, Perfilieva E, Bjork-Eriksson T, Alborn AM, Nordborg C, et al. 1998. Neurogenesis in the adult human hippocampus. *Nature medicine* 4: 1313-7

Faber ES, Sah P. 2003. Calcium-activated potassium channels: multiple contributions to neuronal function. *The Neuroscientist : a review journal bringing neurobiology, neurology and psychiatry* 9: 181-94

Fournier E, Crepel F. 1984. Electrophysiological properties of dentate granule cells in mouse hippocampal slices maintained in vitro. *Brain research* 311: 75-86

Franck JE, Pokorny J, Kunkel DD, Schwartzkroin PA. 1995. Physiologic and morphologic characteristics of granule cell circuitry in human epileptic hippocampus. *Epilepsia* 36: 543-58

Fricke RA, Prince DA. 1984. Electrophysiology of dentate gyrus granule cells. *Journal of neurophysiology* 51: 195-209

Hester MS, Danzer SC. 2013. Accumulation of abnormal adult-generated hippocampal granule cells predicts seizure frequency and severity. *The Journal of neuroscience : the official journal of the Society for Neuroscience* 33: 8926-36

Houser CR, Miyashiro JE, Swartz BE, Walsh GO, Rich JR, Delgado-Escueta AV. 1990. Altered patterns of dynorphin immunoreactivity suggest mossy fiber reorganization in human hippocampal epilepsy. *The Journal of neuroscience : the official journal of the Society for Neuroscience* 10: 267-82

Jakubs K, Nanobashvili A, Bonde S, Ekdahl CT, Kokaia Z, et al. 2006. Environment matters: synaptic properties of neurons born in the epileptic adult brain develop to reduce excitability. *Neuron* 52: 1047-59

Jessberger S, Zhao C, Toni N, Clemenson GD, Jr., Li Y, Gage FH. 2007. Seizure-associated, aberrant neurogenesis in adult rats characterized with retrovirus-mediated cell labeling. *The Journal of neuroscience : the official journal of the Society for Neuroscience* 27: 9400-7

Kron MM, Zhang H, Parent JM. 2010. The developmental stage of dentate granule cells dictates their contribution to seizure-induced plasticity. *The Journal of neuroscience : the official journal of the Society for Neuroscience* 30: 2051-9

Kuhn HG, Dickinson-Anson H, Gage FH. 1996. Neurogenesis in the dentate gyrus of the adult rat: age-related decrease of neuronal progenitor proliferation. *The Journal of neuroscience : the official journal of the Society for Neuroscience* 16: 2027-33

Metz AE, Jarsky T, Martina M, Spruston N. 2005. R-type calcium channels contribute to afterdepolarization and bursting in hippocampal CA1 pyramidal neurons. *The Journal of neuroscience : the official journal of the Society for Neuroscience* 25: 5763-73

Pacheco Otalora LF, Hernandez EF, Arshadmansab MF, Francisco S, Willis M, et al. 2008. Down-regulation of BK channel expression in the pilocarpine model of temporal lobe epilepsy. *Brain research* 1200: 116-31

Parent JM, Elliott RC, Pleasure SJ, Barbaro NM, Lowenstein DH. 2006. Aberrant seizure-induced neurogenesis in experimental temporal lobe epilepsy. *Annals of neurology* 59: 81-91

Parent JM, Murphy GG. 2008. Mechanisms and functional significance of aberrant seizure-induced hippocampal neurogenesis. *Epilepsia* 49 Suppl 5: 19-25

Peng Z, Zhang N, Wei W, Huang CS, Cetina Y, et al. 2013. A reorganized GABAergic circuit in a model of epilepsy: evidence from optogenetic labeling and stimulation of somatostatin interneurons. *The Journal of neuroscience : the official journal of the Society for Neuroscience* 33: 14392-405

Podlogar M, Dietrich D. 2006. Firing pattern of rat hippocampal neurons: a perforated patch clamp study. *Brain research* 1085: 95-101

Ramey WL, Martirosyan NL, Lieu CM, Hasham HA, Lemole GM, Jr., Weinand ME. 2013. Current management and surgical outcomes of medically intractable epilepsy. *Clinical neurology and neurosurgery* 115: 2411-8

Scharfman HE, Goodman JH, Sollas AL. 2000. Granule-like neurons at the hilar/CA3 border after status epilepticus and their synchrony with area CA3 pyramidal cells: functional implications of seizure-induced neurogenesis. *The Journal of neuroscience : the official journal of the Society for Neuroscience* 20: 6144-58

Scharfman HE, Gray WP. 2007. Relevance of seizure-induced neurogenesis in animal models of epilepsy to the etiology of temporal lobe epilepsy. *Epilepsia* 48 Suppl 2: 33-41

Scharfman HE, Pierce JP. 2012. New insights into the role of hilar ectopic granule cells in the dentate gyrus based on quantitative anatomic analysis and three-dimensional reconstruction. *Epilepsia* 53 Suppl 1: 109-15

Selke K, Muller A, Kukley M, Schramm J, Dietrich D. 2006. Firing pattern and calbindin-D28k content of human epileptic granule cells. *Brain research* 1120: 191-201

Staley KJ, Otis TS, Mody I. 1992. Membrane properties of dentate gyrus granule cells: comparison of sharp microelectrode and whole-cell recordings. *Journal of neurophysiology* 67: 1346-58

Su H, Sochivko D, Becker A, Chen J, Jiang Y, et al. 2002. Upregulation of a T-type Ca2+ channel causes a long-lasting modification of neuronal firing mode after status epilepticus. *The Journal of neuroscience : the official journal of the Society for Neuroscience* 22: 3645-55

Surges R, Kukley M, Brewster A, Ruschenschmidt C, Schramm J, et al. 2012. Hyperpolarization-activated cation current Ih of dentate gyrus granule cells is upregulated in human and rat temporal lobe epilepsy. *Biochemical and biophysical research communications* 420: 156-60

Sutula T, Cascino G, Cavazos J, Parada I, Ramirez L. 1989. Mossy fiber synaptic reorganization in the epileptic human temporal lobe. *Annals of neurology* 26: 321-30

Tanner GR, Lutas A, Martinez-Francois JR, Yellen G. 2011. Single K ATP channel opening in response to action potential firing in mouse dentate granule neurons. *The Journal of neuroscience : the official journal of the Society for Neuroscience* 31: 8689-96

von Campe G, Spencer DD, de Lanerolle NC. 1997. Morphology of dentate granule cells in the human epileptogenic hippocampus. *Hippocampus* 7: 472-88

Vreugdenhil M, Hoogland G, van Veelen CW, Wadman WJ. 2004. Persistent sodium current in subicular neurons isolated from patients with temporal lobe epilepsy. *The European journal of neuroscience* 19: 2769-78

Walter C, Murphy BL, Pun RY, Spieles-Engemann AL, Danzer SC. 2007. Pilocarpine-induced seizures cause selective time-dependent changes to adult-generated hippocampal dentate granule cells. *The Journal of neuroscience : the official journal of the Society for Neuroscience* 27: 7541-52

Zhan RZ, Nadler JV. 2009. Enhanced tonic GABA current in normotopic and hilar ectopic dentate granule cells after pilocarpine-induced status epilepticus. *Journal of neurophysiology* 102: 670-81

Zhan RZ, Timofeeva O, Nadler JV. 2010. High ratio of synaptic excitation to synaptic inhibition in hilar ectopic granule cells of pilocarpine-treated rats. *Journal of neurophysiology* 104: 3293-304

Zhang L, Valiante TA, Carlen PL. 1993. Contribution of the low-threshold T-type calcium current in generating the post-spike depolarizing afterpotential in dentate granule neurons of immature rats. *Journal of neurophysiology* 70: 223-31

Zhang W, Yamawaki R, Wen X, Uhl J, Diaz J, et al. 2009. Surviving hilar somatostatin interneurons enlarge, sprout axons, and form new synapses

with granule cells in a mouse model of temporal lobe epilepsy. *The Journal of neuroscience : the official journal of the Society for Neuroscience* 29: 14247-56

Zhao S, Ting JT, Atallah HE, Qiu L, Tan J, et al. 2011. Cell type-specific channelrhodopsin-2 transgenic mice for optogenetic dissection of neural circuitry function. *Nature methods* 8: 745-52

	Granule Cell Layer DGCs (36)	Hilar DGCs (7)	Interneurons (11)
Resting membrane potential (mV)*	-70.47 ± 0.82	-68.81 ± 1.96	-64.18 ± 1.23 ‡
Input resistance (MΩ)*	198.58 ± 15.43	153.32 ± 16.9	142.07 ± 57.04
Sag ratio*	1.12 ± 0.01	1.07 ± 0.04	1.25 ± 0.08 ‡
Action potential threshold (mV)*	-42.98 ± 1.45	-22.87 ± 8.14 ‡	-42.47 ± 2.51 †
Action potential spike height (mV)*	79.69 ± 2.21	53.72 ± 11.37 ‡	69.96 ± 4.01
Action potential half-width (ms)	0.99 ± 0.05	0.92 ± 0.13	0.77 ±0.09

Table 2.1 Specific passive membrane properties were used to differentiate DGCs from interneurons and to investigate differences between hilar DGCs and those in the GCL. Analyses were done using one-way ANOVA with Tukey's post-hoc test for multiple comparisons. AP characteristics were measured from single spike protocol. *Main effect determined by one-way ANOVA. ‡Significantly different from Granule Cell Layer with post-hoc analysis. †Significantly different from hilar DGCs with post-hoc analysis. All data presented as mean ± SEM.

	Normotopic SE (38)	Ectopic SE (7)	Normotopic Sham (6)
Resting membrane potential (mV)*	-71.62 ± 0.65	-65.22 ± 3.15 †	-71.57 ± 1.37
Input resistance (MΩ)	282.50 ± 31.65	273.45 ± 31.75	226.0 ± 32.71
Sag ratio	1.005 ± 0.001	0.999 ± 0.002	1.003 ± 0.001
Action potential threshold (mV)	-40.79 ± 1.20	-41.07 ± 2.59	-37.87 ± 2.29
Action potential spike height (mV)	72.04 ± 2.93	63.48 ± 4.84	67.49 ± 6.53
Action potential half-width (ms)*	0.99 ± 0.03	1.3 ± 0.14 † ‡	0.95 ± 0.07

Table 2.2 Passive membrane properties of all cells recorded from rodents displayed features of DGCs. Ectopic DGCs had depolarized RMP and wider AP than normotopic or sham DGCs respectively. Analyses were done using one-way ANOVA with Tukey's post-hoc test for multiple comparisons. *Main effect determined by one-way ANOVA. †Significantly different from Normotopic SE with post-hoc analysis. ‡Significantly different from Sham with post-hoc analysis. All data presented as mean ± SEM.

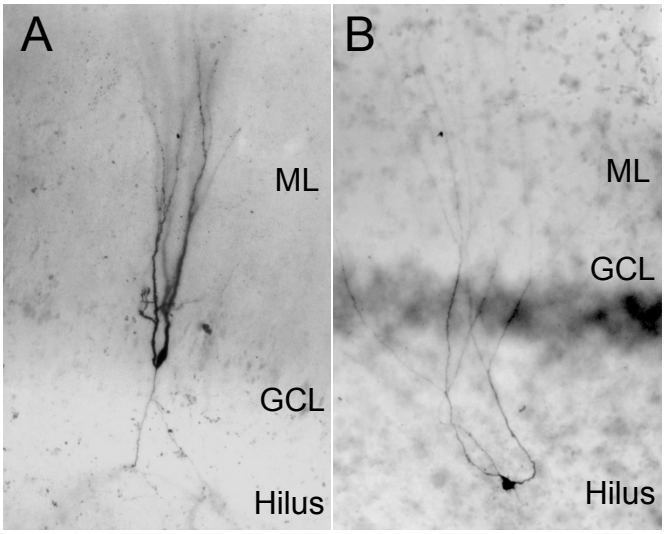

Figure 2.1 Biocytin filled cells display DGC morphology. **A.** Typical human dentate granule cell (DGC) with soma in the granule cell layer (GCL), dendrites in the molecular layer (ML), and axon in the hilus. **B.** Physiologically identified human DGC with hilar ectopic soma.

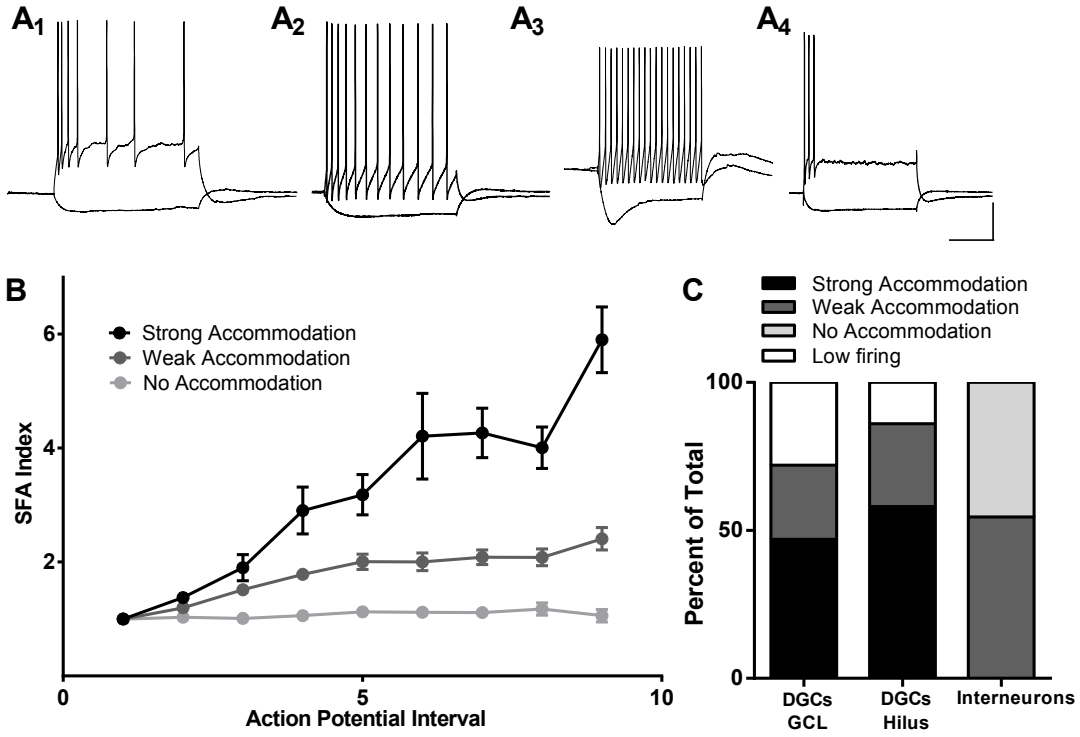

Figure 2.2 Cells display distinct SFA patterns, which help to distinguish DGCs from interneurons**. A.** Representative traces of firing pattern in response to a depolarizing step (500 ms): **A_1**) Strong accommodation (n = 21); **A_2**) Weak accommodation (n = 11); **A_3**) No accommodation (n = 6); **A_4**) Low firing (did not fire more than 3 AP in a spike train at the highest level of stimulation). For such cells (n = 11), SFA index could not be calculated. Scale bar 200 ms, 25 mV. **B**. Plot of SFA index vs AP interval. Strongly accommodating cells reached an SFA index value of at least 3 by the end of the spike train, while the value for weakly accommodating cells never exceeded 2.5, and the value for non-accommodating cells never exceeded 1.2. Error bars represent SEM. **C.** Distribution of SFA types amongst DGCs in the GCL, DGCs cells in the hilus, and cells that do not fit physiological characterization of DGCs (putative interneurons). There was no significant difference in the distribution of firing patterns between DGCs in the hilus or the GCL (p = 0.75, Fisher's Exact test).

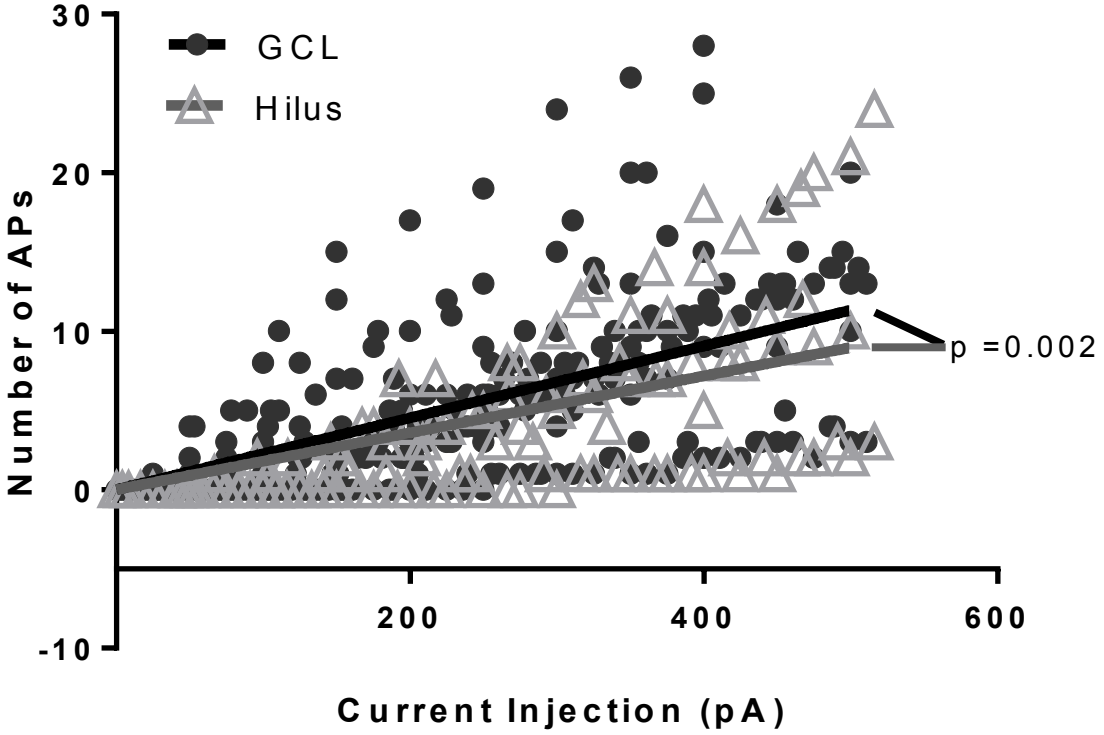

Figure 2.3 Hilar DGCs are slightly, but significantly, less excitable than DGCs in the GCL. All cells fire at least one AP in response to ≥ 300 pA of injected current. The solid black and gray lines were generated by fitting the respective colored scatter plot data with a Poisson regression line that passes through the origin. The slope of the regression line for hilar cells (0.01794 ± 0.001277) is significantly different from the slope of the line for GCL cells (0.02266 ± 0.0015, p = 0.0019), extra sum of squares F test).

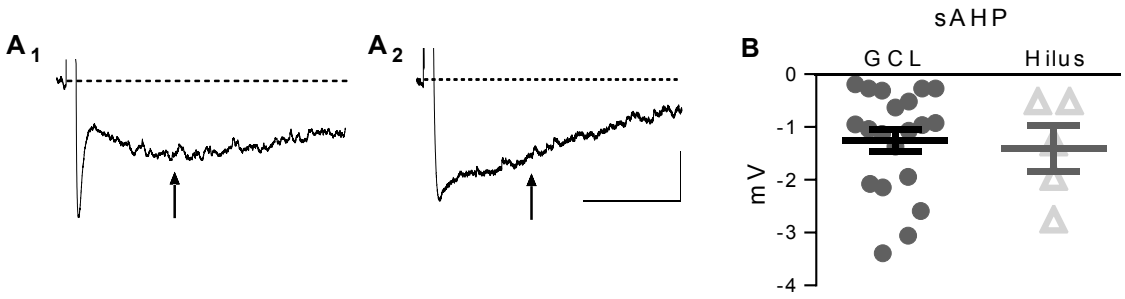

Figure 2.4 Cells in GCL and hilus exhibited a prominent post-burst afterhyperpolarizaion. **A_1**) Sample trace from a cell in the GCL; **A_2**) trace from a cell in the hilus. Arrows indicate when the slow AHP component was measured. **B**. The average amplitude of the slow afterhyperpolarization recorded from cells in the GCL (n=30) and the hilus (n=6) was not significantly different (p = 0.48 unpaired t-test). Data presented as mean ± SEM. Scale bars 1 s, 2 mV.

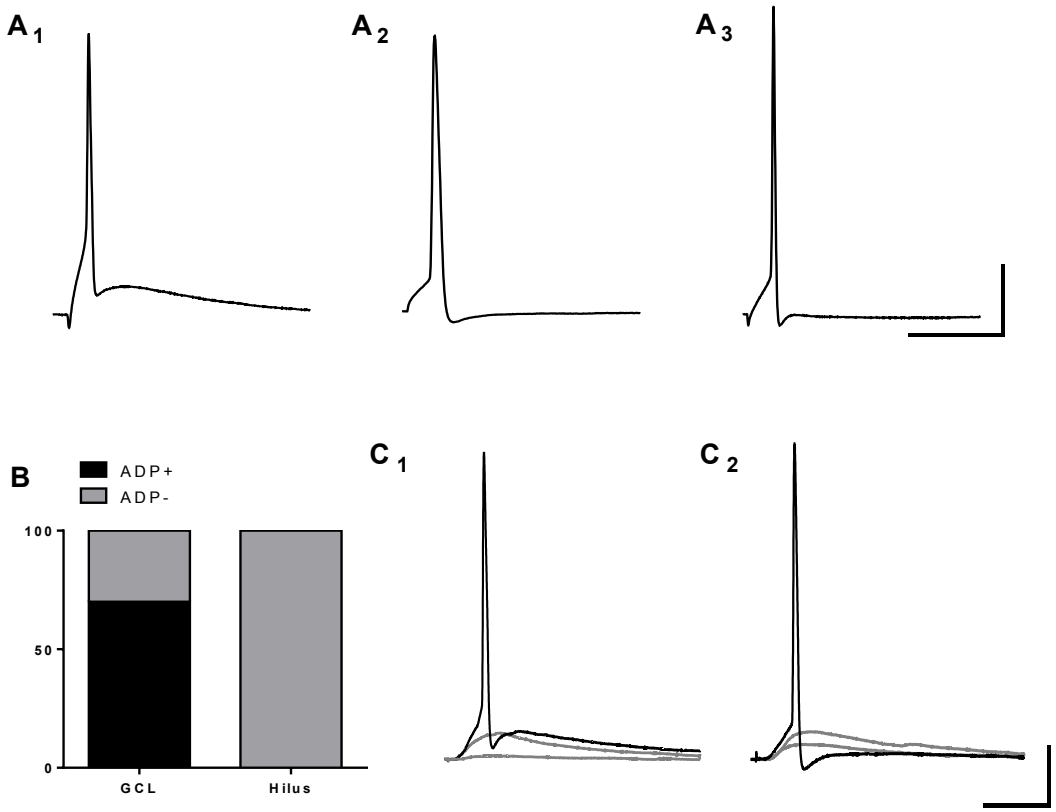

Figure 2.5 Cells in the GCL exhibit two distinct single AP waveforms in response to short depolarizing pulses, while hilar DGCs all exhibit similar waveforms. **A**. Example traces of APs elicited by direct, somatic current injection. Cells in the GCL display AP traces **A_1**) with an after depolarization (ADP), **A_2**) or without an ADP. **A_3**) Hilar cells only exhibit APs without an ADP. **B**. Distribution of cells that fired each type of AP classified by location. The majority of cells in the GCL fired APs with an ADP (25/36) while none of the 7 hilar cells exhibited an ADP. **C**. A subset of cells in both the GCL and hilus could be driven synaptically to fire single APs. Of these cells, some fired an AP **C_1**) with ADP and others fired an AP **C_2**) without ADP. Scale bars 25 ms and 20 mV.

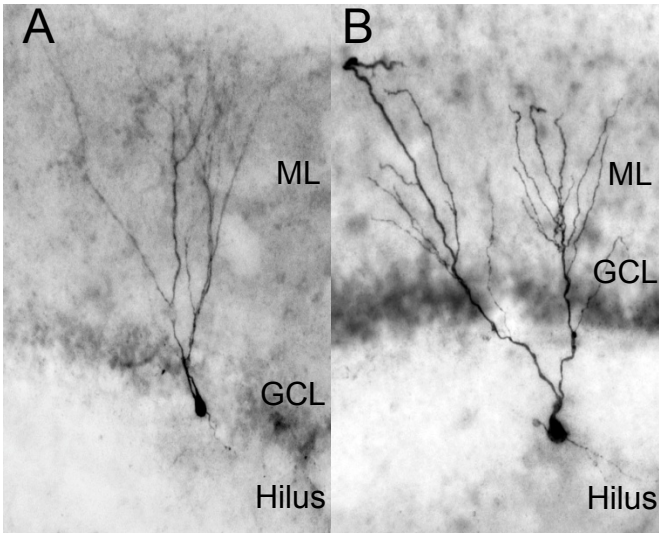

Figure 2.6 Biocytin filled cells display DGC morphology. **A.** Typical rat dentate granule cell (DGC) with soma in the granule cell layer (GCL) and dendrites in the molecular layer (ML). **B.** Rat DGC with hilar ectopic soma.

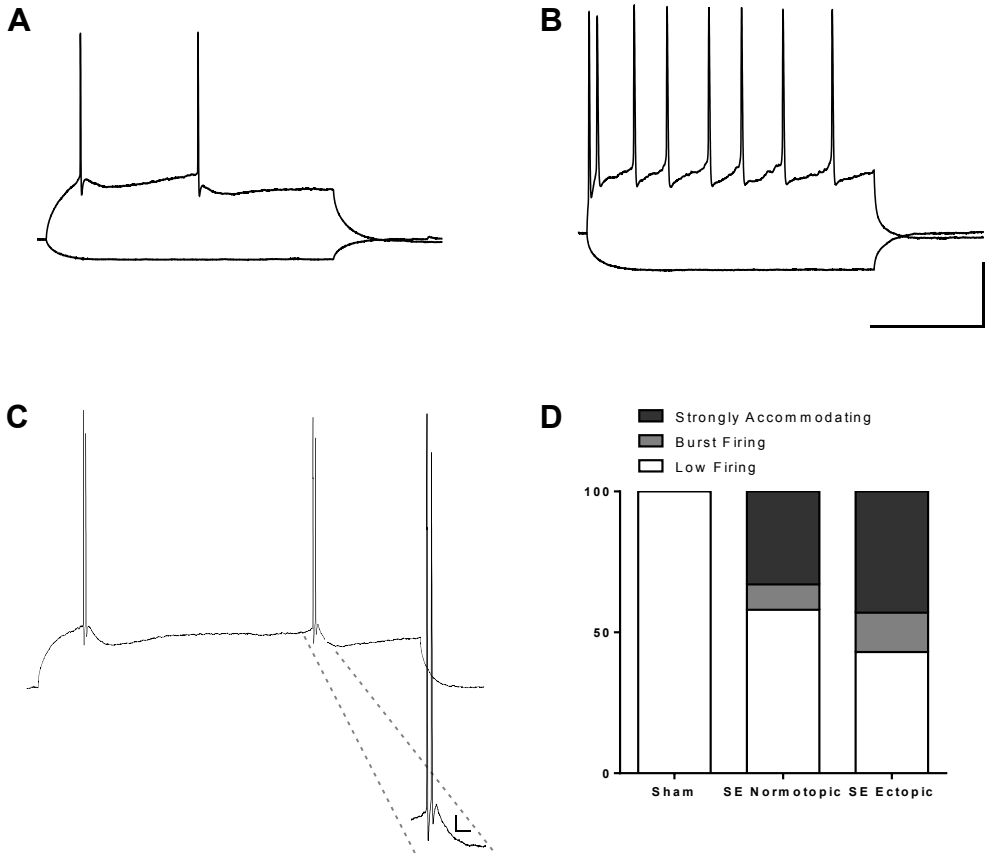

Figure 2.7 All cells from rodent tissue display firing behavior characteristic of dentate granule cells. **A.** Sample trace from a low firing cell. These cells only fired up to 3 AP in response to injected current. **B**. Sample trace from a cell with sustained firing in response to injected current. Cells that fired four or more APs always exhibited strong SFA (an index value of at least 3.0). Scale bars 200 ms, 25 mV. **C**. A small subset of cells from epileptic tissue fired AP doublets, even in response to low levels of current injection. Inset presents a larger image of the doublet. These were classified as burst firing cells. Scale bar 20 ms, 5 mV. **D.** Distribution of firing patterns among cells in each group. There was no significant difference between the firing pattern distributions of normotopic vs. ectopic DGCs ($p = 0.73$ Fisher's Exact test).

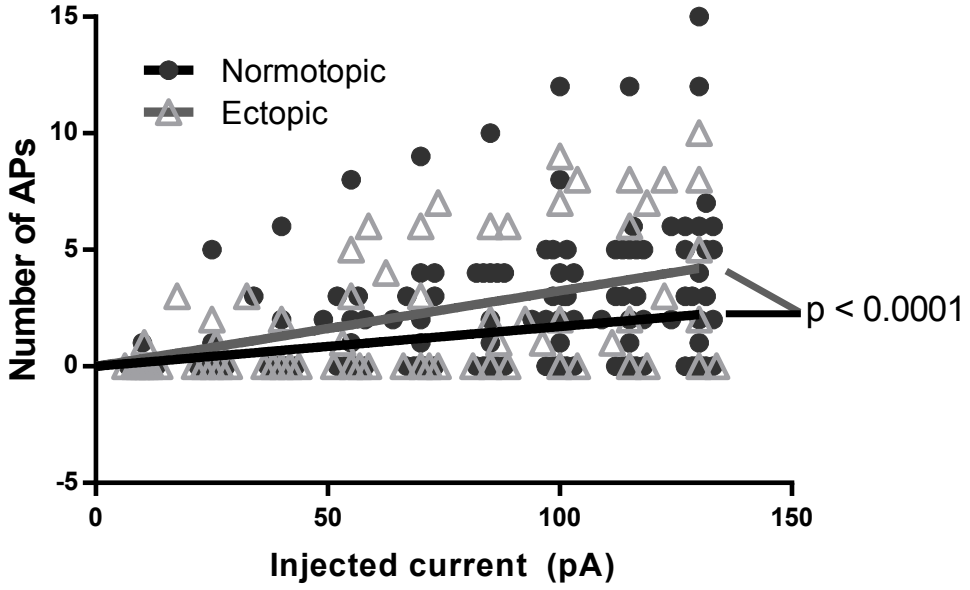

Figure 2.8 Ectopic DGCs from rodent SE tissue exhibit a moderate, but significant, increase in excitability as compared to normotopic DGCs. Both normotopic and ectopic DGCs born after SE exhibit more excitability than age-matched DGCs from sham treated animals. All cells in the sham group were low firing cells, so only cells from SE-treated animals were included for comparison of firing frequency. The solid black and grey lines were generated by fitting the respective colored scatter plot data with a Poisson regression line that passes through the origin. The slope of the line for ectopic DGC firing (0.032 ± 0.0038) is significantly different from the slope of the line for normotopic DGC firing (0.017 ± 0.0014; $p < 0.0001$, Extra sum of squares F test).

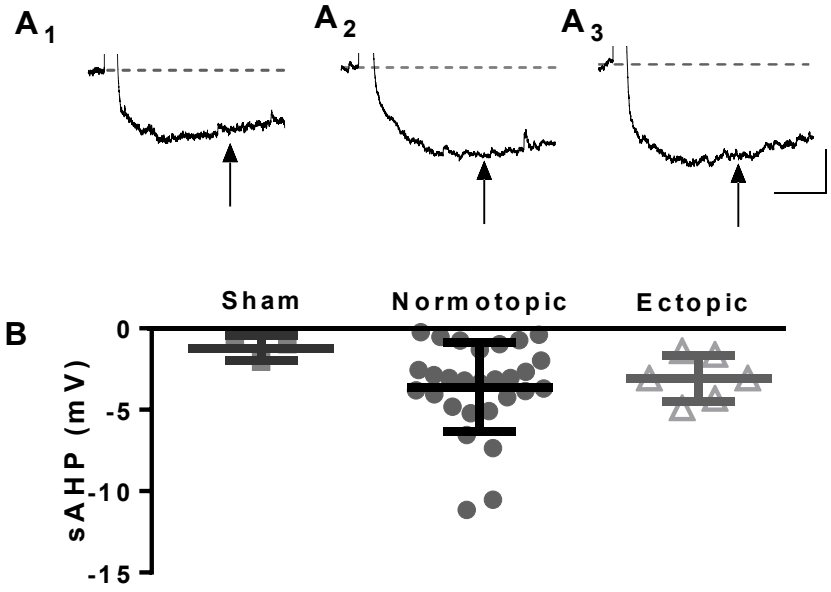

Figure 2.9 A subset of cells from each group exhibited post-burst sAHP. Representative traces from **A_1**) a cell from a sham-treated animal, **A_2**) a normotopic cell from an SE treated animal, and **A_3**) an ectopic cell from an SE treated animal. **B**. There was no significant difference in the mean size of the post-burst sAHP between any of the groups ($p = 0.311$, one-way ANOVA). All data are presented as mean ± SEM. Scale bars 500 ms, 2 mV.

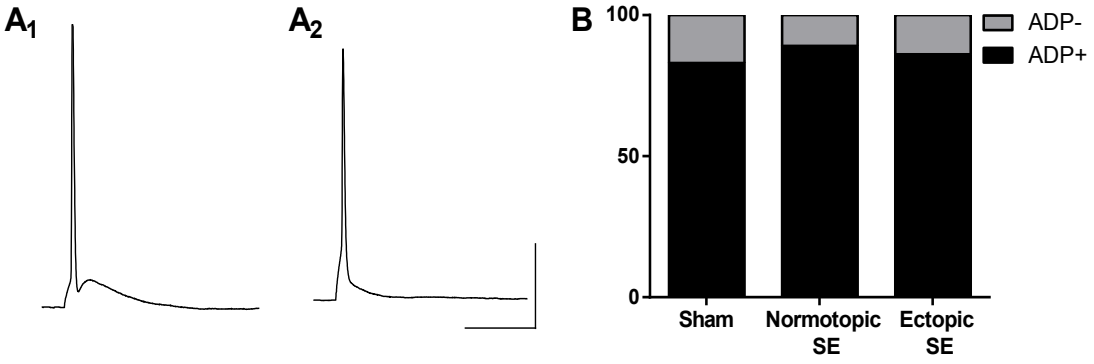

Figure 2.10 Two distinct shapes of single AP traces were observed in all three groups of rodent DGCs. Example trace showing AP **A_1**) with a prominent ADP and **A_2)** without an ADP. **B**. Graph showing the distribution of single spike AP type across all groups. There was no significant difference in the percentage of cells that fired each type of AP across any of the three groups (p = 0.91, Fisher's exact test). Scale bars 20 ms, 25 mV.

Chapter 3

Axonal plasticity of age-defined dentate granule cells in a rat model of temporal lobe epilepsy

Summary

Dentate granule cell (DGC) mossy fiber sprouting (MFS) in TLE is thought to underlie the creation of aberrant circuitry which promotes the generation or spread of spontaneous seizure activity. Understanding the extent to which subpopulations of DGCs participate in this circuitry could help determine how it develops and potentially identify therapeutic targets for regulating the aberrant activity of these circuits. In this study, we investigated the potential role of DGC birthdate in MFS into the inner molecular layer (IML) as well as other aspects of axonal plasticity. We used a retrovirus (RV) carrying a synaptophysin-yellow fluorescent protein (syp-YFP) fusion gene to birthdate cells and brightly label their axon terminals. With this approach, we studied DGCs born during the neonatal period and in adulthood from animals that underwent pilocarpine-SE or sham treatment. We found that both neonatal and adult-born populations of DGCs participate, to the same extent, in MFS within the inner molecular layer and in CA2. Interestingly, we did not observe changes in boutons within the hilus for either population of DGCs in SE tissue when compared to control. These data

indicate that axonal reorganization is independent of DGC birthdate in the rat TLE model.

Introduction

Dentate granule cell (DGC) axonal reorganization is a common feature of dentate gyrus histopathology in patients with temporal lobe epilepsy (TLE) that is recapitulated in many animal models of the disease (Sutula & Dudek 2007). Schleibel and colleagues first discovered the presence of aberrant terminals of DGC axons, known as mossy fibers, in the inner molecular layer (IML) of TLE patients in 1974 (Scheibel et al 1974). In rodent models of TLE, mossy fiber sprouting (MFS) into the IML creates a functional excitatory feedback loop, primarily forming synapses onto DGC apical dendrites, with a minority of sprouted synapses in the IML onto interneurons (Buckmaster et al 2002, Scharfman et al 2003). MFS has been linked with reverberant firing of the DGC network (Tauck & Nadler 1985) and positively correlated with the number of spontaneous seizures (Hester & Danzer 2013, Xu et al 2004). However, the role of MFS in epileptogenesis has recently been called into question by data that suggests it may not be involved in spontaneous seizure activity (Buckmaster 2014, Buckmaster et al 2009). Importantly, the focus of most research on DGC axonal reorganization in TLE has been on IML MFS, but this plasticity occurs throughout the hilus and CA region as well.

The mechanisms that drive axonal reorganization of DGCs in TLE models are not fully understood. IML sprouting has been correlated with seizure-induced changes such as cell death, changes in extracellular matrix protein expression, and loss of axon guidance cues (Cavazos et al 1991, Cavazos & Sutula 1990, Holtmaat et al 2003, Pollard et al 1994). Plasticity of MFs in CA3 can occur in response to physiological stimuli such as exercise, in addition to seizures, and has been linked to loss of synaptic contacts in CA3 in a TLE model (Danzer et al 2010, McAuliffe et al 2011, Schwarzer et al 1995, Toscano-Silva et al 2010). While nothing is known about seizure-related plasticity at the MF-CA2 synapse, recent data indicates that this synapse can be modulated by exercise and inflammation (Llorens-Martin et al 2015).

In addition to these external stimuli, there are cell-autonomous factors, such as mTOR signaling, that influence axonal reorganization within individual DGCs (Buckmaster et al 2009). Not every DGC contributes to MFS (Buckmaster & Dudek 1999), but it is not known what influences the likelihood to contribute. DGC birthdate is one potential influence because of the well-documented role of adult-born DGCs in seizure-related plasticity (Jessberger et al 2007, Kron et al 2010, Walter et al 2007). Previous research suggested that DGCs developing during or after an epileptogenic insult are responsible for most, if not all, MFS in the IML (Kron et al 2010). However, the retroviral (RV) GFP labeling used in these experiments did not allow for reliable resolution of small MF boutons in the IML and hilus, and extensive dendritic labeling made it difficult to distinguish GFP+ axons in the IML. In addition, a potential relationship between DGC

birthdate and axonal plasticity within the hilus and hippocampal pyramidal cell regions has not previously been investigated.

In this study, we compared MF structural plasticity of DGCs born in the neonatal period, and thus mature at the time of injury, with those generated in adulthood after injury in the rat pilocarpine model of TLE. To more specifically label the synaptic boutons of birthdated DGCs, we utilized a construct carrying the synaptophysin (syp) gene fused to yellow fluorescent protein (YFP) to direct YFP to synaptic vesicles (Umemori et al 2004), and this construct was packaged in a RV vector to limit infection to actively dividing cells.

With this tool, we found that both neonatal and adult-born populations of DGCs participate in MFS in the pilocarpine SE model of TLE, with some subtle but significant differences in other forms of aberrant axonal remodeling. We also found that the DG-CA2 “alternative trisynaptic circuit” is altered after SE. Our findings suggest that both pre-existing, mature DGCs and those generated after SE contribute to various aspects of seizure-induced axonal plasticity.

Methods

Virus production

We generated the syp-YFP RV using a vesicular stomatitis virus G-protein (VSV-G) pseudotyped Moloney murine Leukemia virus backbone in which the expression of syp-YFP is driven by the human synapsin-1 promoter. The synaptophysin-YFP fusion gene was amplified from the pCMV-synaptophysin-

YFP plasmid (generously provided by Dr. Hisashi Umemori (Umemori et al 2004)) via PCR using primers 5'-cgagctcaaggatccaattctgcagtcg-3' and 5'-ctgattatgatcacgcgtcgcggcc-3'. To express the syp-YFP under the control of the synapsin promoter, the amplified and isolated syp-YFP fragment was subcloned into the RV vector pCAG-mCherry-WPRE (woodchuck post-transcriptional regulatory element) by replacing the mCherry fragment between pCAG and WPRE. The accuracy of the cloned syp-YFP fragment in the construct was verified by DNA sequencing and the expression of syp-YFP was tested by transfecting HEK 293 cells using LIpofectamine^{TM} (Invitrogen, CA). The cells were cultured at 37^{o}C for 3 days prior to analysis. We also used a GFP-expressing RV as described previously (Kron et al 2010).

High-titer, replication incompetent pseudotyped RV was produced as described previously (Kron et al 2010) by co-transfection of CAG-GFP-WPRE and VSV-G plasmids into GP_2-293 packaging cell line (Clontech, CA). Cells were plated in 10 ml DMEM supplemented with 10% FBS the day prior to transfection. The co-transfection was performed using calcium phosphate precipitation. The transfected cells were incubated at 37^{O}C for 6 hours, the medium was replaced and cells were allowed to grow for 65 hours. The supernatant containing RVs were harvested and filtered through a 0.45-μM pore size filter (Gelman Sciences, MI). The filtered supernatant was concentrated by centrifugation in a Sorvall model *RC 5C PLUS* at 50,000xg at 4^{O}C for 90 min. The RV-containing pellet was resuspended in 1X PBS, aliquoted, and was stored at -80^{O}C until use. Final RV

titers ranged between 2-5 X 10^8 cfu/ml as measured by YFP or GFP colony formation on NIH 3T3 cells.

Animals

Animal procedures were performed using protocols approved by the University Committee on Use and Care of Animals of the University of Michigan. Animals were purchased from Charles River and kept under a constant 12 hour light/dark cycle with access to food and water *ad libitum.* Epileptic animals (n = 32) and sham controls (n = 11) were generated as described previously (Kron et al 2010). Briefly, eight week-old male Sprague Dawley rats were pretreated with atropine methylbromide (5 mg/kg i.p.; Sigma-Aldrich, St. Louis, MO) 20 minutes prior to induction of SE with pilocarpine hydrochloride (340 mg/kg i.p.; Sigma-Aldrich, St. Louis, MO) for epileptic animals, or an equivalent volume of 0.9% saline for sham animals. After 90 minutes of SE, seizures were terminated with diazepam (10 mg/kg i.p.; Hospira Inc, Lake Forest, IL). Sham controls were treated with diazepam two hours after the saline injection.

Intrahippocampal RV injections

Animals were injected with Syp-YFP RV, or in some cases GFP RV, bilaterally into the dorsal dentate gyrus at either postnatal day 7 (P7) or postnatal day 60 (P60) as described previously (Kron et al 2010). Briefly, male P7 rat pups were anesthetized on ice and placed on an ice cold neonatal rat stereotax adaptor (Stoelting, Wood Dale, IL) in a Kopf (Tujunga, CA) stereotaxic frame.

Bilateral burr holes were drilled in the skull and 1 μl of RV was injected, using a Hamilton syringe and microinjection pump, at 0.1 μl/min into each hemisphere with the following coordinates (in mm from bregma and mm below the skull): caudal 2.0, lateral 1.5, deep 2.7. P60 male rats were anesthetized with a ketamine/xyelzine mixture and placed in a Kopf stereotaxic frame. Bilateral burr holes were drilled in the skull and 2.5 μl of RV was injected the same as for neonatal rats but with the following coordinates (in mm from bregma and mm below the skull): caudal 3.9, lateral 2.3, deep 4.2.

Immunohistochemistry

At 1, 2, 4, or 8-10 weeks post SE or sham treatment, rats were deeply anesthetized with pentobarbital and transcardially perfused with 0.9% saline and 4% paraformaldehyde (PFA). Brains were removed and post-fixed overnight in 4% PFA. Sixty μm sections were cut in the coronal plane using a vibrating blade microtome (VT1000S, Leica Microsystems Inc, Buffalo Grove, IL). Representative sections (4-6 sections, 720 μm apart) through the rostro-caudal axis of the brain were processed with standard fluorescent immunohistochemical techniques using the following primary and secondary antibodies: mouse anti-bassoon (1:1000, Enzo Life Sciences), rabbit or chicken anti-GFP (1:2000 both, Invitrogen and Aves), mouse anti-striatal enriched phosphatase (STEP) (1:1000, Cell Signalling), rabbit anti-zinc transporter-3 (Znt3) (1:3000, Synaptic Systems). Fluorescent signals were achieved using Alexa Fluor secondary antibodies: goat

anti-mouse 594, goat anti-mouse 647, goat anti-rabbit 488 and 594, and goat anti-chicken 488.

Microscopy

Images were acquired using a Zeiss LSM 510-META Laser Scanning Confocal Microscope or Leica Upright SP5X Confocal Microscope. For confirmation of co-localization and analysis of bouton size and density, images were acquired with a 63x objective at 2x optical zoom as 1 μm stacks through the z-plane with the pinhole set at 1 Airy unit and 0.5 μm step size. For analysis of amount of axon sprouting into the IML and pyramidal cell regions, sections were imaged at 2048 resolution with a 10x objective at 1 or 2x optical zoom, as 40-60 μm stacks through the z-plane with the pinhole set at 1 Airy unit and a 6 μm step size.

Image analysis and statistics

Image files were imported into ImageJ for analysis. Statistical analyses were performed using GraphPad Prism 6.0 software. Co-localization of YFP-positive bouton-like structures was first established using 1 μm optical slice images, prior to further image processing. To calculate IML and hilar bouton density, axon segments were first traced through image stacks and straightened. Images were then made binary and the analyze particle function was used to count all boutons with at least 10% circularity and an area larger than 0.25 μm^2. The number of boutons was then divided by the length of axon segment to

determine bouton density. The average density was determined for each animal, and group means were compared with a one-way ANOVA and Sidak's multiple comparisons test.

Relative amounts of sprouting into the IML by birthdated DGCs was determined from z-projections by identifying regions within tissue sections containing IML sprouting where labeled axons were present but labeled apical dendrites were not. Regions in the IML were outlined using the Region of Interest (ROI) function in ImageJ, The same sized ROI was then copied and placed over the hilus directly below the GCL. Using the same ROI for both areas of each section allowed for direct comparison of the percentage of YFP labeling within the ROI. Once ROIs were determined for all sections within the image, the image was made binary and the number of labeled and unlabeled pixels was determined using the histogram function. From these data, the percentage of labeled pixels was determined for each ROI. The percent of labeling in the IML ROI was divided by the percent of labeling in the hilar ROI to determine the sprouting ratio for that section. The sprouting ratios for all sections from a given animal were averaged to determine a single sprouting ratio for each animal. Group means were statistically compared using student's t-test.

Length of CA2 was determined for each section containing syp-YFP labeled boutons by using the segmented line function in ImageJ and tracing the cell body layer of STEP-labeled cells. The borders of CA2 were defined by a sharp reduction in STEP label intensity. Sections for which the borders of CA2 could not be clearly delineated were not included in the analysis. The amount of

syp-YFP innervation in the CA2 region was measured with the segmented line function by starting from the CA3/CA2 border and tracing to the furthest syp-YFP labeled structure within the STEP. The length of the syp-YFP-containing region in CA2 was divided by the length of CA2 within an individual slice to determine percent of CA2 that is innervated by labeled axons.

Results

Synaptophysin-YFP retrovirus labels DGC axon terminals

Previous work from our lab and others has used RV carrying a cytoplasmic GFP reporter as a means of birthdating and labeling subsets of DGCs to study them after they mature (Jessberger et al 2007, Kron et al 2010, van Praag et al 2002). This tool is excellent for studying changes in soma location, dendritic morphology, and giant MF boutons, but its utility is limited for studying changes in finer axon structures. Given our interest in seizure-induced plasticity of MF axons, we therefore developed a RV that preferentially labels axon structures to better visualize axonal changes.

Synaptophysin is a synaptic vesicle-associated protein that is abundant in synaptic terminals (Li & Murthy 2001). The syp-YFP fusion protein is comprised of full-length synaptophysin directly conjugated to full-length YFP, such that YFP expression is highly enriched in synaptic boutons. Delivering this construct in a RV vector thus allows us to simultaneously birthdate DGCs and intensely label the MF terminals to a much greater extent than the cytoplasmic GFP RV (**Figure**

3.1 $A_{1,2}$). RV overexpression of syp-YFP often leads to diffuse, albeit weaker, labeling in the soma and dendrites (**Figure 3.1 A_2, arrowheads**) in addition to strong labeling at putative MF boutons. While the difference in label intensity between MF boutons and non-bouton labeled structures provides a straightforward means of distinguishing them, we also used immunohistochemistry (IHC) to identify co-labeling of syp-YFP+ MF boutons with the synaptic protein bassoon, which is expressed exclusivel in pre-synaptic terminals (tom Dieck et al 1998) (**Figure 3.1 C**). Most tissues showed well-delineated bassoon immunoreactivity, and all syp-YFP-labeled putative boutons (identified on the basis of their size and shape) were co-labeled with bassoon.

Both adult- and neonatal-born DGCs contribute to MFS in the IML

Previous work from our laboratory using a GFP-expressing RV showed that neonatal-born DGCs that were 7 weeks old when animals underwent SE did not exhibit gross anatomical hallmarks of seizure-induced plasticity, whereas DGCs born after SE exhibited the most aberrant plasticity, including HBDs, ectopic locations, or MFS (Kron et al 2010). To better assess seizure-induced axonal changes, we used syp-YFP RV to label similar DGC cohorts and examined YFP immunolabeling in hippocampal sections. Rats received syp-YFP RV at P7 or P60, underwent pilocarpine-induced SE at P56 and were euthanized 8 weeks later. These two time points were chosen for RV injection to label DGCs at two different stages of development during epileptogenesis: pre-existing, mature DGCs and those generated 4 days after SE.

The syp-YFP RV allowed us to clearly distinguish between axons and dendrites in the IML and also to identify low levels of MFS, because axon terminals in the IML were visible even at low magnification and were labeled to a much greater extent than with eGFP RV (**Figure 3.1 B**). Using this approach, we found that both neonatal and adult-born DGC populations contributed to MFS in the IML at 8 weeks after SE (**Figure 3.2 A**). Others have shown that sprouted MF terminals begin to appear in the IML early after SE in rodent models and continue to increase in number until the IML is densely packed with MF terminals (Cavazos et al 1991, Mello et al 1993). We performed a time course experiment in which tissues were collected at 2 and 4 weeks after SE to determine when the two populations of cells began to contribute to MFS. We found that sprouted MFs from neonatal-born DGCs, but not adult-born DGCs, were present in the IML by 2 weeks post SE (**Figure 3.2 B**). At 4 weeks post SE, sprouted MF from both populations could be observed in the IML (**Figure 3.2 C**), and the amount of MFS appeared to increase by 8 weeks post-SE (**Figure 3.2 D**). To further support the finding that MFS from neonatal-born DGCs, which are mature at the time of SE, begins sooner after SE than for adult-born DGCs, we also examined the neonatal-born DGCs at 1 week after SE. We observed fairly robust sprouting at this time point in 2 of 4 animals (**Figure 3.2 E**). These data support the idea that syp-YFP+ DGCs labeled by P7 injections were mature at the time of SE, rather than arising from from P7 labeling of NSCs that continued to generate DGCs into adulthood.

Features of IML and hilar MF boutons are similar between adult- and neonatal-born DGCs after SE

To investigate the relationship between DGC birthdate and amount of IML sprouting, we determined a sprouting ratio for each animal by measuring the percentage of bouton labeling in the IML vs. hilus of discreet regions within the dentate gyrus (excluding the apex). There was no significant difference in the mean sprouting ratio between birthdated groups (**Figure 3.3;** p = 0.65, student's t-test).

We next examined the density of boutons on individual sprouted fibers in the IML and hilus from pilocarpine- and sham-treated animals. We identified axon segments that could be easily distinguished from other structures and determined the average number of boutons per micron for each animal. The dentate hilus undergoes substantial structural changes during epileptogenesis that may influence local MF synapses. These include rapid loss of interneurons and a progressive increase in aberrant DGC dendrites, either from HBDs or ectopic cells (Althaus & Parent 2014, Buckmaster & Dudek 1997). We found no significant difference in bouton density across the 4 populations (P7 vs. P60 birthdate and SE vs. sham) of DGCs (**Figure 3.4 A,B**. However, axon segments of adult-born DGCs, but not neonatal-born DGCs, had a greater bouton density in the IML than in hilus (**Figure 3.4 B**; p = 0.0052, one-way ANOVA with Sidak's multiple comparison's test).

Plasticity of pyramidal cell innervation by MFs

DGCs synapse onto CA3 pyramidal neurons as part of the classic trisynaptic circuit in the hippocampus. The giant boutons form synapses primarily onto the basal dendrites of pyramidal cells in stratum lucidum. Under normal conditions, a small proportion of MF boutons also synapse onto apical dendrites in stratum oriens (Blaabjerg & Zimmer 2007). In some TLE models, MFs sprout additional collaterals into more caudal regions of SO (Schwarzer et al 1995). We observed syp-YFP labeled axons in CA3 SO of DGCs in all four treatment groups (data not shown). In sham treated animals, axon terminals from both neonatally generated and adult-born DGCs were present in SO of rostral sections. However, we did not observe any apparent differences in amount of SO labeling across any of the groups.

An “alternative trisynaptic circuit” was recently identified in which small boutons of DGCs functionally innervate CA2 pyramidal neurons (Kohara et al 2014). We investigated whether this changes after SE and if so, whether there is a difference between neonatal and adult-born DGCs. Using an antibodies against the CA2-specific markers STEP, we observed considerable damage to CA2 neurons in many animals that had undergone SE (**Figure 3.5 A, B**). When we compared the size of the CA2 region across animals, we found that it was significantly smaller in animals that underwent SE (**Figure 3.5 B**; $p = 0.0006$, student’s t-test). As a result, we normalized each measurement to the length of CA2 within individual sections to determine the percent by length of CA2 that was innervated by syp-YFP labeled axons. We found that labeled axons from both neonatal and adult-born DGCs innervate a greater percentage of CA2 after SE

when compared to sham-treated animals (**Figure 3.5 C**; p = 0.01, one-way ANOVA with Sidak's multiple comparisons test), but there was no difference between birthdated populations within the same treatment group.

Discussion

The goal of this study was to determine the relative contributions of age-defined cohorts of DGCs to aberrant axonal organization in a rat TLE model. Using syp-YFP RV to birthdate neonatal- and adult-born DGCs and label their axon terminals, we found that cells that are mature at SE and cells that are born after contribute similarly to seizure-related axonal plasticity. We also report a novel type of seizure-induced plasticity, which involves changes to mossy fiber innervation of CA2 pyramidal cells.

Initially, we were surprised to find sprouted MF axons from neonatal-born DGCs in the IML after SE. Previous work from our laboratory found that DGCs that were born neonatally and were 7 weeks old when animals underwent SE were resistant to seizure-related plasticity, whereas many DGCs born after SE exhibited HBDs, ectopic somas, or MFS (Kron et al 2010). This study also found that intermediate-aged cells exhibited intermediate levels of seizure-induced plasticity; about 15% of DGCs that were 4 weeks at SE and about 35% that were 2 weeks at SE retained HBD and cells of both ages contributed to MFS, but none from either population migrated ectopically (Kron et al 2010). These data suggest that susceptibility to seizure-induced plasticity is commensurate with a cell's

developmental stage. Indeed, this study found that neonatal-born DGCs, which were mature at the onset of SE, do not contribute to IML sprouting (Kron et al 2010). However, those results were obtained using a cytoplasmic eGFP RV, which causes strong somatic and dendritic labeling, but weaker labeling of axon processes and small boutons. With the syp-YFP RV, we identified labeled axons from both birthdated populations in the IML after SE and confirmed the presence of synaptic boutons by double labeling with bassoon.

The RV vector that we use only infects cells that are dividing at the time of the intrahippocampal injections (Zhao et al 2006). However, we considered the possibility that a small number of radial glia-like (RG-like) neural stem cells could have been infected when RV was injected in neonatal animals. RG-like cells are relatively quiescent and so could retain the label and divide after SE to produce post-SE, adult-born DGCs, which might be responsible for the observed MFS after P7 RV injections. The time course data indicate, however, that the labeled fibers do indeed arise from DGCs that were born neonatally and were mature at SE because MFS arises from this population within one week post-SE, while MFS could not be detected from the adult-born population until four weeks post SE.

It is interesting that the axons of adult-born DGCs examined at 2 weeks post-SE are not yet found in the IML, considering the fact that they are already present in the hilus. This points to factors above and beyond the initial injury as being involved in the regulation of axon innervation of the IML. Excitatory synaptic activity, via LTP induction in the perforant path, induces MFS in the

absence of the deleterious effects of SE (Adams et al 1997), suggesting that differential synaptic activity could account for differences in timing of sprouting or even the identity of individual cells that participate in sprouting. To label adult-born DGCs, the RV is injected four to five days after SE. Therefore, these cells are 9-10 days old at 2 weeks post-SE. At this stage in normal rodents, adult-born DGCs have short processes and do not receive excitatory synaptic input (Overstreet-Wadiche et al 2006a, Zhao et al 2006). After SE, adult-born DGCs have been shown to develop more rapidly (Overstreet-Wadiche et al 2006b), but 10 day-old cells are still unlikely to be receiving significant amounts of excitatory synaptic input.

We observed that the amount of labeled axons in the IML varied among animals at the 8 week post-SE time point, and wondered whether DGC birthdate impacts contribution to MFS. To determine relative amount of MFS, we calculated a sprouting ratio for each animal, which was variable across animals, but not different between the neonatal- and adult-born populations. From these data, we cannot determine whether the degree of sprouting is determined by small subpopulations of DGCs exhibiting very robust MFS, or by large proportions of DGCs that develop less extensive MFS. Interestingly, the mean sprouting ratio was about 30% for both populations, which supports the hypothesis that a subset of cells participate in MFS at any given time.

We did find a significant difference in bouton density between IML and hilar axon segments of adult-born DGCs, but not between IML and hilar axon segments of neonatal-born DGCs. Without a measurement of total axon length in

IML vs hilus, it is difficult to speculate on the net impact of this increased bouton density. Several comprehensive studies examining the structure of DGC axon arbors from epileptic and intact tissue indicate that there is an increase in the total axon length of DGCs in epileptic tissue (Acsady et al 1998, Buckmaster & Dudek 1999, Claiborne et al 1986, Sutula et al 1998). One study, using the kainic acid SE model of TLE, also found a significant increase in IML bouton density when compared to hilar bouton density, as well as a small, but significant increase in hilar bouton density when compared with control animals (Sutula et al 1998). None of the aforementioned studies identified DGC birthdate. Our finding of greater IML bouton density on adult-born DGCs is consistent with the idea that this population is more involved in recurrent excitation of DGCs than the neonatal-born population.

In addition to axonal reorganization within the dentate gyrus, we examined seizure-related plasticity of DGC axons in pyramidal cell layers CA3 and CA2. While others have found sprouting of MF axons into SO of CA3, we were unable to consistently detect axons of birthdated cells – either neonatal or adult-born – in this region. This is likely due to variability in viral infection and location of labeled DGCs within the granule cell layer, because the path of DGC axons is influenced by their location within the different blades of the layer (Claiborne et al 1986).

To our knowledge, this is the first report of seizure-induced plasticity at the MF-CA2 synapse. Pyramidal cell death occurs throughout the CA subfields, including CA2 in the pilocarpine-SE model of TLE (Fujikawa 1996). Our data also indicate substantial cell death in CA2, since the average length of the CA2

pyramidal cell body layer is shorter in animals that underwent SE. We found that MFs of both birthdated populations of DGCs extend further into CA2 in epileptic tissue than in controls, even when controlling for the shorter length of CA2. More work is needed to determine the functional implications of this plasticity, but it is consistent with an increase in DG output to CA2 pyramidal cells in this TLE model.

The data presented in this chapter show that both neonatal- and adult-born DGCs, participate in MFS in the IML and axonal plasticity in the hippocampus proper. Recent data from others have called into question the role of MFS in the IML for epileptogenesis. While the impact of axonal plasticity in TLE appears to be a net increase in excitatory post-synaptic output, the functional implications of this plasticity for spontaneous seizure activity are still unclear (Buckmaster 2014, Buckmaster & Lew 2011, Buckmaster et al 2002, Sutula et al 1998). Inhibiting MFS with rapamycin treatment may not be the most effective means of studying the impact of this plasticity because it has off target effects that compromise the interpretation of the data. Instead, more work needs to be done to determine the proportion of DGCs that participate in MFS, what factors influence individual DGCs to participate, and how the physiology of sprouting cells compares to non-sprouting cells in both TLE and control tissue.

References

Acsady L, Kamondi A, Sik A, Freund T, Buzsaki G. 1998. GABAergic cells are the major postsynaptic targets of mossy fibers in the rat hippocampus. *The Journal of neuroscience : the official journal of the Society for Neuroscience* 18: 3386-403

Adams B, Lee M, Fahnestock M, Racine RJ. 1997. Long-term potentiation trains induce mossy fiber sprouting. *Brain research* 775: 193-7

Althaus AL, Parent JM. 2014. Role of adult neurogenesis in seizure-induced hippocampal remodeling and epilepsy. In *Endogenous Stem Cell-Based Brain Remodeling in Mammals*, ed. J M.-P., KS G. Boston, MA: Springer US : Imprint: Springer

Blaabjerg M, Zimmer J. 2007. The dentate mossy fibers: structural organization, development and plasticity. *Progress in brain research* 163: 85-107

Buckmaster PS. 2014. Does mossy fiber sprouting give rise to the epileptic state? *Advances in experimental medicine and biology* 813: 161-8

Buckmaster PS, Dudek FE. 1997. Neuron loss, granule cell axon reorganization, and functional changes in the dentate gyrus of epileptic kainate-treated rats. *The Journal of comparative neurology* 385: 385-404

Buckmaster PS, Dudek FE. 1999. In vivo intracellular analysis of granule cell axon reorganization in epileptic rats. *Journal of neurophysiology* 81: 712-21

Buckmaster PS, Ingram EA, Wen X. 2009. Inhibition of the mammalian target of rapamycin signaling pathway suppresses dentate granule cell axon sprouting in a rodent model of temporal lobe epilepsy. *The Journal of neuroscience : the official journal of the Society for Neuroscience* 29: 8259-69

Buckmaster PS, Lew FH. 2011. Rapamycin suppresses mossy fiber sprouting but not seizure frequency in a mouse model of temporal lobe epilepsy. *The Journal of neuroscience : the official journal of the Society for Neuroscience* 31: 2337-47

Buckmaster PS, Zhang GF, Yamawaki R. 2002. Axon sprouting in a model of temporal lobe epilepsy creates a predominantly excitatory feedback circuit. *The Journal of neuroscience : the official journal of the Society for Neuroscience* 22: 6650-8

Cavazos JE, Golarai G, Sutula TP. 1991. Mossy fiber synaptic reorganization induced by kindling: time course of development, progression, and

permanence. *The Journal of neuroscience : the official journal of the Society for Neuroscience* 11: 2795-803

Cavazos JE, Sutula TP. 1990. Progressive neuronal loss induced by kindling: a possible mechanism for mossy fiber synaptic reorganization and hippocampal sclerosis. *Brain research* 527: 1-6

Claiborne BJ, Amaral DG, Cowan WM. 1986. A light and electron microscopic analysis of the mossy fibers of the rat dentate gyrus. *The Journal of comparative neurology* 246: 435-58

Danzer SC, He X, Loepke AW, McNamara JO. 2010. Structural plasticity of dentate granule cell mossy fibers during the development of limbic epilepsy. *Hippocampus* 20: 113-24

Fujikawa DG. 1996. The temporal evolution of neuronal damage from pilocarpine-induced status epilepticus. *Brain research* 725: 11-22

Hester MS, Danzer SC. 2013. Accumulation of abnormal adult-generated hippocampal granule cells predicts seizure frequency and severity. *The Journal of neuroscience : the official journal of the Society for Neuroscience* 33: 8926-36

Holtmaat AJ, Gorter JA, De Wit J, Tolner EA, Spijker S, et al. 2003. Transient downregulation of Sema3A mRNA in a rat model for temporal lobe epilepsy. A novel molecular event potentially contributing to mossy fiber sprouting. *Experimental neurology* 182: 142-50

Jessberger S, Zhao C, Toni N, Clemenson GD, Jr., Li Y, Gage FH. 2007. Seizure-associated, aberrant neurogenesis in adult rats characterized with retrovirus-mediated cell labeling. *The Journal of neuroscience : the official journal of the Society for Neuroscience* 27: 9400-7

Kohara K, Pignatelli M, Rivest AJ, Jung HY, Kitamura T, et al. 2014. Cell type-specific genetic and optogenetic tools reveal hippocampal CA2 circuits. *Nature neuroscience* 17: 269-79

Kron MM, Zhang H, Parent JM. 2010. The developmental stage of dentate granule cells dictates their contribution to seizure-induced plasticity. *The Journal of neuroscience : the official journal of the Society for Neuroscience* 30: 2051-9

Li Z, Murthy VN. 2001. Visualizing postendocytic traffic of synaptic vesicles at hippocampal synapses. *Neuron* 31: 593-605

Llorens-Martin M, Jurado-Arjona J, Avila J, Hernandez F. 2015. Novel connection between newborn granule neurons and the hippocampal CA2 field. *Experimental neurology* 263: 285-92

McAuliffe JJ, Bronson SL, Hester MS, Murphy BL, Dahlquist-Topala R, et al. 2011. Altered patterning of dentate granule cell mossy fiber inputs onto CA3 pyramidal cells in limbic epilepsy. *Hippocampus* 21: 93-107

Mello LE, Cavalheiro EA, Tan AM, Kupfer WR, Pretorius JK, et al. 1993. Circuit mechanisms of seizures in the pilocarpine model of chronic epilepsy: cell loss and mossy fiber sprouting. *Epilepsia* 34: 985-95

Overstreet-Wadiche LS, Bensen AL, Westbrook GL. 2006a. Delayed development of adult-generated granule cells in dentate gyrus. *The Journal of neuroscience : the official journal of the Society for Neuroscience* 26: 2326-34

Overstreet-Wadiche LS, Bromberg DA, Bensen AL, Westbrook GL. 2006b. Seizures accelerate functional integration of adult-generated granule cells. *The Journal of neuroscience : the official journal of the Society for Neuroscience* 26: 4095-103

Pollard H, Khrestchatisky M, Moreau J, Ben-Ari Y, Represa A. 1994. Correlation between reactive sprouting and microtubule protein expression in epileptic hippocampus. *Neuroscience* 61: 773-87

Scharfman HE, Sollas AL, Berger RE, Goodman JH. 2003. Electrophysiological evidence of monosynaptic excitatory transmission between granule cells after seizure-induced mossy fiber sprouting. *Journal of neurophysiology* 90: 2536-47

Scheibel ME, Crandall PH, Scheibel AB. 1974. The hippocampal-dentate complex in temporal lobe epilepsy. A Golgi study. *Epilepsia* 15: 55-80

Schwarzer C, Williamson JM, Lothman EW, Vezzani A, Sperk G. 1995. Somatostatin, neuropeptide Y, neurokinin B and cholecystokinin immunoreactivity in two chronic models of temporal lobe epilepsy. *Neuroscience* 69: 831-45

Sutula T, Zhang P, Lynch M, Sayin U, Golarai G, Rod R. 1998. Synaptic and axonal remodeling of mossy fibers in the hilus and supragranular region of the dentate gyrus in kainate-treated rats. *The Journal of comparative neurology* 390: 578-94

Sutula TP, Dudek FE. 2007. Unmasking recurrent excitation generated by mossy fiber sprouting in the epileptic dentate gyrus: an emergent property of a complex system. *Progress in brain research* 163: 541-63

Tauck DL, Nadler JV. 1985. Evidence of functional mossy fiber sprouting in hippocampal formation of kainic acid-treated rats. *The Journal of neuroscience : the official journal of the Society for Neuroscience* 5: 1016-22

tom Dieck S, Sanmarti-Vila L, Langnaese K, Richter K, Kindler S, et al. 1998. Bassoon, a novel zinc-finger CAG/glutamine-repeat protein selectively localized at the active zone of presynaptic nerve terminals. *The Journal of cell biology* 142: 499-509

Toscano-Silva M, Gomes da Silva S, Scorza FA, Bonvent JJ, Cavalheiro EA, Arida RM. 2010. Hippocampal mossy fiber sprouting induced by forced and voluntary physical exercise. *Physiology & behavior* 101: 302-8

Umemori H, Linhoff MW, Ornitz DM, Sanes JR. 2004. FGF22 and its close relatives are presynaptic organizing molecules in the mammalian brain. *Cell* 118: 257-70

van Praag H, Schinder AF, Christie BR, Toni N, Palmer TD, Gage FH. 2002. Functional neurogenesis in the adult hippocampus. *Nature* 415: 1030-4

Walter C, Murphy BL, Pun RY, Spieles-Engemann AL, Danzer SC. 2007. Pilocarpine-induced seizures cause selective time-dependent changes to adult-generated hippocampal dentate granule cells. *The Journal of neuroscience : the official journal of the Society for Neuroscience* 27: 7541-52

Xu B, McIntyre DC, Fahnestock M, Racine RJ. 2004. Strain differences affect the induction of status epilepticus and seizure-induced morphological changes. *The European journal of neuroscience* 20: 403-18

Zhao C, Teng EM, Summers RG, Jr., Ming GL, Gage FH. 2006. Distinct morphological stages of dentate granule neuron maturation in the adult mouse hippocampus. *The Journal of neuroscience : the official journal of the Society for Neuroscience* 26: 3-11

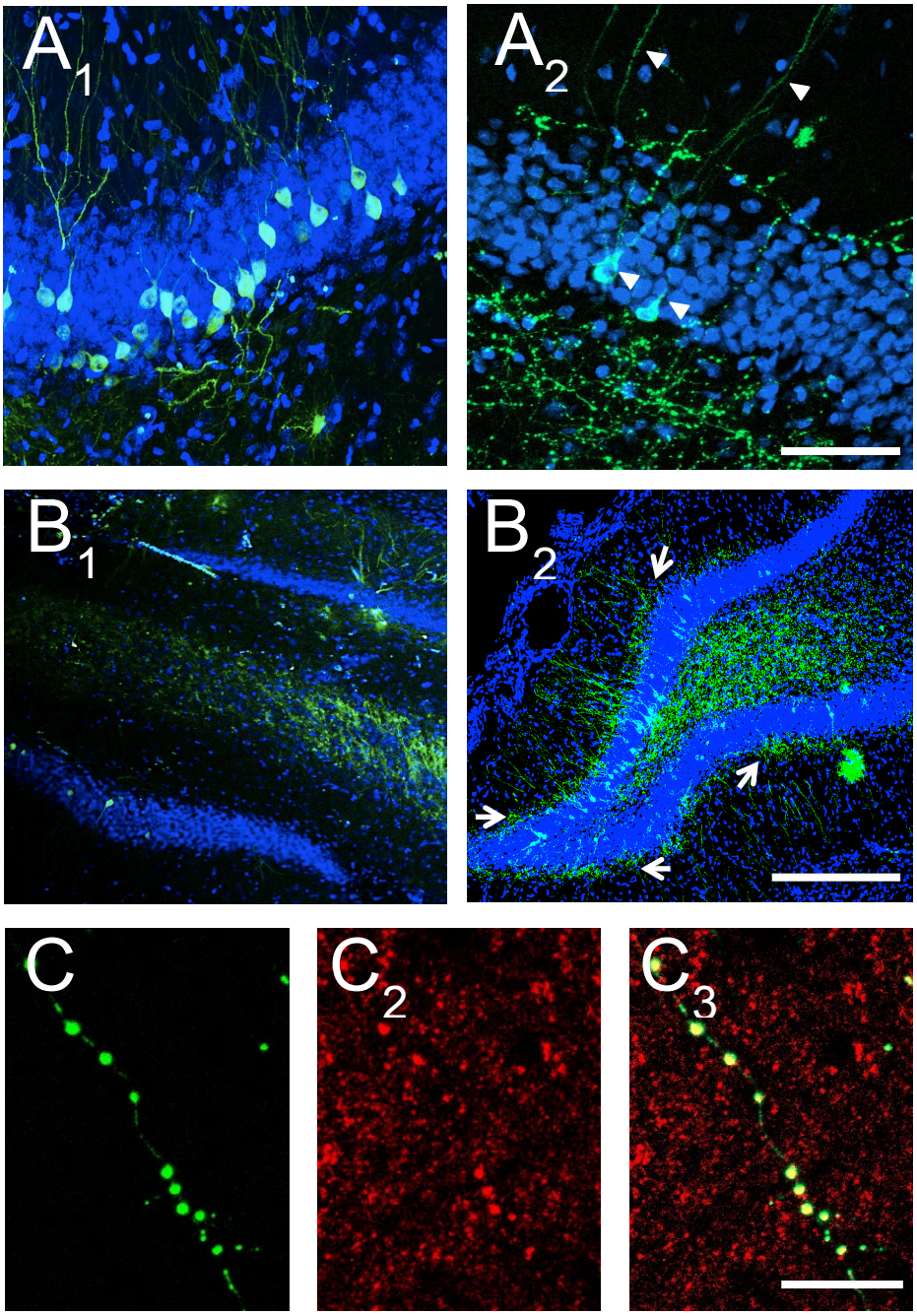

Figure 3.1 The syp-YFP RV allows better resolution of small MF boutons in the hilus and IML of the DGC as compared to eGFP RV. Blue channel is Hoescht, green channel is YFP or GFP, and red channel is bassoon. **A**. 40x confocal z-stacks of **A_1)** eGFP or **A_2)** syp-YFP expressing DGCs from a SE-treated animal. Note the lack of hilar axon labeling of eGFP expressing cells as compared to syp-YFP expressing cells. Arrows indicate MFS in the IML. Arrowheads indicate dendritic and somatic labeling from syp-YFP overexpression. Scale bar = 50 μm **B.** Representative images (10x objective) from rats that experienced SE and 4 days later received injections of **B_1)** eGFP or **B_2)** syp-YFP RV to label DGC

progenitors. Rats were euthanized 8 weeks later. MFS and hilar boutons can be detected at this magnification from DGCs that express syp-YFP (**B_2**). Arrows indicate MFS in the IML. Scale bar = 250 μm **C.** Confocal z-stack images obtained with a 63x objective and 2x optical zoom of a hilar axon segment from a syp-YFP expressing DGC. **C_1)** YFP alone **C_2)** Bassoon, a pre-synaptic terminal maker. **C_3)** YFP/Bassoon overlay showing co-localization of YFP and bassoon in boutons.

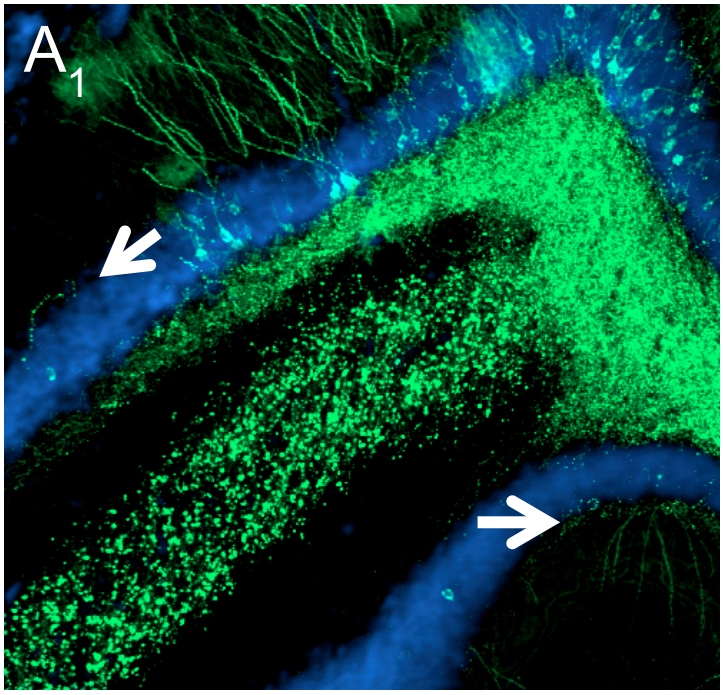
A1

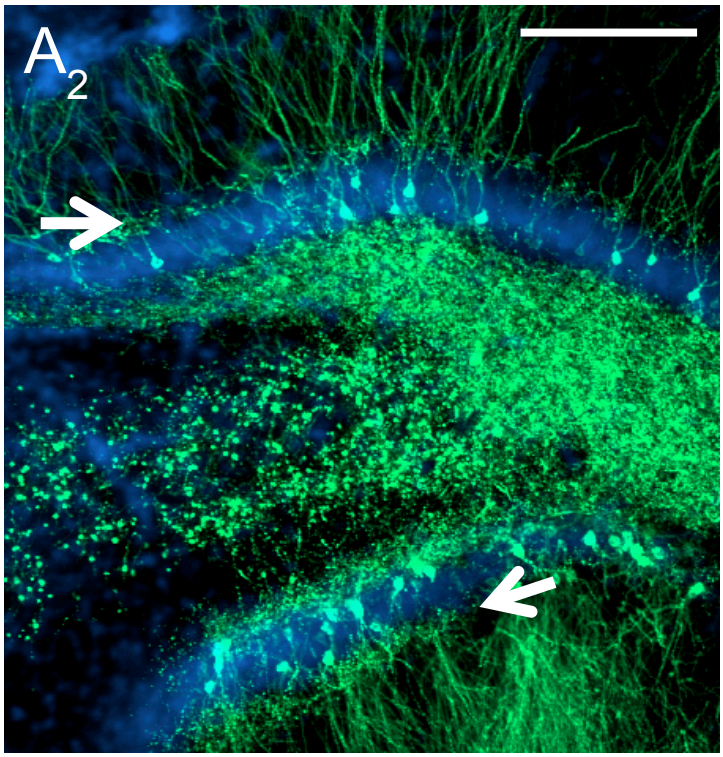
A2

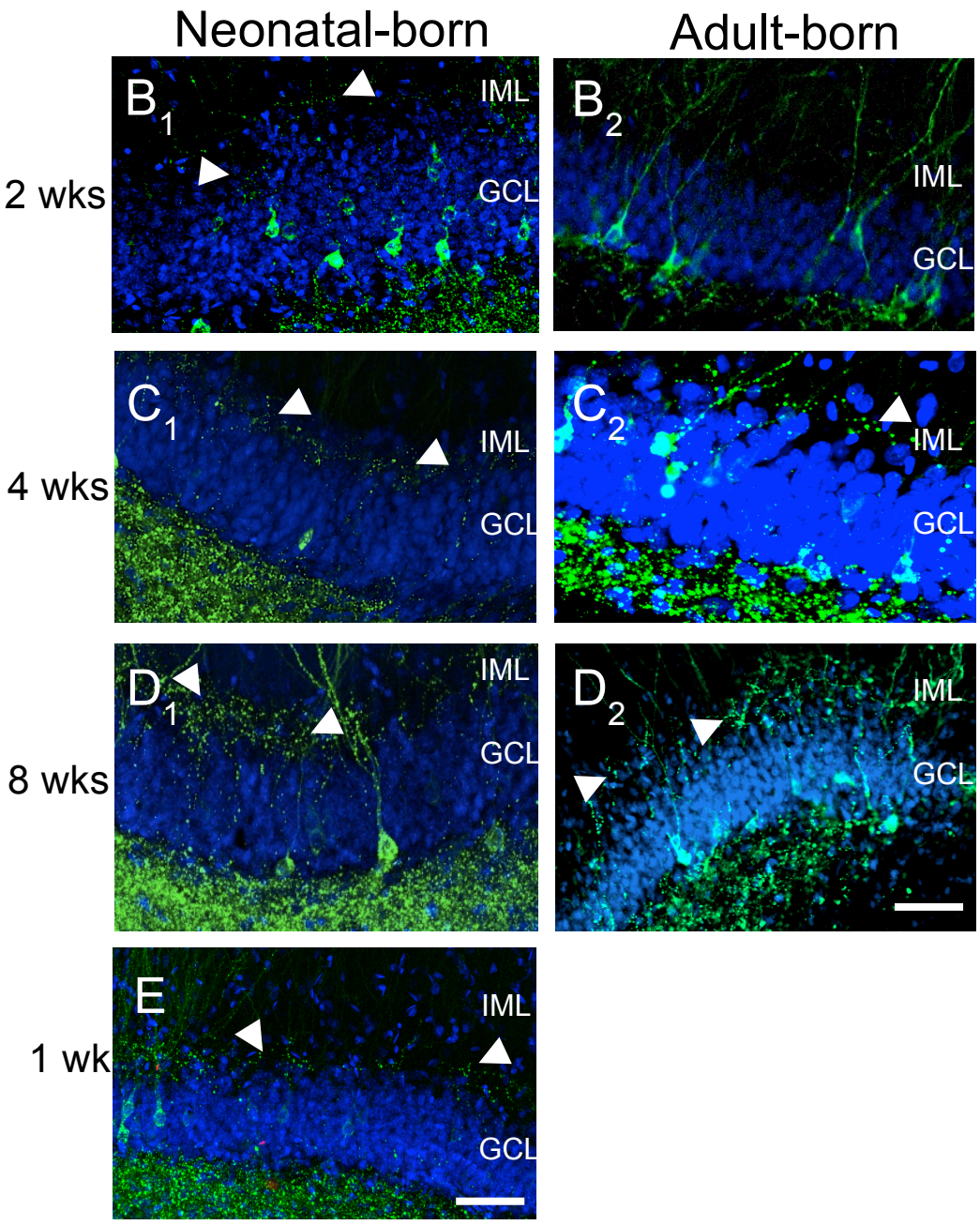

Figure 3.2 Both neonatal- and adult-born DGCs contribute to MFS in the IML. **A.** 10x images of **A_1)** neonatal-born and **A_2)** adult-born DGCs showing syp-YFP labeling of putative axon terminals in the IML. Scale bar = 250 μm **B-D.** 20x images showing neonatal-born and adult-born DGCs at **B)** 2 weeks, **C)** 4 weeks, and **D)** 8 weeks post SE. Arrowheads indicate putative axon terminals in the IML. Note the absence of labeling in **B_2** at 2 weeks post SE for adult-born DGCs. **E.** 20x image of neonatal born DGCs at 1 week post SE. Arrowheads indicate IML labeling. Scale bar = 50 μm.

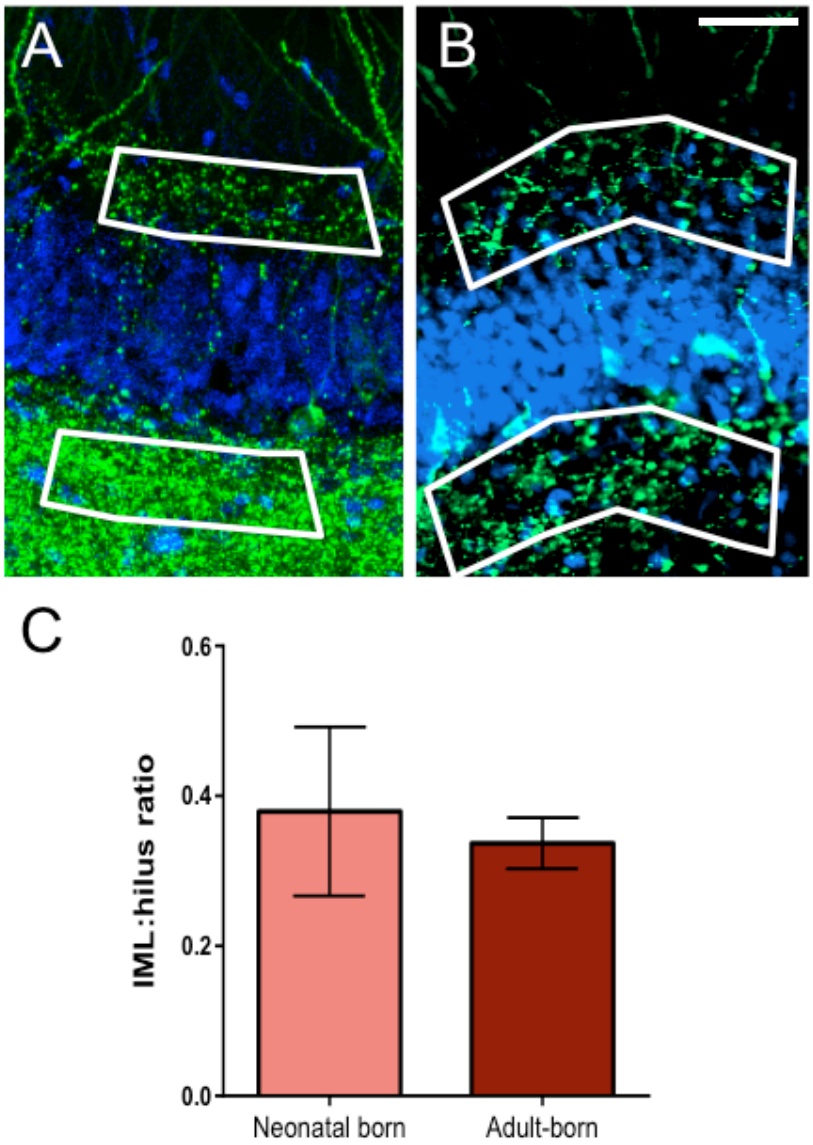

Figure 3.3 Neonatal-born and adult-born DGC populations contribute to a similar degree to MFS in the IML. **A.** MFS in the IML from neonatal-born DGCs. **B.** MFS in the IML from adult-born DGCs. White outlines indicate ROI segments which were measured for number of labeled pixels and compared to determine MFS ratio for that section and correct for variability in the degree of labeling. Scale bar = 50 μm. **C.** Histogram of mean MFS ratio for neonatal-born and adult-born DGCs. The means of the two populations were not significantly different (p = 0.65, student's t-test).

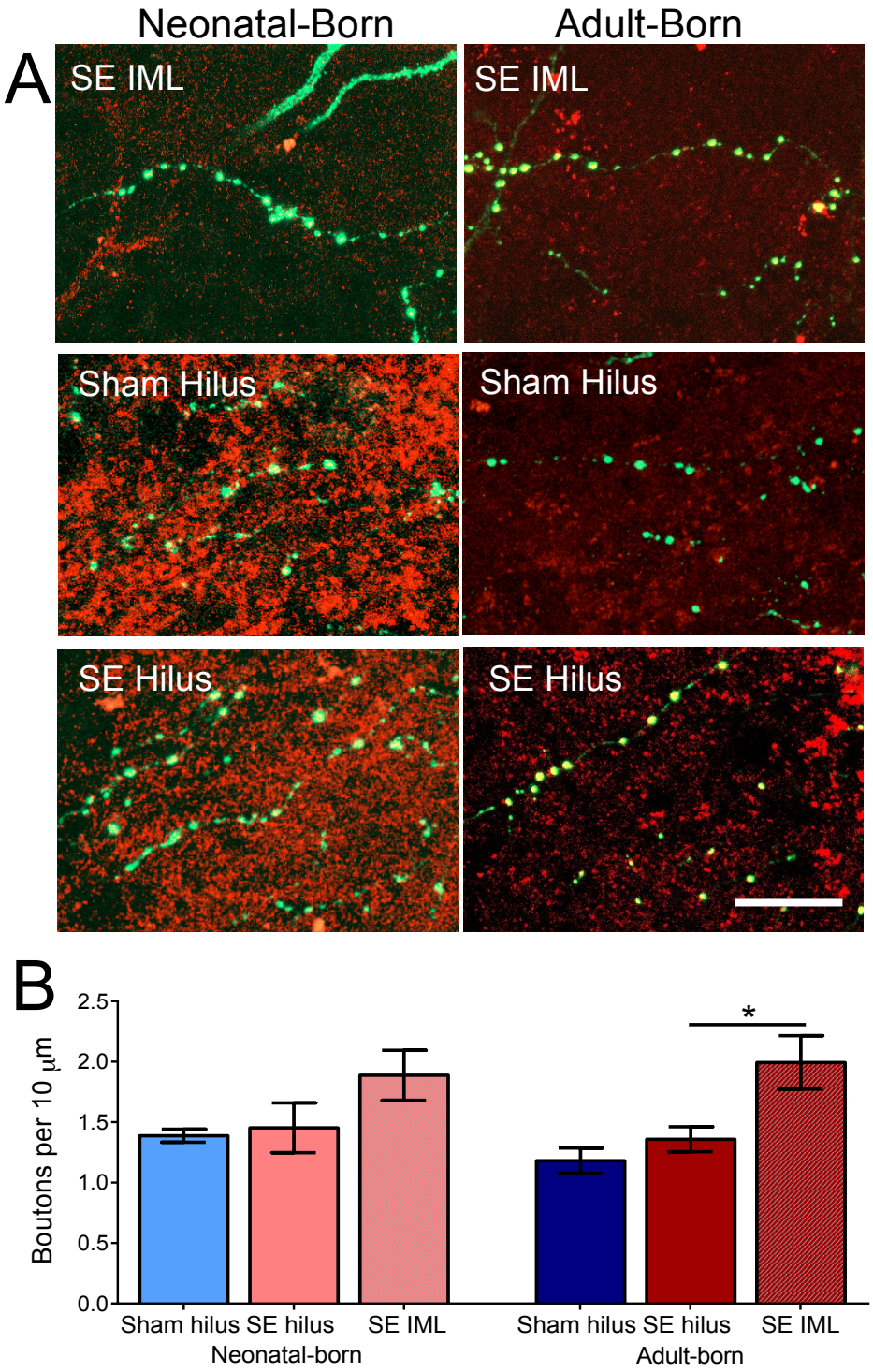

Figure 3.4 Hilar bouton density is not influenced by SE or DGC birthdate, but adult-born DGCs have increased bouton density in the IML than in the hilus after SE. **A.** Representative images of axon segments from each respective group. All images are z-projections from confocal stacks acquired with a 63x objective at 2x optical zoom. Bassoon labeling is the red channel, syp-YFP labeling is in the

green channel. Scale bar = 20 μm. **B.** Histograms of average bouton density. The increase in density for IML boutons compared to hilar boutons of adult-born DGCs in SE tissue is statistically significant ($p = 0.03$, one-way ANOVA, Sidak's multiple comparisons test.

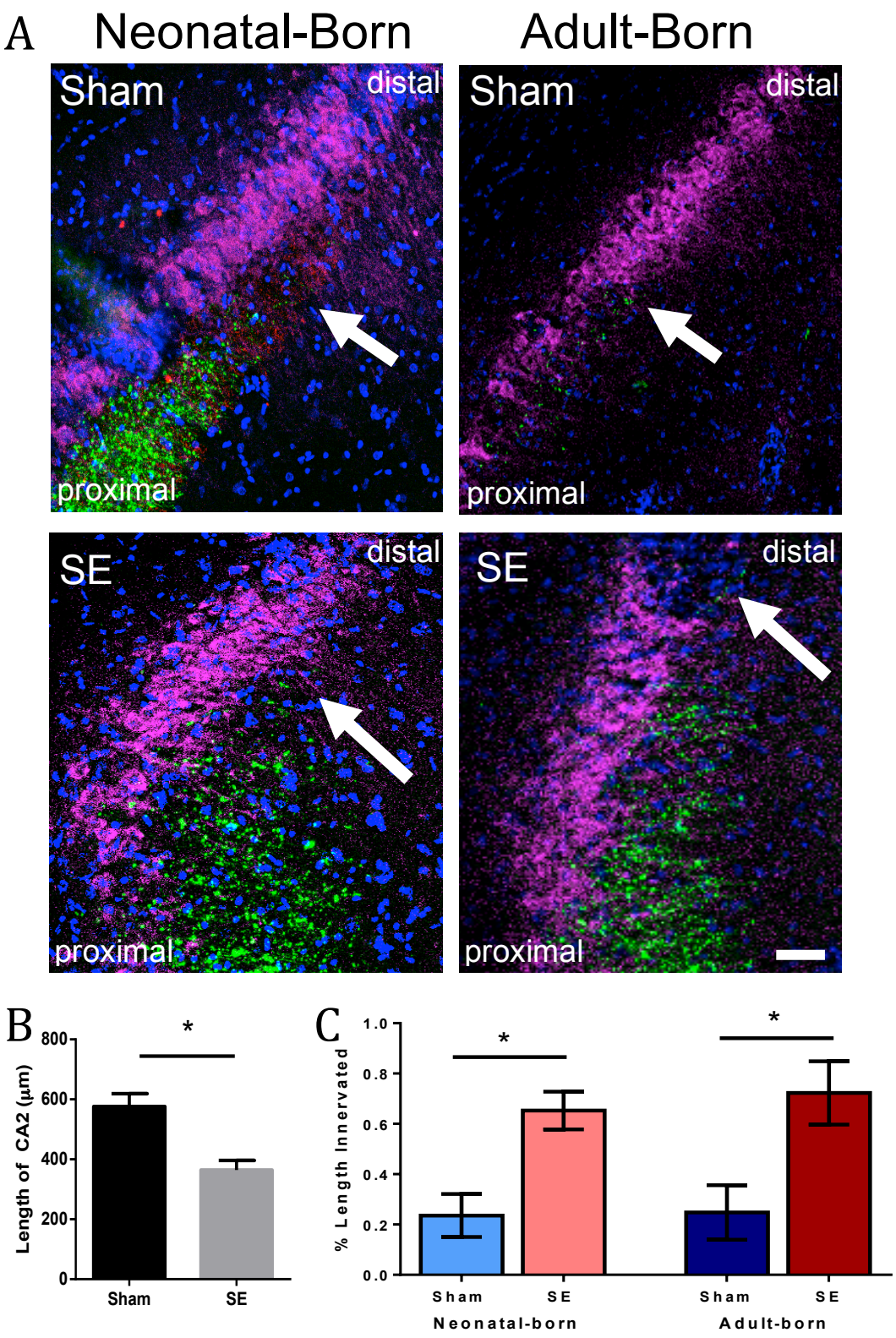

Figure 3.5 Seizures are associated with CA2 damage and cell death. Axon terminals from both neonatal-born and adult-born DGCs extend further into CA2 after SE. **A.** Representative images from all four groups (acquired with 10x

objective) of syp-YFP labeling into CA2. White arrows indicate the location where syp-YFP labeling ends in CA2. Proximal refers to the CA3-CA2 border, distal refers to the CA2-CA1 border. STEP labeling is in the purple channel, Hoescht nuclear stain is in the blue channel, syp-YFP labeling is in the green channel. Scale bar = 50 μm. **B.** Graph showing total length of CA2 in sham and SE (data from sham and SE animals for this measurement were not separated according to age at RV injection). There was a significant reduction in size of CA2 for SE animals ($p = 0.0006$, student's t-test). **C.** Graph showing percent, by length, of CA2 that is innervated by syp-YFP labeled terminals. The differences were significant between SE vs sham treated animals for both neonatal born and adult-born DGCs, but there was no difference among sham or SE animals ($p = 0.01$ one-way ANOVA, Sidak' multiple comparisons test).

Chapter 4

Electrophysiological properties of age-defined dentate granule cells in a rodent model of temporal lobe epilepsy.

Summary

Dysregulated hippocampal neurogenesis is a prominent feature of temporal lobe epilepsy (TLE). Anatomical data indicate that most dentate granule cells (DGCs) generated in response to an epileptic insult develop features that promote increased excitability, including ectopic location, persistent hilar basal dendrites (HBDs) and mossy fiber sprouting (Jessberger et al 2007, Kron et al 2010, Walter et al 2007). However, some appear to integrate normally, and even exhibit reduced excitability compared to other DGCs (Jakubs et al 2006, Murphy et al 2011). Using a retroviral (RV) enhanced green fluorescent protein (eGFP) reporter to birthdate DGCs, our laboratory found that DGCs that were mature at status epilepticus (SE) were resistant to morphological abnormalities, while the majority of those born after SE display TLE-related pathology (Kron et al 2010). This may suggest that post-SE generated DGCs promote pathological function while established DGCs retain normal function. Much of what is known about aberrant DGC neurogenesis comes from anatomical data; relatively few studies have investigated the physiological properties of age-defined cells. To examine the relationship between DGC age and activity within an epileptic network, we

recorded from RV birth-dated DGCs born either neonatally, or during adulthood in an epileptic or intact animal. We found that, in TLE tissues, both adult-born and neonatal-born populations of DGCs appear to receive increased excitatory input compared with age-matched controls in intact tissues. Furthermore, adult-born DGCs that display aberrant morphology in TLE tissue receive more excitatory input than their normotopic counterparts in TLE.

Introduction

Since it was discovered that seizures potently upregulate dentate granule cell (DGC) neurogenesis, many studies have investigated the role of post-seizure born DGCs in epileptogenesis (Scharfman & McCloskey 2009). A considerable amount of anatomical data has implicated DGCs that are developing after an epileptogenic insult as the likeliest to drive hyperexcitability of the dentate gyrus network (Althaus & Parent 2014, Scharfman & McCloskey 2009). Importantly, this population is an exceptionally heterogeneous group; some DGCs born post-insult appear morphologically normal, while others have a variety of dendritic, axonal, and somatic abnormalities (Jessberger et al 2007, Kron et al 2010, Murphy et al 2011, Walter et al 2007). This is in contrast to cells that are mature at the onset of epileptogenesis, which primarily maintain normal morphology (Kron et al 2010, Walter et al 2007).

One recent study suggested that these post-insult born DGCs exhibit reduced excitatory and increased inhibitory synaptic inputs when compared to

cells that were presumably mature at insult, thereby having a net homeostatic effect on network excitability (Jakubs et al 2006). However, this study did not include ectopically integrated DGCs, which comprise up to 25% of post-injury born DGCs (Kron et al 2010, Walter et al 2007). In a different study, which did not report DGC age, ectopic cells were found to receive a greater proportion of excitatory inputs, relative to normotopic DGCs (Zhan et al 2010). In addition, ectopic DGCs exhibited greater intrinsic excitability when compared to age-matched normotopic DGCs in SE and sham tissue (Scharfman et al 2000, Zhan & Nadler 2009).

While individual DGCs may contribute to network excitability in a variety of heterogeneous ways, identifying subpopulations that are particularly prone to hyperexcitability may help to identify therapeutic windows and potential treatments. Therefore, the goal of the study described in this chapter is to better understand the relationship between age, morphology, and excitability of individual DGCs in a model of TLE. To investigate this question, we birthdated DGC cohorts with a GFP-expressing retrovirus (GFP-RV) and recorded the excitatory synaptic inputs onto DGCs from epileptic or sham-treated animals. These experiments are part of an ongoing investigation and will be combined with additional excitatory data as well as recordings of inhibitory synaptic inputs onto the same cohorts of cells.

Methods

Animals

Animal procedures were performed using protocols approved by the University Committee on Use and Care of Animals of the University of Michigan. Animals were purchased from Charles River and kept under a constant 12 hour light/dark cycle with access to food and water *ad libitum.* Epileptic animals and sham controls were generated as described previously (Kron et al 2010). Briefly, postnatal day 56 (P56) male Sprague Dawley rats were pretreated with atropine methylbromide (5 mg/kg i.p.; Sigma) 20 minutes prior to pilocarpine hydrochloride (340 mg/kg i.p.; Sigma) for epileptic animals, or an equivalent volume of 0.9% saline for sham animals. After 90 minutes of SE, seizures were terminated with diazepam (10 mg/kg i.p.; Hospira Inc). Sham controls were treated with diazepam two hours after the saline injection. Acute slice recordings were made 3-5 months after SE/sham treatment.

Bilateral intrahippocampal RV

Animals were injected with GFP-YFP RV bilaterally into the dentate gyrus at either P7 or P60 as described previously (Kron et al 2010). Briefly, to label neonatal-born DGCs, male P7 rat pups were anesthetized on ice and placed on an ice cold neonatal rat stereotax adaptor (Stoelting) in a Kopf stereotaxic frame. Bilateral burr holes were drilled in the skull and 1 μl of RV was injected, using a Hamilton syringe and microinjection pump, at 0.1 μl/min into each hemisphere with the following coordinates (in mm from bregma and mm below the skull): caudal 2.0, lateral 1.5, deep 2.7. To label adult-born (AB) DGCs, P60 male rats

were anesthetized with a ketamine/xyelzine mixture and placed in a Kopf stereotaxic frame. Bilateral burr holes were drilled in the skull and 2.5 μl of RV was injected at 0.1 μl/min into each hemisphere with the following coordinates (in mm from bregma and mm below the skull): caudal 3.9, lateral 2.3, deep 4.2.

Slice preparation

Animals were anesthetized with isoflourane (Vet One) and transcardially perfused for 60 seconds with ice-cold cutting solution containing (mM): 206 sucrose, 2.8 KCl, 1 $MgCl_2 \cdot 6H_2O$, 1.25 NaH_2PO_4, 1 $CaCl_2$, 10 D-Glucose, 26 $NaHCO_3$, 0.4 Ascorbic Acid (pH 7.4). After decapitation, brains were rapidly removed and rested for 2 minutes in ice cold oxygenated, cutting solution. Brains were then blocked to isolate the hippocampus and 400 μm-thick coronal slices were cut with a vibrating blade microtome (VT1000S, Leica Microsystems Inc) in ice cold, oxygenated cutting solution. Slices were allowed to recover for 15 minutes in 34^0C, oxygenated N-methyl D-glutamine (NMDG) based solution containing (mM): 92 NMDG (Sigma), 2.5 KCl, 1.2 NaH_2PO_4, 30 $NaHCO_3$, 20 HEPES, 25 Glucose, 5 sodium ascorbate (Sigma), 2 thiourea (Sigma), 3 sodium pyruvate (Gibco Life Technologies), 10 $MgSO_4 \cdot 7H_2O$ (Sigma), 0.5 $CaCl_2 \cdot 2H_2O$. (pH adjusted to 7.35 with 10N HCl). We find that recovery in this solution provides a significant improvement in the health of slices made from aged, epileptic rats (Zhao et al 2011). Slices were then rested for at least 1 hour at room temperature in aCSF containing (mM): 124 NaCl, 2.8 KCl, 2 $MgSO_4$, 1.25 NaH_2PO_4, 2 $CaCl_2$, 10 D-Glucose, 26 $NaHCO_3$, 0.4 Ascorbic acid (pH 7.4) before

being transferred individually to the recording chamber and continuously perfused (~1.5mL/min) with oxygenated aCSF heated to 32^0C. To record spontaneous EPSCs (sEPSCs), 100 μm picrotoxin (PTX) was added to the aCSF, to record mini EPSCs (mEPSCs), 100 μm PTX and 1 μm tetrodotoxin (TTX) were added to the aCSF.

Electrophysiological recordings and analysis

GFP+ DGCs were first identified under epifluorescence (525 nm emission filter), then visualized and patched using infrared differential interference contrast (IR-DIC) optics. Recordings were obtained using borosilicate glass electrodes (Sutter Instruments) with a 4-7 MΩ open tip resistance. Pipettes contained 0.3% biocytin (Sigma) in cesium gluconate-based internal solution (in mM, all from Sigma): 100 Gluconic Acid, 0.2 EGTA, 5 $MgCl_2$, 40 HEPES, 2 Mg-ATP, 0.3 Na-GTP, pH to 7.2 with concentrated CsOH. A Dagan Cornerstone amplifier in bridge mode was used, and data were filtered at 3 kHz and digitized at 10 kHz. Data were acquired using pClamp 10.0 (Molecular Devices). Seal resistances of > 1 GΩ were achieved before breaking into whole cell mode. Once successful break-in was achieved, capacitance was compensated and series resistance was monitored. Cells were held at -70 mV. sEPSCs and mEPSCs were recorded gapfree for 5 minutes and analysis was performed off-line using MiniAnalysis 6.0 (Synaptosoft, Inc).

For both sEPSCs and mEPSCs, events were identified manually as having a fast rise time to a peak that was >3x the root mean square of the noise.

Statistical analysis was performed using using Prism 6.0 (GraphPad). Cumulative fractions were compared using a Kruskal-Wallis test, with Dunn's post-hoc correction for multiple comparisons and group means were compared using one-way ANOVA with Sidak's post-hoc correction for multiple comparisons.

Immunohistochemistry

Following recording, slices were immediately placed in 4% paraformaldehyde (Sigma) in phosphate buffered saline (PBS) (pH 7.4), and refrigerated for up to 1 week. For biocytin visualization, slices were rinsed with PBS and endogenous peroxidase activity was quenched with 0.1% hydrogen peroxide in 10% methanol and PBS. After a second wash in PBS, slices were permeabilized with 2% Triton X-100 (Sigma) in PBS and then incubated at room temperature in avidin/biotinylated enzyme complex (Vector Labs). After 1-2 days, slices were rinsed with PBS and then reacted with 3,3'-Diaminobenzidine (Invitrogen) until the cells could be visualized. Slices were slide-mounted before cresyl violet counterstaining and coverslipping. Images were acquired on a Leica DSM-IRB inverted microscope (Leica Microsystems Inc) connected to a SPOT Flex digital camera (SPOT Imaging Solutions).

Results

The results presented herein represent the preliminary findings of an investigation into how age and morphology affect the synaptic integration of

individual DGCs in a model of TLE. This work will be followed up during a post-doctoral position in Dr. Jack Parent's lab in collaboration with Drs. Geoffrey Murphy and Shannon Moore.

Identification of DGC morphology

GFP-expressing DGCs were identified under epifluorescence and patched under IR-DIC. To confirm correct targeting, we imaged the patched cell under both epilfluoresence and IR DIC (**Figure 4.1 A**) to see the electrode in the GFP+ cell. We observed cell morphologies in the live slices, and confirmed them with biocytin staining in a subset of cells. All cells with somas in the GCL that lacked HBDs were classified as normotopic. Cells born post-SE that had somas in the GCL and HBD were classified as HBD+, and those with somas in the hilus or molecular layer were classified as ectopic. Normotopic DGCs were found in slices from all groups, while HBD+ and ectopic cells were only collected from the adult-born, post-SE population (**Figure 4.1 B-F**). Under normal conditions, as DGCs mature and age, they migrate away from the sub-granular zone (SGZ), toward the molecular layers and populate the outer region of the GCL (Ma et al 2009). Therefore, in addition to GFP-expressing neonatal-born DGCs, an outer granule cell layer (OGCL) cohort was recorded from both SE and sham treated animals to assess synaptic input onto cells that should have been mature at the time of insult. OGCL cells displayed morphology similar to normotopic DGCs. DGCs from all groups were patched from the dentate gyrus (**Figure 4.2)**.

DGCs in TLE model tissue receive larger amplitude, greater frequency sEPSCs than DGCs in sham tissue

The amplitudes of individual sEPSCs were measured and plotted as both the cumulative fraction of all events as well as mean amplitudes for each cell. When we examined the effect of treatment (SE vs Sham), we observed a shift toward larger amplitude sEPSCs after SE for both neonatal- and adult-born DGCs relative their age-matched counterparts in sham tissue (**Figure 4.3 A**). When we examined the effect of age (neonatal- vs adult-born), we observed that the neonatal population exhibited a small number of sEPSCs that are much larger in amplitude than the adult-born population both after SE and in sham tissue. However, these events did not affect shape of the overlapping portion of the curves for either sham or seizure animals (**Figure 4.3 B**). Interestingly, there appeared to be no difference in the mean amplitudes for individual cells between any of the populations (**Figure 4.3$_{\text{insets}}$**).

Frequency was calculated as events per second for each cell, as well as interevent interval (IEI) for all events. IEI was plotted as the cumulative fraction and mean frequency was plotted as a bar graph. We found a similar effect of treatment on sEPSC frequency; both neonatal- and adult-born DGCs in SE tissue received more frequent sEPSC input when compared to birthdated DGCs in sham tissue. This was true for both IEI and mean cell frequency (**Figure 4.4 A, A$_{\text{inset}}$**). When we compared neonatal- to adult-born DGCs in sham tissue, we observed a slight shift toward shorter IEI for adult-born DGCs, but no difference

in mean cell frequency. The neonatal- and adult-born DGCs in SE tissue did not differ in either IEI or mean cell frequency (**Figure 4.4 B, B_{inset}**).

Ectopic and HBD+ DGCs exhibit the largest amplitude, highest frequency sEPSCs

We observed considerable variability in the mean amplitude and frequency of individual DGCs within the population of DGCs born after SE. To examine whether this was related to variability in DGC morphology among this population, we analyzed adult-born DGCs from SE tissue separated into normotopic, ectopic, and HBD+ DGC subgroups. We found that the normotopic population exhibits the lowest frequency (longest IEI) and smallest amplitude sEPSCs, while the ectopic and HBD+ populations both exhibit sEPSCs with larger amplitude and higher frequency (not different from each other) (**Figure 4.5 A,B**).

DGC position in the OGCL as a proxy for cell age

Prospectively birthdating DGCs born during the neonatal period is a powerful and reliable method of identifying cells that are mature in adulthood. We chose to use this method to identify DGCs that are mature at SE. However, another means of identifying cells that are likely mature at the time of SE is to record from cells in the OGCL. We recorded from this population in addition to the prospectively birthdated, neonatal-born population to replicate previously published experiments that exclusively used the OGCL population as the cohort

of mature DGCs (Jakubs et al 2006). In sham treated animals, amplitude and frequency of sEPSCs were different between the neonatal-born RV-labeled DGCs and the OGCL population. However, there was a slight rightward shift of OGCL DGCs in SE when compared to neonatal-born DGCs in SE (**Figure 4.6**). We hypothesize that it could be related to the fact that after SE the organization of the GCL can change in a variety of ways. There is often dispersion of the normally compact GCL and newborn DGCs can migrate aberrantly toward the molecular layer (Parent et al 2006). Therefore, this OGCL population in SE could be comprised of both cells mature at SE which retained an OGCL location, as well as cells born at any other time which are normotopically integrated, but do not truly belong to the mature population. Overall, we believe that these data support the of our prospective labeling approach and suggest that this is critical for studying the relationship between DGC age and features of TLE.

Adult-born, post-SE DGCs exhibit larger, more frequent mESPCs

sEPSCs are comprised of both TTX-insensitive and TTX-sensitive synaptic events, and therefore can include action potential-dependent neurotransmitter release. Miniature ESPCs (mEPSCs) are excitatory post-synaptic currents that are recorded in the presence of TTX to block voltage-gated sodium channels. When sESPC and mESPC data are considered together, it provides a better understanding of how cells are integrated into the network and whether the observed changes are the result of pre- or post-synaptic changes. Thus far, mEPSC data have only been acquired from a subset of the age- and

morphology-defined groups, but appear to be following a similar trend as the sEPSC data. Adult-born DGCs exhibited the largest and most frequent mEPSCs, as compared to neonatal-born and OGCL DGCs in SE tissue, and OGCL DGCs in sham tissue (**Figure 4.7**).

Discussion

The goal of this study is to determine how DGC age and morphology affect synaptic activity onto DGCs in a rat TLE model. We recorded both sEPSCs and mEPSCs from age-defined populations of DGCs in slices from SE and sham-treated animals. This work is ongoing, but our preliminary findings suggest that there is considerable heterogeneity among adult-born DGCs in SE, with aberrantly integrated cells exhibiting the largest, most frequent sEPSCs.

Thus far, we have observed an increase in sEPSC amplitude and frequency onto both neonatal- and adult-born DGCs from animals that underwent SE, which indicates an increase in excitatory input onto DGCs in the TLE model. The data are consistent with some previous reports of synaptic activity onto DGCs in various TLE models (Wuarin & Dudek 2001, Zhan et al 2010, Zhang et al 2012). Increases in excitatory input onto DGCs after SE can be observed early in epileptogenesis and become more pronounced as the disease progresses (Wuarin & Dudek 2001). We performed all experiments when animals were between 2.5 and 5 months of age, which allows sufficient time for adult-born DGCs to mature. Previous reports of sEPSCs and mEPSCs onto DGCs in the

GCL from animals with chronic epilepsy indicate a significant increase in both amplitude and frequency when compared to DGCs from sham animals (Wuarin & Dudek 2001, Zhan et al 2010). In addition, Zhan and colleagues recorded mESPCs onto hilar ectopic DGCs and found an even greater increase in frequency for this population (Zhan et al 2010). However, DGC age was unknown in these studies.

In order to specifically investigate adult-born DGCs in a rat TLE model, Jakubs and colleagues retrovirally birthdated DGCs after electrical SE or running control treatment. They found that adult-born DGCs in epileptic tissue received less excitatory synaptic input when compared to both unlabeled DGCs in epileptic tissue and to adult-born DGCs in control tissue (Jakubs et al 2006). From these data, they concluded that the post-SE born population serves a homeostatic function to dampen overall excitation within the network. Notably, nearly all of the adult-born cells in this study were normotopically integrated (2 had HBDs, none were ectopic) (Jakubs et al 2006).

Our data set provides evidence that may reconcile these two, seemingly disparate findings. We found that cells with aberrant morphology were driving much of the observed increase in excitatory input among the adult-born DGCs. Indeed, when we separated the this population into morphologically-defined subgroups, we found that ectopic and HBD+ DGCs have larger amplitude and higher frequency sEPSCs than normotopic post-SE born. In fact, we actually find that normotopic exhibit sEPSC amplitudes and frequency that are similar to adult-born DGCs in sham treated animals. Therefore, adult-born normotopic

DGCs receive reduced excitatory input, when compared to both adult-born DGCs with aberrant morphology and neonatal-born DGCs.

Larger EPSC amplitudes are thought to be driven by changes in post-synaptic channel density (O'Brien et al 1998), but this may be less applicable when measuring spontaneous currents, since larger amplitude currents could also result from the summation of multiple synaptic events. Similarly, more frequent events are believed to reflect pre-synaptic changes like greater release probability or the presence of more synapses (Redman 1990) but this cannot be determined from sEPSC data alone because increased frequency could be due to a more active network. In order to gain more insight into the mechanisms driving the changes we observe in sEPSCs, we began to record mESPCs from the same populations of DGCs. At this stage, we are finding that post-SE born DGCs exhibit the largest amplitude, highest frequency mEPSCs. However, it is important to note that there is considerable heterogeneity within this group, and due to our current small sample size, this conclusion should be adopted cautiously.

The data presented herein suggest an interesting relationship between DGC age, morphology, and synaptic excitability. Neonatal-born DGCs retain a mostly normal morphology, but still receive increased excitatory input when compared to same-aged DGCs in sham tissue. Adult-born DGCs that integrate in the GCL receive less excitatory input than same-aged DGCs with aberrant morphology but similar input when compared to same-aged DGCs in sham tissue. In addition to increasing the number of cells in each of these age and

morphologically defined groups, we will need to determine the spontaneous and miniature inhibitory inputs onto all populations. Understanding the balance of excitation and inhibition for these populations is required in order to assess the potential impact of these cell populations on the activity within the epileptic network.

References

Althaus AL, Parent JM. 2014. Role of adult neurogenesis in seizure-induced hippocampal remodeling and epilepsy. In *Endogenous Stem Cell-Based Brain Remodeling in Mammals*, ed. J M.-P., KS G. Boston, MA: Springer US : Imprint: Springer

Jakubs K, Nanobashvili A, Bonde S, Ekdahl CT, Kokaia Z, et al. 2006. Environment matters: synaptic properties of neurons born in the epileptic adult brain develop to reduce excitability. *Neuron* 52: 1047-59

Jessberger S, Zhao C, Toni N, Clemenson GD, Jr., Li Y, Gage FH. 2007. Seizure-associated, aberrant neurogenesis in adult rats characterized with retrovirus-mediated cell labeling. *The Journal of neuroscience : the official journal of the Society for Neuroscience* 27: 9400-7

Kron MM, Zhang H, Parent JM. 2010. The developmental stage of dentate granule cells dictates their contribution to seizure-induced plasticity. *The Journal of neuroscience : the official journal of the Society for Neuroscience* 30: 2051-9

Ma DK, Bonaguidi MA, Ming GL, Song H. 2009. Adult neural stem cells in the mammalian central nervous system. *Cell research* 19: 672-82

Murphy BL, Pun RY, Yin H, Faulkner CR, Loepke AW, Danzer SC. 2011. Heterogeneous integration of adult-generated granule cells into the epileptic brain. *The Journal of neuroscience : the official journal of the Society for Neuroscience* 31: 105-17

O'Brien RJ, Kamboj S, Ehlers MD, Rosen KR, Fischbach GD, Huganir RL. 1998. Activity-dependent modulation of synaptic AMPA receptor accumulation. *Neuron* 21: 1067-78

Parent JM, Elliott RC, Pleasure SJ, Barbaro NM, Lowenstein DH. 2006. Aberrant seizure-induced neurogenesis in experimental temporal lobe epilepsy. *Annals of neurology* 59: 81-91

Redman S. 1990. Quantal analysis of synaptic potentials in neurons of the central nervous system. *Physiological reviews* 70: 165-98

Scharfman HE, Goodman JH, Sollas AL. 2000. Granule-like neurons at the hilar/CA3 border after status epilepticus and their synchrony with area CA3 pyramidal cells: functional implications of seizure-induced neurogenesis. *The Journal of neuroscience : the official journal of the Society for Neuroscience* 20: 6144-58

Scharfman HE, McCloskey DP. 2009. Postnatal neurogenesis as a therapeutic target in temporal lobe epilepsy. *Epilepsy research* 85: 150-61

Walter C, Murphy BL, Pun RY, Spieles-Engemann AL, Danzer SC. 2007. Pilocarpine-induced seizures cause selective time-dependent changes to adult-generated hippocampal dentate granule cells. *The Journal of neuroscience : the official journal of the Society for Neuroscience* 27: 7541-52

Wuarin JP, Dudek FE. 2001. Excitatory synaptic input to granule cells increases with time after kainate treatment. *Journal of neurophysiology* 85: 1067-77

Zhan RZ, Nadler JV. 2009. Enhanced tonic GABA current in normotopic and hilar ectopic dentate granule cells after pilocarpine-induced status epilepticus. *Journal of neurophysiology* 102: 670-81

Zhan RZ, Timofeeva O, Nadler JV. 2010. High ratio of synaptic excitation to synaptic inhibition in hilar ectopic granule cells of pilocarpine-treated rats. *Journal of neurophysiology* 104: 3293-304

Zhang W, Huguenard JR, Buckmaster PS. 2012. Increased excitatory synaptic input to granule cells from hilar and CA3 regions in a rat model of temporal lobe epilepsy. *The Journal of neuroscience : the official journal of the Society for Neuroscience* 32: 1183-96

Zhao S, Ting JT, Atallah HE, Qiu L, Tan J, et al. 2011. Cell type-specific channelrhodopsin-2 transgenic mice for optogenetic dissection of neural circuitry function. *Nature methods* 8: 745-52

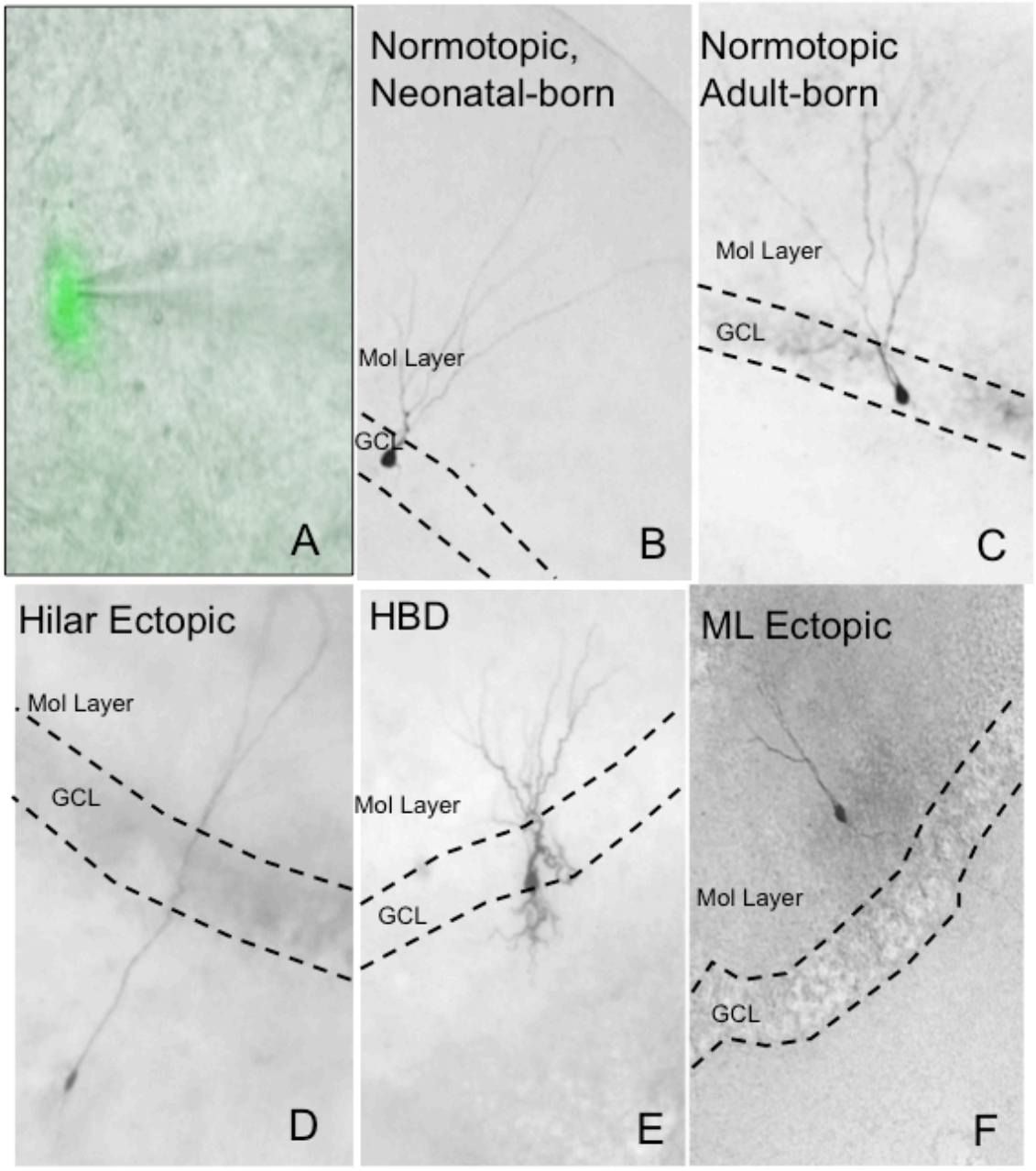

Figure 4.1 We visualized GFP labeling and ectopic location or presence of HBD online, and confirmed the morphology of biocytin-filled DGCs offline with immunohsitochemistry. All GFP labeled cells are identified under fluorescence and patched using IR-DIC. **A.** Overlay of the two images to confirms that we recorded from the target cell. **B-F:** Representative DGCs from each birthdate or morphology defined group, all from SE tissue **B.** Neonatal-born **C-F** adult-born. The morphology of neonatal-born was similar between sham and TLE tissue. The morphology of adult-born in sham tissue was similar to normotopic, adult-born in SE tissue.

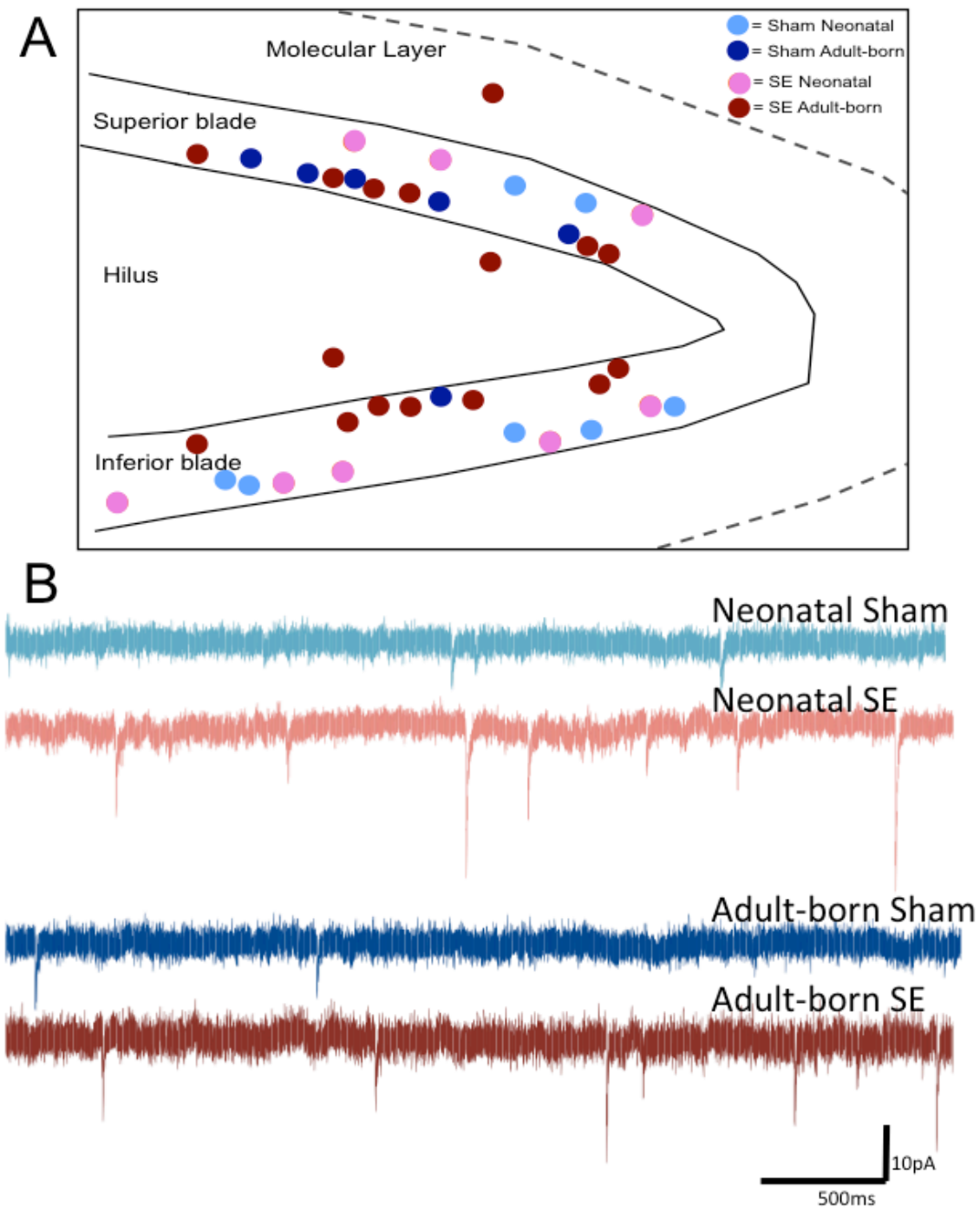

Figure 4.2 DGCs were patched from throughout the dentate gyrus for recording spontaneous activity. **A.** Schematic of the locations of a sample of cells from each of the birthdated populations. **B**. Representative traces for each of the birthdated populations.

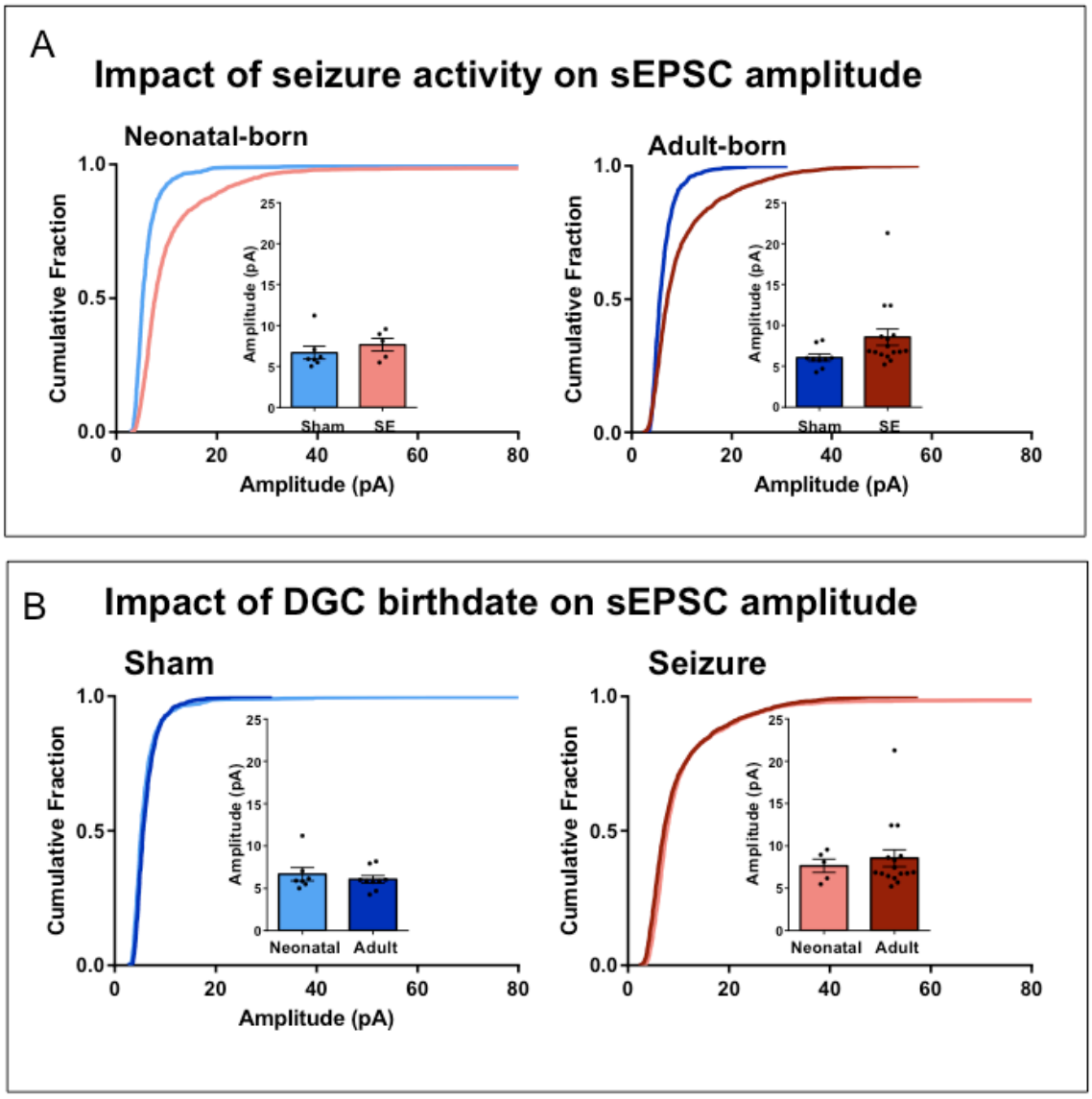

Figure 4.3 Both neonatal- and adult-born DGCs exhibited larger amplitude sEPSCs in TLE model tissue/ **A.** There was a rightward shift in the cumulative histogram comparing neonatal-born in sham to neonatal-born in SE as well as the histogram comparing adult-born in sham to adult-born in SE. This shift reached statistical significance for the adult-born populations ($p < 0.001$). **A_{inset}.** There was a trend toward larger mean amplitude as measured by cells when comparing adult-born SE to adult-born sham. **B.** The cumulative fraction curves for neonatal- and adult-born in sham and for neonatal- and adult-born in SE overlap except for a small fraction of sEPSC very large events in the neonatal-born populations for both treatment conditions. **B_{inset}.** The cell mean values did not differ for any groups.

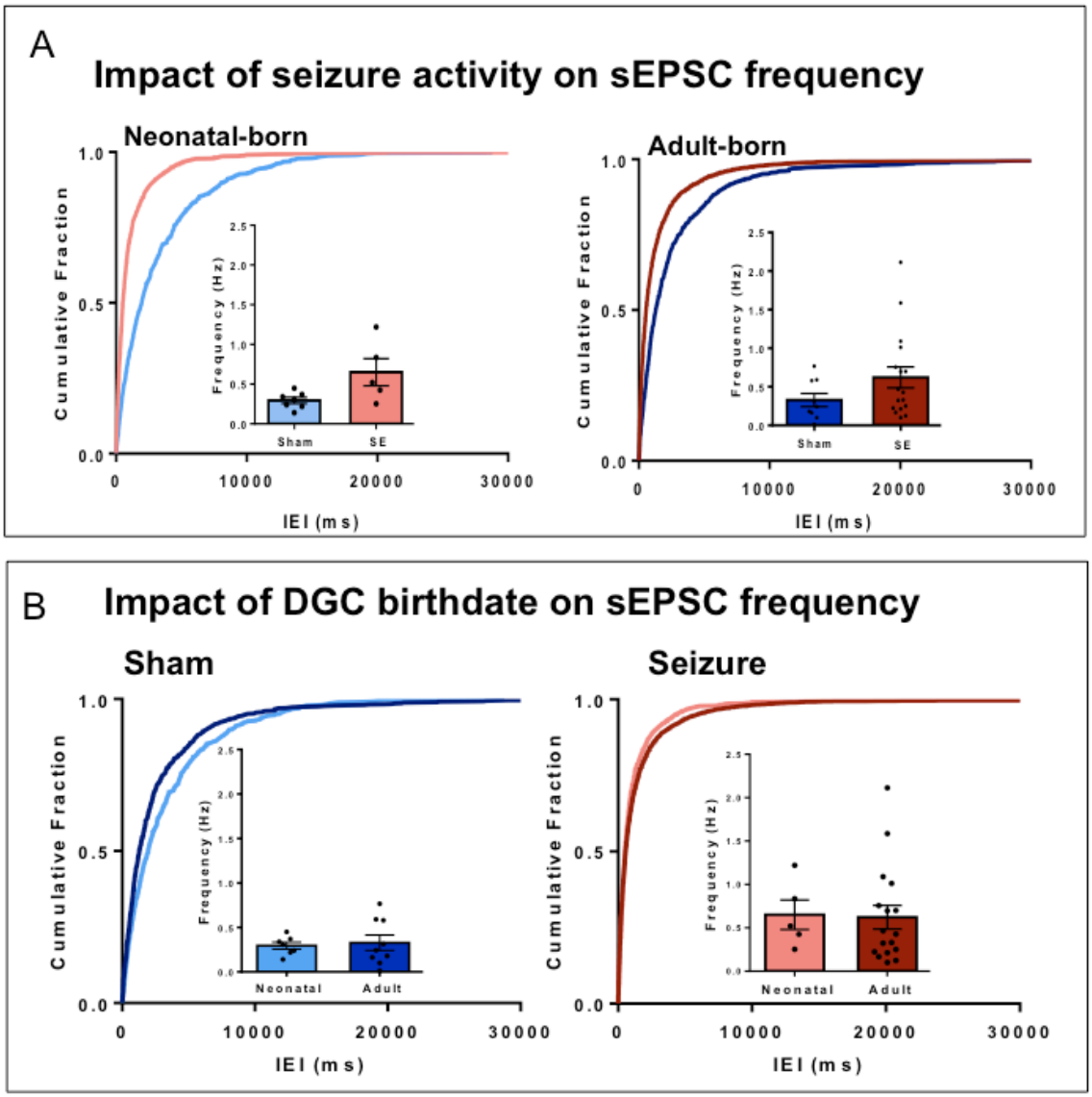

Figure 4.4 DGCs in SE tissue exhibited more frequent sEPSCs when compared to same-age DGCs in sham tissue. **A.** There was a leftward shift in the cumulative histograms when comparing neonatal-born in sham to neonatal-born in SE and adult-born in sham to adult-born in SE (**inset)**. Further, there was a trend (which does not reach statistical significance) toward more frequent sEPSCs when comparing cell means between these groups. **B.** There was a slight leftward shift in the cumulative histogram for adult-born DGCs compared to neonatal-born in sham tissue, but no difference in cell means (**inset**). The cumulative histogram and cell means were not different when comparing neonatal- and adult-born DGCs in SE tissue.

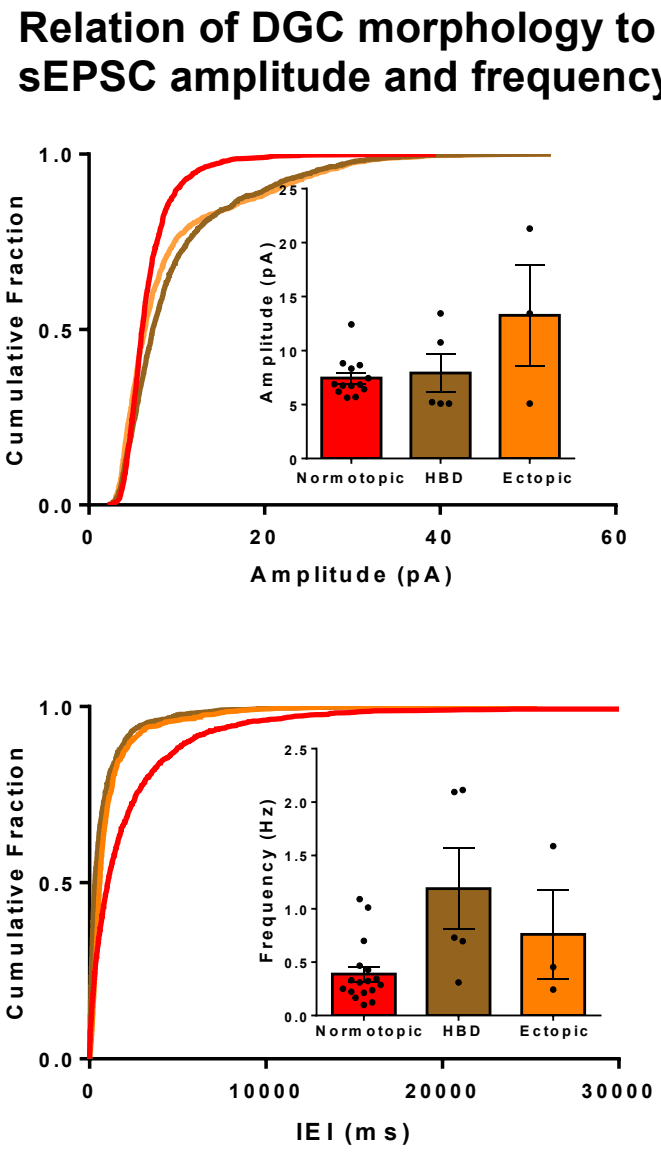

Figure 4.5 When the adult-born, post-SE DGC population was separated into subgroups according to morphology, the cumulative frequency plots of DGCs with HBD or ectopic soma were right-shifted for amplitude, indicating larger amplitude, and left-shifted for IEI, indicating higher frequency. The cell mean values for both amplitude and frequency were highly variable for all groups.

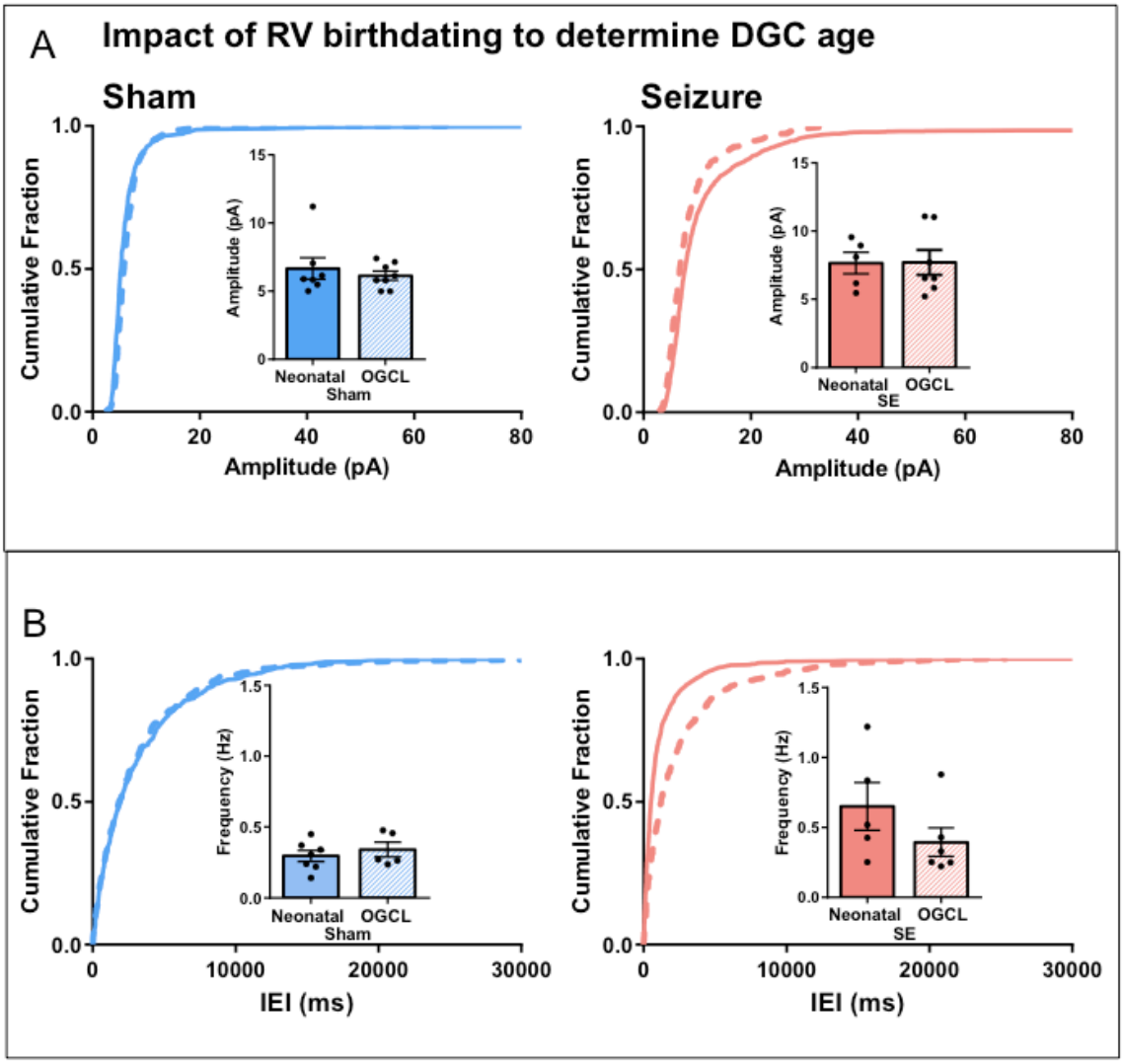

Figure 4.6 OGCL DGCs are not necessarily equivalent to prospectively birthdated NB DGCs. **A.** sEPSC amplitude was similar for neonatal-born and OGCL DGCs from sham, but slightly right-shifted for the neonatal-born population compared to OGCL DGCs in SE. Cell means for amplitude were not different between any of the groups (**insets**). **B.** IEI was similar for neonatal-born and OGCL DGCs from sham, but slightly left-shifted for the neonatal-born compared to OGCL populations in SE. The mean frequency also tended to be greater for neonatal-born compared to OGCL in SE tissue, but not different in sham tissue (**insets)**.

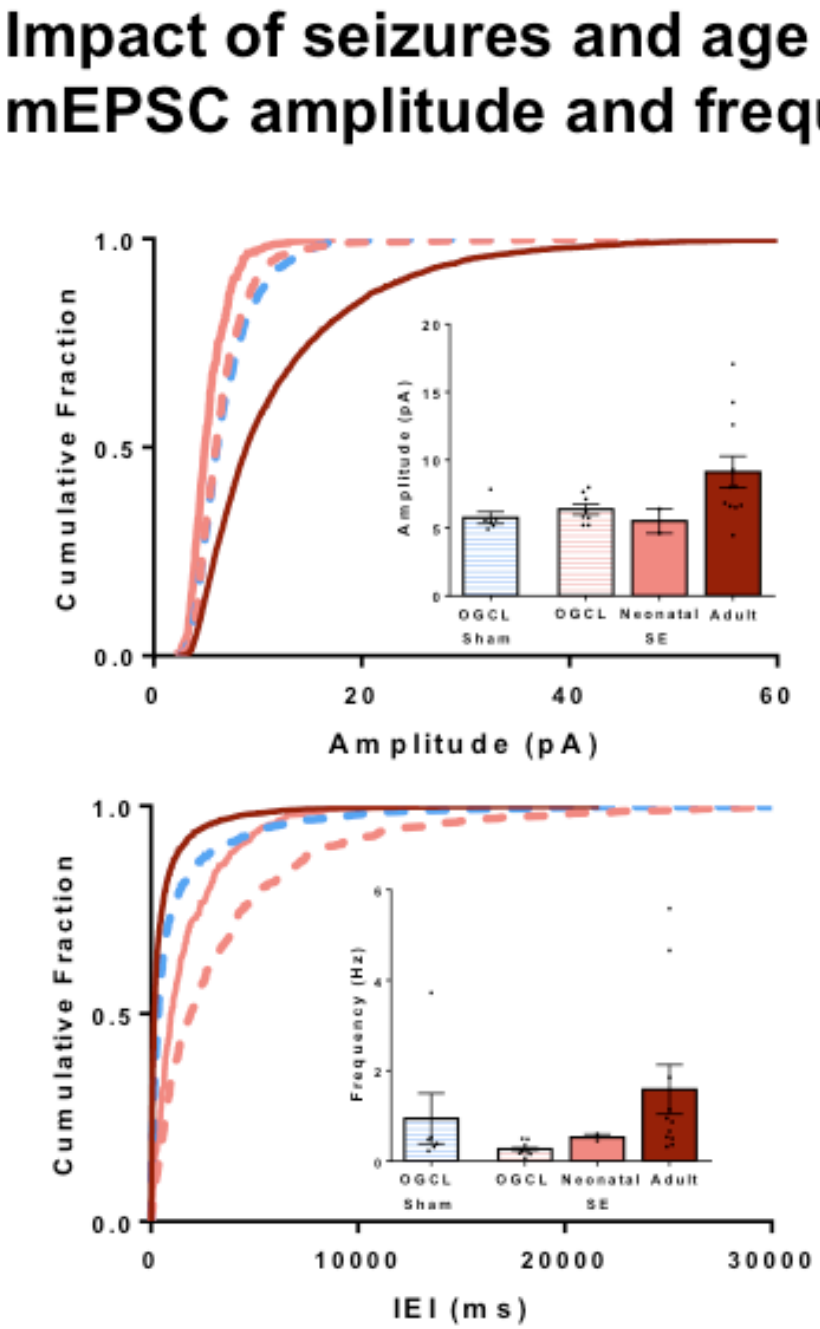

Figure 4.7 Adult-born DGCs exhibited largest amplitude, highest frequency mEPSCs of any groups measured thus far, but outliers were present in both OGCL sham and adult-born SE populations. Further work will be necessary to determine the significance of these observations.

Chapter 4

Discussion

Summary of results

Pathphysiological changes of dentate granule cells (DGCs) in temporal lobe epilepsy (TLE) appear to function as a positive feedback loop, with increased network activity eliciting DGC plasticity, which, in turn, increases the activity of the network. However, it is not yet known how the various aspects of seizure-related plasticity individually affect network excitability. Some may be homeostatic or neutral, in which case interfering with these aspects of seizure-related induced plasticity could exacerbate seizures. The long-term goal of the experiments described in this dissertation is to understand the relationship between ongoing DGC neurogenesis and epileptogenesis in TLE. The results of the completed and ongoing studies indicate that, while adult neurogenesis impacts the development of aberrant circuits in TLE, the mature, pre-existing population of DGCs also contributes to seizure-related plasticity and aberrant connectivity.

MFS involves axons of both neonatal- and adult-born DGCs

MFS into the dentate gyrus inner molecular layer (IML), which creates novel excitatory connections between DGCs, is hypothesized to participate in the generation or spread of seizure activity through the hippocampus because of the correlations observed between the presence of MFS and reverberant firing of DG neurons (Sutula & Dudek 2007). Under normal conditions, the dentate gyrus is believed to act as a "gate" for excitatory input coming in to the hippocampus (Heinemann et al 1992). In models of epilepsy, this gating function can be compromised, allowing excitatory activity to spread more easily through the DG to the hippocampus proper (Heinemann et al 1992, Mello et al 1993, Pathak et al 2007). As a result, much research has focused on trying to identify and understand the mechanisms that drive MFS in the hopes that intervening to block or reverse the development of this pathology would ameliorate seizure activity.

Previous work revealed that DGCs that are developing during or after an epileptogenic insult are responsible for most instances of aberrant DGC morphology, and that DGCs that are mature prior to epileptogenesis do not exhibit aberrant features (Jessberger et al 2007, Kron et al 2010, Walter et al 2007). These data suggested that developmental mechanisms are a necessary aspect of aberrant plasticity for DGCs in TLE. However, our use of a novel retrovirus (RV) to fluorescently label axon terminals with synaptophysin-YFP, showed that that neonatal-born and adult-born DGCs appear to participate equally in MFS in the IML (**Figure 3.3**), as well as in axonal plasticity in CA2 (**Figures 3.5**). In fact, time-course data suggested that cells that are more mature participate readily in MFS, since sprouted fibers could be detected among this

population very early after SE, while sprouted fibers from the adult-born population were not detected until 4 weeks after SE (**Figure 3.2**). Thus, MFS is not only caused by the disruption of normal DGC development, but rather involves plasticity of both mature and developing DGCs. The latter is evidenced by our finding of MFS within 4 weeks after SE arising from adult-born DGCs labeled 24 days earlier.

Axonal plasticity of mature neurons is required for normal brain function, so it is perhaps not surprising that mature neurons participate in axonal plasticity in epilepsy. DGC axonal plasticity, even IML MFS, can occur in response to physiological stimuli, albeit to a much lesser extent than occurs after SE (Adams et al 1997, Schwarzer et al 1995, Toscano-Silva et al 2010). Perhaps, then, MFS in TLE is an extension of this normal plasticity. It has been posited that MFS may not even be pathological or pro-epileptogenic (Buckmaster 2014). Recent work showed that seizure-induced MFS could be blocked by continuous treatment with rapamycin (Buckmaster et al 2009, Zeng et al 2009). Interestingly, this treatment does not reliably affect seizure frequency, and MFS in the IML can recover once rapamycin treatment is stopped (Buckmaster et al 2009, Buckmaster & Lew 2011, Lew & Buckmaster 2011). These data indicate that MFS is not necessary for the development of spontaneous seizure activity in rodent TLE models, and that there is no critical window during epileptogenesis for the development of MFS.

Importantly, however, DGC MFS is not the only feature of seizure-related plasticity that is affected by continuous rapamycin treatment. Rapamycin acts to

block m-Tor signaling, which is involved in many cellular processes, including new protein synthesis (Sandsmark et al 2007). Rapamycin treatment also blocks inhibitory axon sprouting, which is hypothesized to be an important homeostatic mechanism to reduce network excitability (Buckmaster & Wen 2011). In addition, the effects of this treatment on axonal plasticity in the dentate hilus, CA3 and CA2, or on other aspects of seizure-related plasticity have not been fully examined. Therefore, the effect of rapamycin treatment on seizure activity should not be regarded as equivalent to the effect blocking MFS on seizure activity.

Still, MFS could certainly be a neutral or even homeostatic type of plasticity. MFS into the IML has long been associated with aberrant recurrent excitability and excess excitatory input onto DGCs, but the total number of excitatory inputs onto DGCs in the IML is actually reduced in an animal model of TLE (Yamawaki et al 2015). In a normal, healthy dentate gyrus, excitatory input to DGCs in the IML comes primarily from mossy cells, which are innervated by DGCs, and provide a form of positive feedback onto DGCs, though the net effect of mossy cells on DGCs is not known (Scharfman & Myers 2012). Additionally, the pattern of excitatory innervation of DGCs from the entorhinal cortex is such that many DGCs are innervated by single cortical cells (Tamamaki & Nojyo 1993). Thus, widespread excitatory and feedback activation of DGCs is not unique to the epileptic dentate gyrus, and MFS may be an attempt to restore this type of activation after mossy cell death. In a healthy dentate network, inhibitory activity regulates the sparse activation of DGCs (Yu et al 2013). Perhaps in

epileptic networks, it is the loss of inhibition, rather than the increase in MFS, that is critical for epileptogenic hyperexcitability.

There is still much work that needs be done in order to determine the net impact of DGC axonal reorganization on network hyperexcitability. The data discussed in Chapter 3 shows that both adult-born and neonatal-born DGCs can participate in all aspects of seizure-related axonal plasticity. However, these data also indicate that only a subset of cells from both populations do so. It will need to be determined which DGCs participate in MFS, what factors govern their participation, and whether the extent of axonal plasticity varies for individual cells. Previous approaches to labeling DGC axons did not allow for distinguishing axons of individual, birthdated DGCs. In vivo biocytin labeling has been used effectively to trace individual axons, but this approach is very low throughput and does not allow for DGC birthdating. The RV mediated labeling could be adjusted to reduce cell infection rate, which would allow for tracing the axon arbors of individual, birthdated DGCs, but this approach would still be very low throughput.

Fortunately, recently developed technology offers an intermediate approach that provides both higher throughput data acquisition and the ability to resolve individual, birth-dated DGCs. Gomez-Nicola and colleagues established a system of viral vector labeling that drives the expression of up to three different fluorescent proteins in infected cells, thereby allowing for single cell identification via a unique combination of the three fluorescent markers being expressed in each cell (Gomez-Nicola et al 2014). When packaged into a RV, these fluorescent proteins distinguished individual adult-born DGCs and provided

identification of individual cells' boutons in CA3 (Gomez-Nicola et al 2014). To study hilar and IML axons, the system could be modified to drive expression of three different colors of synaptophysin-conjugated fluorescent proteins. With this approach, the axons of birthdated DGCs could be identified both at the population level and at the individual cell level. This would reveal the proportion of DGCs that participate in MFS, the extent to which individual cells participate (e.g. length of axon and width/breadth of axon arbor), and could help identify which factors might account for an individual cell's propensity for MFS.

Aberrant DGC morphology contributes to increased excitability in a rodent TLE model

Part of the utility of animal models of TLE is that they recapitulate histopathology observed in tissue from many TLE patients. This includes ectopic DGCs in the hilus or molecular layer and increased presence of hilar basal dendrites (HBDs) on DGCs. Both of these aberrant features are consistent with an increased opportunity for excitatory input, especially from other DGCs: the presence of a HBD results in a net increase in excitatory inputs onto DGCs (Thind et al 2008), and ectopic DGCs receive a greater proportion of excitatory inputs than their normotopic counterparts and DGCs from control tissue (Zhan et al 2010). One interesting recent hypothesis is that these aberrantly integrated cells are acting as "hubs" for integrating and propagating excitatory activity. This hypothesis was developed using computational modeling studies which showed that a network in which a small number of DGCs are hyper-connected to one

another is more effective for promoting seizure-like activity than one in which all DGCs have increased inter-connectivity relative to the control condition (Morgan & Soltesz 2008). Owing to their role in the epileptic network, these hyper-connected cells were termed “hub cells” (Morgan & Soltesz 2008).

It is not known whether hub-like cells actually exist in epileptic dentate gyrus networks, but if they do, then identifying them and understanding their function could provide promising new targets for therapeutic intervention. DGCs with HBDs or ectopic location are candidates for these potential hub-like cells because of both their increased excitatory input and their relative scarcity within the network. Interestingly, a recent study using inducible transgenic alteration of mTOR signaling to disrupt normal development of a minority of post-natal born DGCs provides a biological proof-of-principal for the idea that the aberrant development of a subset of DGCs is sufficient to induce spontaneous seizures (Pun et al 2012). However, it remains unknown whether such a mechanism can underlie seizures in a TLE model.

The preliminary findings presented in chapter 4 indicate that these aberrant subpopulations do indeed receive greater functional excitatory input relative to age-matched, normotopic DGCs (**Figure 4.4**). However, the increased input onto the adult-born, aberrant populations is similar to the increased input onto neonatal born DGCs after SE. Thus the difference between aberrantly integrated and normotopic adult-born DGCs appears to be caused by lower levels of excitatory input onto normotopic DGCs rather than greater input onto aberrant DGCs. These results only include the spontaneous excitatory input, and

data on inhibitory and miniature excitatory inputs are needed to put these results in context. However, a decrease in excitatory input has been reported for post-SE born DGCs that are normotopically integrated in another TLE model (Jakubs et al 2006). These data suggest that post-SE born DGCs can participate in both pro- and anti-epileptogenic types of seizure-related plasticity.

One question that arises from these preliminary data is whether aberrantly integrated DGCs could still function as hub-like cells even if they do not have dramatically increased excitatory input when compared to neonatal-born DGCs. In the computational model, hub cells are defined by their anatomical, excitatory synaptic connectivity (Morgan & Soltesz 2008). However, biological hub-like cells might exhibit a variety of anatomical and physiological features that converge to make them more likely to receive and send excitatory activity. One way in which this could be accomplished is if inhibitory inputs were reduced in this aberrant population relative to the normotopic adult- or neonatal-born DGC populations. This would lead to a shift in excitatory/inhibitory input ratio, which has been reported for ectopic DGCs, relative to normotopic (Zhan et al 2010), but has not been investigated in DGCs with HBDs. The current ongoing investigation described in chapter 4 will assess this question directly by measuring both excitatory and inhibitory inputs onto these populations.

Additionally, aberrantly integrated DGCs could still function as hub-like cells if they were more likely to functionally innervate greater numbers of downstream targets. Data from the previously proposed study using the RV driving expression in three different synaptophysin-conjugated fluorescent

proteins would provide anatomical information about the synaptic output of aberrantly integrated compared to normotopic DGCs. In addition, the physiological effects of these cells on their downstream targets must be determined in order assess their potential role as hub-like cells. Recently, Yu and colleagues combined two live imaging techniques, voltage-sensitive dye and multicellular calcium imaging, in an elegant study designed to examine the response of cells in the dentate gyrus and CA3 to activation of the perforant path (Yu et al 2013). This approach is well suited for exploring the physiological impact of individual DGC activity on post-synaptic partners because it is sensitive enough to resolve the activity of individual cells and allows for the visualization of both sub-threshold and action potential activity of the post-synaptic cells (Yu et al 2013). Individual, birthdated DGCs would be driven to fire action potentials in acute, live slices loaded with voltage-sensitive and calcium-sensitive dyes, so that the post-synaptic responses could be visualized and compared between aberrantly integrated and normotopic adult-born DGCs as well as neonatal-born DGCs. In this way, the impact of individual DGC activity within the network could be determined. Finally, these aberrantly integrated cells could still function as hub-like cells if they have greater intrinsic excitability, which would mean similar levels of excitatory synaptic input could more reliably result in action potential firing and activation of downstream cells.

Intrinsic neurophysiological properties of DGCs from both human and rodent model tissue are affected in TLE

Changes in synaptic inputs are one way in which network activity can be modified, but changes in intrinsic excitability of DGCs may also play an important role in the development of network hyperexcitability. Most studies examining intrinsic neurophysiology of DGCs in animal models of TLE have reported only minor or subtle changes in membrane or firing properties(Mody & Staley 1994). However, many of these studies did not account for DGC birthdate or aberrant morphology, and therefore other changes may not have been detected. Indeed, the studies that investigated the physiology of hilar ectopic DGCs reported spontaneous AP firing as well as less polarized resting membrane potential in ectopic DGCs compared to those that are normotopic (Scharfman et al 2000, Zhan & Nadler 2009). In these studies, neither the normotopic nor ectopic populations were birthdated, but nearly all ectopic DGCs in rodent TLE models are born after SE (Kron et al 2010, Walter et al 2007), while most DGCs in the granule cell layer are already mature when SE is induced in adulthood. Thus, it is not known whether the observed changes in intrinsic excitability are due to the fact that ectopic cells have aberrant morphology or that they were born after SE.

The data reported in Chapter 2 of this dissertation showed that ectopic DGCs in the rat TLE model exhibit a less polarized resting membrane potential and a greater firing rate when compared to normotopic post-SE born DGCs and adult-born DGCs in sham tissue (**Figure 2.8, Table 2.2**). This is consistent with increased intrinsic excitability and therefore with the hypothesis that this population acts as hub-like cells to promote excitatory activity in TLE. Interestingly, however, ectopic DGCs from patient tissue exhibit reduced firing

rate and less polarized action potential threshold when compared to normotopic (**Figure 2.3, Table 2.1**), both of which are consistent with reduced intrinsic excitability. Additionally, variability in spike frequency accommodation and action potential waveform were observed among DGCs from patient tissue but not the rat model. These discrepancies between data from patient and rat model tissue raise questions about the validity of animal models and the potential role of ongoing plasticity in TLE.

The question of appropriate animal models is an ongoing area of concern in TLE research. The utility of any given animal model should always be considered in relation to a particular research question. For example, the pilocarpine-induced SE rat model is useful for studying the contribution of aberrant DGC plasticity because it reliably produces many morphological abnormalities observed in TLE. In addition, it is a commonly used model, which provides a large framework of pre-existing data within which to evaluate the meaning of newly collected data. In fact, in this sense, data from animal models can be more reliable than data from human tissue. Due to the wide range in patient age, disease severity, and medication history, the variability we observed among DGCs from patient tissue could result from many different influences and is difficult to interpret. Thus, when discrepancies are observed between the disease and disease model, data from the disease model is often favored. This is unfortunate because access to living human brain tissue provides a rare and precious opportunity to study the neurophysiology of human cells.

A much larger data set of the neurophysiological properties of human DGCs is needed in order to understand the implications of the heterogeneity described in Chapter 2. Anterior temporal lobectomy is performed on many TLE patients every year, but the majority of resected tissue is not used for neurophysiological studies. A large-scale effort across many universities to characterize the anatomy and physiology of all available neuronal subtypes from resected temporal lobe structures should be undertaken to build a database of human neuronal activity. This would provide a framework for understanding not only TLE-related heterogeneity, but also, potentially, age- or medication- related heterogeneity. Moreover, studying samples from patients who undergo surgery early in their disease course would be particularly informative.

As discussed in Chapter 2, one likely cause of discrepancies between the human and rat data was the difference in disease duration between the patient population and the rodent population. Perhaps ectopic DGCs exhibited reduced excitability in human tissue because of homeostatic mechanisms that come into play in later stages of the disease. Plasticity that is presumed to be homeostatic, such as inhibitory axon sprouting, accumulates over time in animal models (Peng et al 2013, Zhang et al 2009). However, plasticity that is presumed to be pathological, including ectopic DGCs, also accumulates over time in animal models (Parent et al 2006). The relationship between disease duration and pathology needs to be better elucidated in the rat model. For intrinsic physiology of ectopic DGCs, this could be accomplished with fairly straightforward time course experiments in which the birthdated DGCs are examined at six-month

intervals starting six months after SE. These experiments should include both DGCs born soon after SE and DGCs born later in the chronic stage of epilepsy, such as one year after SE, in order to distinguish between how intrinsic properties may change over time and how newly added DGCs may respond to the changing environment.

A look to the future

Identifying which aspects of brain injury-induced plasticity lead to epilepsy and why, is a primary focus of TLE research. The long-term goal is to develop ways to block or reverse the plasticity in order to treat the cause of epilepsy rather than just the symptoms. However, this line of research might be based on incorrect assumptions about distinctions between pro- and anti-epileptogenic plasticity. The mechanisms of epileptogenesis are likely to involve interaction of multiple aspects of aberrant plasticity. The contribution of any one feature may not be truly separable from others, and may, in fact, vary among individuals and even change over the course of disease.

Studies in animal models have attempted to block aspects of seizure-related plasticity that are presumed to be epileptogenic with mixed results. The effects of blocking MFS were discussed previously in this chapter and illustrate the difficulty in separating one aspect of seizure-related plasticity from the others and determining the net impact of a given feature. Another attempt to interfere with epileptogenic plasticity has been to block the post-SE upregulation of

neurogenesis. Some studies reported a reduction in seizure activity when neural stem cell proliferation is blocked with antimitotic drugs or by reducing inflammatory signals (Jung et al 2004, Jung et al 2006), while others found that reducing adult-born neurons with irradiation or genetic manipulation can increase the response to SE and does not reduce spontaneous seizure activity (A. Althaus, unpublished observations) (Iyengar et al 2014). Perhaps some of the discrepancy in these results can be explained by the use of different methods of suppressing neurogenesis, different models of epilepsy, and even different rodent species in these experiments. Importantly, as with the MFS data, off-target effects of these treatments have to be considered when interpreting the results. Targeting the inflammatory response or general cell division reduces activated microglia in addition to neurogenesis, and can affect cell death and other features associated with SE (Jung et al 2004, Jung et al 2006). Thus, the impact of blocking neurogenesis in these experiments cannot be separated from the effects of interfering with these other types of plasticity.

Of course, data that challenge pre-conceived ideas about what types of plasticity are pro- or anti-epileptogenic must be considered carefully, and not simply explained away. It is certainly possible that MFS is not pro-epileptogenic and there is now a considerable amount of data suggesting that adult-neurogenesis contributes to both pro- and anti-epileptogenic plasticity. However, eliminating a phenomenon to determine its overall impact may not be the best approach for investigating this type of reactive plasticity, even if it could be accomplished without interfering with other aspects of plasticity. When

considering the effect of blocking any type of plasticity, one must also consider potential compensatory mechanisms employed by the network in response to the loss. Loss of neurogenesis in otherwise normal laboratory mice results in compensatory plasticity throughout the rest of the dentate gyrus that eventually restores activity thought to be normally mediated by immature neurons (Singer et al 2011). While this is not necessarily an indication of how a diseased network would respond, it suggests the possibility for compensatory mechanisms that could confound data interpretation. Rather than eliminating various aspects of DGC pathology outright, a better strategy for therapeutic intervention in epilepsy would be to focus on understanding ongoing plasticity in chronic epilepsy, as in the time course experiment proposed for studying potential homeostatic changes in ectopic DGCs.

Intervening in seizure-related plasticity prior to the onset of epilepsy may be ideal, but it is currently impossible. Many patients with TLE do not experience an obvious precipitating injury and there is no way of knowing whether an individual patient who experiences a precipitating injury such as SE will go on to develop epilepsy (Harvey et al 1997). Some progress is being made toward the identification of factors that are associated with eventual development of TLE, and therefore toward a potential ability for pre-epileptogenic intervention (Choy et al 2014, Lewis et al 2014), but there is an immediate need for better treatment options for patients who currently have epilepsy. An elegant study by Hunt and colleagues recently offered promising evidence of the potential for restoring normal function to a network damaged by SE, which was accomplished by

transplantation of inhibitory interneurons (Hunt et al 2013). However, this required invasive transplantation and a fetal mouse stem cell donor into a mouse TLE model. Ongoing plasticity has been described for existing inhibitory interneurons that promotes inhibition of the dentate gyrus in TLE models (Halabisky et al 2010, Houser et al 2012, Zhan & Nadler 2009, Zhang et al 2009). Additionally, the development of inhibitory circuitry is, at least at some stages, differentially regulated from the development of excitatory circuitry, and therefore could be differentially targeted for intervention (Terauchi & Umemori 2012). Thus, exploring the mechanisms that drive plasticity of inhibitory networks, in particular with an eye to identifying mechanisms that are unique to inhibitory circuit development, could provide novel therapeutic opportunities.

The effort to understand seizure-related plasticity in DGCs is an important step in the study of TLE, and the data presented in this dissertation provide novel insight into the impact of cell age and morphology on TLE plasticity. However, a comprehensive understanding of how aspects of seizure-related plasticity affect excitability, both individually and in coordination with other features, will likely require large-scale computational modeling. Modeling allows for both the isolated manipulation of variables without off-target effects (eg altering only DGC axon sprouting, but retaining inhibitory axon sprouting), and the concurrent manipulation of variables that often cannot be concurrently studied in bioloigical experiments (eg altering dendritic morphology and ion channel composition). A number of computational studies have already explored the contribution of aberrant DGC morphology to hyperexcitability in TLE and their findings have

generated important new hypothesis, including the hub cell hypothesis discussed above (Tejada & Roque 2014). Of course, the construction of good computational models requires good experimental data and open communication among scientists. The current primary means of sharing data is inefficient for facilitating widespread collaborative efforts. Technological advancements in data storage and sharing could be better utilized by the scientific community to create free, open access to one anothers' raw and analyzed data. This would maximize resources, reduce waste, and speed scientific progress.

References

Adams B, Lee M, Fahnestock M, Racine RJ. 1997. Long-term potentiation trains induce mossy fiber sprouting. *Brain research* 775: 193-7

Buckmaster PS. 2014. Does mossy fiber sprouting give rise to the epileptic state? *Advances in experimental medicine and biology* 813: 161-8

Buckmaster PS, Ingram EA, Wen X. 2009. Inhibition of the mammalian target of rapamycin signaling pathway suppresses dentate granule cell axon sprouting in a rodent model of temporal lobe epilepsy. *The Journal of neuroscience : the official journal of the Society for Neuroscience* 29: 8259-69

Buckmaster PS, Lew FH. 2011. Rapamycin suppresses mossy fiber sprouting but not seizure frequency in a mouse model of temporal lobe epilepsy. *The Journal of neuroscience : the official journal of the Society for Neuroscience* 31: 2337-47

Buckmaster PS, Wen X. 2011. Rapamycin suppresses axon sprouting by somatostatin interneurons in a mouse model of temporal lobe epilepsy. *Epilepsia* 52: 2057-64

Choy M, Dube CM, Patterson K, Barnes SR, Maras P, et al. 2014. A novel, noninvasive, predictive epilepsy biomarker with clinical potential. *The Journal of neuroscience : the official journal of the Society for Neuroscience* 34: 8672-84

Gomez-Nicola D, Riecken K, Fehse B, Perry VH. 2014. In-vivo RGB marking and multicolour single-cell tracking in the adult brain. *Scientific reports* 4: 7520

Halabisky B, Parada I, Buckmaster PS, Prince DA. 2010. Excitatory input onto hilar somatostatin interneurons is increased in a chronic model of epilepsy. *Journal of neurophysiology* 104: 2214-23

Harvey AS, Berkovic SF, Wrennall JA, Hopkins IJ. 1997. Temporal lobe epilepsy in childhood: clinical, EEG, and neuroimaging findings and syndrome classification in a cohort with new-onset seizures. *Neurology* 49: 960-8

Heinemann U, Beck H, Dreier JP, Ficker E, Stabel J, Zhang CL. 1992. The dentate gyrus as a regulated gate for the propagation of epileptiform activity. *Epilepsy research. Supplement* 7: 273-80

Houser CR, Zhang N, Peng Z, Huang CS, Cetina Y. 2012. Neuroanatomical clues to altered neuronal activity in epilepsy: from ultrastructure to signaling pathways of dentate granule cells. *Epilepsia* 53 Suppl 1: 67-77

Hunt RF, Girskis KM, Rubenstein JL, Alvarez-Buylla A, Baraban SC. 2013. GABA progenitors grafted into the adult epileptic brain control seizures and abnormal behavior. *Nature neuroscience* 16: 692-7

Iyengar SS, LaFrancois JJ, Friedman D, Drew LJ, Denny CA, et al. 2014. Suppression of Adult Neurogenesis Increases the Acute Effects of Kainic Acid. *Experimental neurology* 264C: 135-49

Jakubs K, Nanobashvili A, Bonde S, Ekdahl CT, Kokaia Z, et al. 2006. Environment matters: synaptic properties of neurons born in the epileptic adult brain develop to reduce excitability. *Neuron* 52: 1047-59

Jessberger S, Zhao C, Toni N, Clemenson GD, Jr., Li Y, Gage FH. 2007. Seizure-associated, aberrant neurogenesis in adult rats characterized with retrovirus-mediated cell labeling. *The Journal of neuroscience : the official journal of the Society for Neuroscience* 27: 9400-7

Jung KH, Chu K, Kim M, Jeong SW, Song YM, et al. 2004. Continuous cytosine-b-D-arabinofuranoside infusion reduces ectopic granule cells in adult rat hippocampus with attenuation of spontaneous recurrent seizures following pilocarpine-induced status epilepticus. *The European journal of neuroscience* 19: 3219-26

Jung KH, Chu K, Lee ST, Kim J, Sinn DI, et al. 2006. Cyclooxygenase-2 inhibitor, celecoxib, inhibits the altered hippocampal neurogenesis with attenuation of spontaneous recurrent seizures following pilocarpine-induced status epilepticus. *Neurobiology of disease* 23: 237-46

Kron MM, Zhang H, Parent JM. 2010. The developmental stage of dentate granule cells dictates their contribution to seizure-induced plasticity. *The Journal of neuroscience : the official journal of the Society for Neuroscience* 30: 2051-9

Lew FH, Buckmaster PS. 2011. Is there a critical period for mossy fiber sprouting in a mouse model of temporal lobe epilepsy? *Epilepsia* 52: 2326-32

Lewis DV, Shinnar S, Hesdorffer DC, Bagiella E, Bello JA, et al. 2014. Hippocampal sclerosis after febrile status epilepticus: the FEBSTAT study. *Annals of neurology* 75: 178-85

Mello LE, Cavalheiro EA, Tan AM, Kupfer WR, Pretorius JK, et al. 1993. Circuit mechanisms of seizures in the pilocarpine model of chronic epilepsy: cell loss and mossy fiber sprouting. *Epilepsia* 34: 985-95

Mody I, Staley KJ. 1994. Cell properties in the epileptic hippocampus. *Hippocampus* 4: 275-80

Morgan RJ, Soltesz I. 2008. Nonrandom connectivity of the epileptic dentate gyrus predicts a major role for neuronal hubs in seizures. *Proceedings of the National Academy of Sciences of the United States of America* 105: 6179-84

Parent JM, Elliott RC, Pleasure SJ, Barbaro NM, Lowenstein DH. 2006. Aberrant seizure-induced neurogenesis in experimental temporal lobe epilepsy. *Annals of neurology* 59: 81-91

Pathak HR, Weissinger F, Terunuma M, Carlson GC, Hsu FC, et al. 2007. Disrupted dentate granule cell chloride regulation enhances synaptic excitability during development of temporal lobe epilepsy. *The Journal of neuroscience : the official journal of the Society for Neuroscience* 27: 14012-22

Peng Z, Zhang N, Wei W, Huang CS, Cetina Y, et al. 2013. A reorganized GABAergic circuit in a model of epilepsy: evidence from optogenetic labeling and stimulation of somatostatin interneurons. *The Journal of neuroscience : the official journal of the Society for Neuroscience* 33: 14392-405

Pun RY, Rolle IJ, Lasarge CL, Hosford BE, Rosen JM, et al. 2012. Excessive activation of mTOR in postnatally generated granule cells is sufficient to cause epilepsy. *Neuron* 75: 1022-34

Sandsmark DK, Pelletier C, Weber JD, Gutmann DH. 2007. Mammalian target of rapamycin: master regulator of cell growth in the nervous system. *Histology and histopathology* 22: 895-903

Scharfman HE, Goodman JH, Sollas AL. 2000. Granule-like neurons at the hilar/CA3 border after status epilepticus and their synchrony with area CA3 pyramidal cells: functional implications of seizure-induced neurogenesis. *The Journal of neuroscience : the official journal of the Society for Neuroscience* 20: 6144-58

Scharfman HE, Myers CE. 2012. Hilar mossy cells of the dentate gyrus: a historical perspective. *Frontiers in neural circuits* 6: 106

Schwarzer C, Williamson JM, Lothman EW, Vezzani A, Sperk G. 1995. Somatostatin, neuropeptide Y, neurokinin B and cholecystokinin immunoreactivity in two chronic models of temporal lobe epilepsy. *Neuroscience* 69: 831-45

Singer BH, Gamelli AE, Fuller CL, Temme SJ, Parent JM, Murphy GG. 2011. Compensatory network changes in the dentate gyrus restore long-term potentiation following ablation of neurogenesis in young-adult mice. *Proceedings of the National Academy of Sciences of the United States of America* 108: 5437-42

Sutula TP, Dudek FE. 2007. Unmasking recurrent excitation generated by mossy fiber sprouting in the epileptic dentate gyrus: an emergent property of a complex system. *Progress in brain research* 163: 541-63

Tamamaki N, Nojyo Y. 1993. Projection of the entorhinal layer II neurons in the rat as revealed by intracellular pressure-injection of neurobiotin. *Hippocampus* 3: 471-80

Tejada J, Roque AC. 2014. Computational models of dentate gyrus with epilepsy-induced morphological alterations in granule cells. *Epilepsy & behavior : E&B* 38C: 63-70

Terauchi A, Umemori H. 2012. Specific sets of intrinsic and extrinsic factors drive excitatory and inhibitory circuit formation. *The Neuroscientist : a review journal bringing neurobiology, neurology and psychiatry* 18: 271-86

Thind KK, Ribak CE, Buckmaster PS. 2008. Synaptic input to dentate granule cell basal dendrites in a rat model of temporal lobe epilepsy. *The Journal of comparative neurology* 509: 190-202

Toscano-Silva M, Gomes da Silva S, Scorza FA, Bonvent JJ, Cavalheiro EA, Arida RM. 2010. Hippocampal mossy fiber sprouting induced by forced and voluntary physical exercise. *Physiology & behavior* 101: 302-8

Walter C, Murphy BL, Pun RY, Spieles-Engemann AL, Danzer SC. 2007. Pilocarpine-induced seizures cause selective time-dependent changes to adult-generated hippocampal dentate granule cells. *The Journal of neuroscience : the official journal of the Society for Neuroscience* 27: 7541-52

Yamawaki R, Thind K, Buckmaster PS. 2015. Blockade of excitatory synaptogenesis with proximal dendrites of dentate granule cells following rapamycin treatment in a mouse model of temporal lobe epilepsy. *The Journal of comparative neurology* 523: 281-97

Yu EP, Dengler CG, Frausto SF, Putt ME, Yue C, et al. 2013. Protracted postnatal development of sparse, specific dentate granule cell activation in the mouse hippocampus. *The Journal of neuroscience : the official journal of the Society for Neuroscience* 33: 2947-60

Zeng LH, Rensing NR, Wong M. 2009. The mammalian target of rapamycin signaling pathway mediates epileptogenesis in a model of temporal lobe epilepsy. *The Journal of neuroscience : the official journal of the Society for Neuroscience* 29: 6964-72

Zhan RZ, Nadler JV. 2009. Enhanced tonic GABA current in normotopic and hilar ectopic dentate granule cells after pilocarpine-induced status epilepticus. *Journal of neurophysiology* 102: 670-81

Zhan RZ, Timofeeva O, Nadler JV. 2010. High ratio of synaptic excitation to synaptic inhibition in hilar ectopic granule cells of pilocarpine-treated rats. *Journal of neurophysiology* 104: 3293-304

Zhang W, Yamawaki R, Wen X, Uhl J, Diaz J, et al. 2009. Surviving hilar somatostatin interneurons enlarge, sprout axons, and form new synapses with granule cells in a mouse model of temporal lobe epilepsy. *The Journal of neuroscience : the official journal of the Society for Neuroscience* 29: 14247-56